Kéage Laboratory of Nuclear Science
Decennial Report 1955-1965

Kiichi KIMURA*

(Kimura Laboratory)

(*Received November 17, 1965*)

The works in various fields done by using the Kyoto University Cyclotron in the period from 1955 to 1965 are summarized and reviewed. The activities of the cyclotron laboratory which are not yet published are also presented. This report contains some topical problems as follows.

1. Introduction. .... (499)
2. Site and Building. .... (500)
3. Facilities and Technique Development. .... (503)
4. Research in Nuclear Physics. .... (509)
5. Research in Radiation Biology and Related Problems. .... (553)
6. Publications. .... (562)

1. INTRODUCTION

In December 1955, proton beam of about 7.5 MeV was observed to brighten a quartz plate inserted in the acceleration chamber of the Kyoto University Cyclotron. The acceleration of ions by the cyclotron was successfully achieved. Since then, a decade has flowed away over the Laboratory of Nuclear Science. As a Japanese proverb goes, "ten years is an epoch," an enormous progress was made in nuclear physics, in radiation chemistry and in radiation biology during this decade. In the field of nuclear physics, many new phenomena have been found and a number of new conceptions have been proposed, and many body aspects or cooperative nature of nucleons in the nucleus have become more clear. The author is not acquainted with the field of nuclear chemistry or radiation biology, but it seems to him that, hot atom chemistry, activation analysis, molecular level bio-chemistry and so on are the most pronounced field investigated recently with the aid of nuclear radiations.

To limit the topics in our laboratory, various affairs have occurred and the cyclotron has become ten years old.

In the following, the history of the Laboratory of Nuclear Science, Institute for Chemical Research, is described. In section 2, the changes of the site and building of this laboratory, in section 3 the information of research apparatus installed and the development of laboratory techniques, in section 4 research works done in the field of nuclear physics, in section 5, studies by physicians on radiation injuries upon living bodies and radiochemical researches by chemists in other laboratories are introduced, and finally in section 6, the scientific articles are listed

---

* 木村毅一

up which were written by members of the laboratory and by researchers who performed their works using the Kyoto University Cyclotron.

The Kyoto University Cyclotron was born by the good will of many persons in Kyoto University, and has been expected to contribute to the researches in various fields of nuclear science. Here we have a pleasure to present ten years history of the laboratory of nuclear science, which is nothing but the memoirs of the growth of the cyclotron.

2. SITE AND BUILDING

The Kéage Cyclotron Laboratory was installed in an old brick building, which was used as a hydro-electric power station until 1936. When we entered in this building for the first time, there were nothing except floors with large holes, roofs with large holes, windows with many holes as well as a heap of dust. The first work we had to do was to light the inside of the building and to sweep out the dust.

The building consists of the 2nd basement, the 1st basement, the ground floor and the mezzanine floor. In former days, the 2nd basement was used as a water exhaust channel, the 1st basement supported five big bend tubes, on the ground floor were set five hydraulic turbins and electric power generators and on the mezzanine floor control systems of the hydroelectric power station were installed. To utilize this building as a laboratory for nuclear science, the reinforcement of the floors, the partition of the large hall, the construction of new rooms and the radiation shielding walls and ceilings were necessary.

The present arrangements of the laboratory are shown in Fig. 2-1. This final form was established in Dec. 1961, six years later from the date of the first operation of the cyclotron. The reader may ask why such a long time was needed to rebuild the laboratory. This was caused mainly by the lack of funds. In the following, the sequence of the constructions are described.

In Dec. 1955, when the cyclotron was operated for the first time, the radiation shielding wall only covered the front of the control desk, and soon it became clear that the radiation doses were far above the safety level even at the control desk. The wall thickness was enough to attenuate the direct radiation under the safety level, thus the skyshine effect and the reflections from the roofs were the main reason of the high radiation level. In 1956, the shielding wall was extended so as to surround the cyclotron, and in 1957 the ceiling of 80 cm thick concrete covered the cyclotron.

In 1958, the radiation shielding wall of 50 cm thick concrete divided the main hall on the ground floor into two rooms. One room near the cyclotron was devoted to as an experimental area, into this room the beam was extracted and the scattering chamber and other equipments were installed. Ceilings of 50 cm thick concrete were also provided to shield the radiations generated in the experimental area.

In 1959, started the partition of the building into the rooms for office, chemical

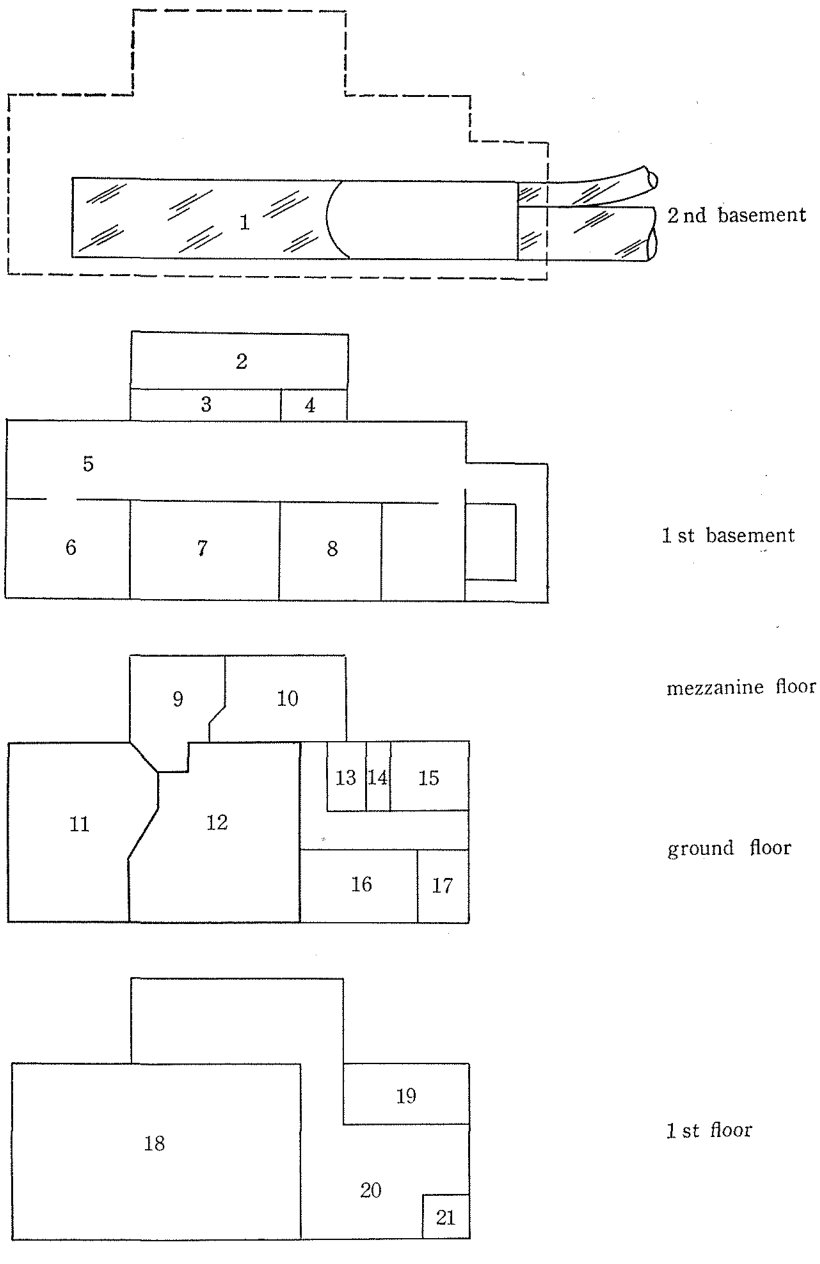

Fig. 2-1. Present arrangements of the laboratory.

1) Water pool.
2) Mechanical shop.
3) Main generator room.
4) Nitrogen liquefier room.
5) Heat exchanger for cyclotron.
6) Heat exchanger for R. F.
7) Beta ray spectrometer room.
8) Target preparation room.
9) Control room.
10) Counting room.
11) Cyclotron area.
12) Experimental area.
13) Developing machine room.
14) Balance room.
15) Chemical operation room.
16) Electronic shop.
17) Office room.
18) Safety area.
19) Library.
20) Office room.
21) Microscopic scanning room.

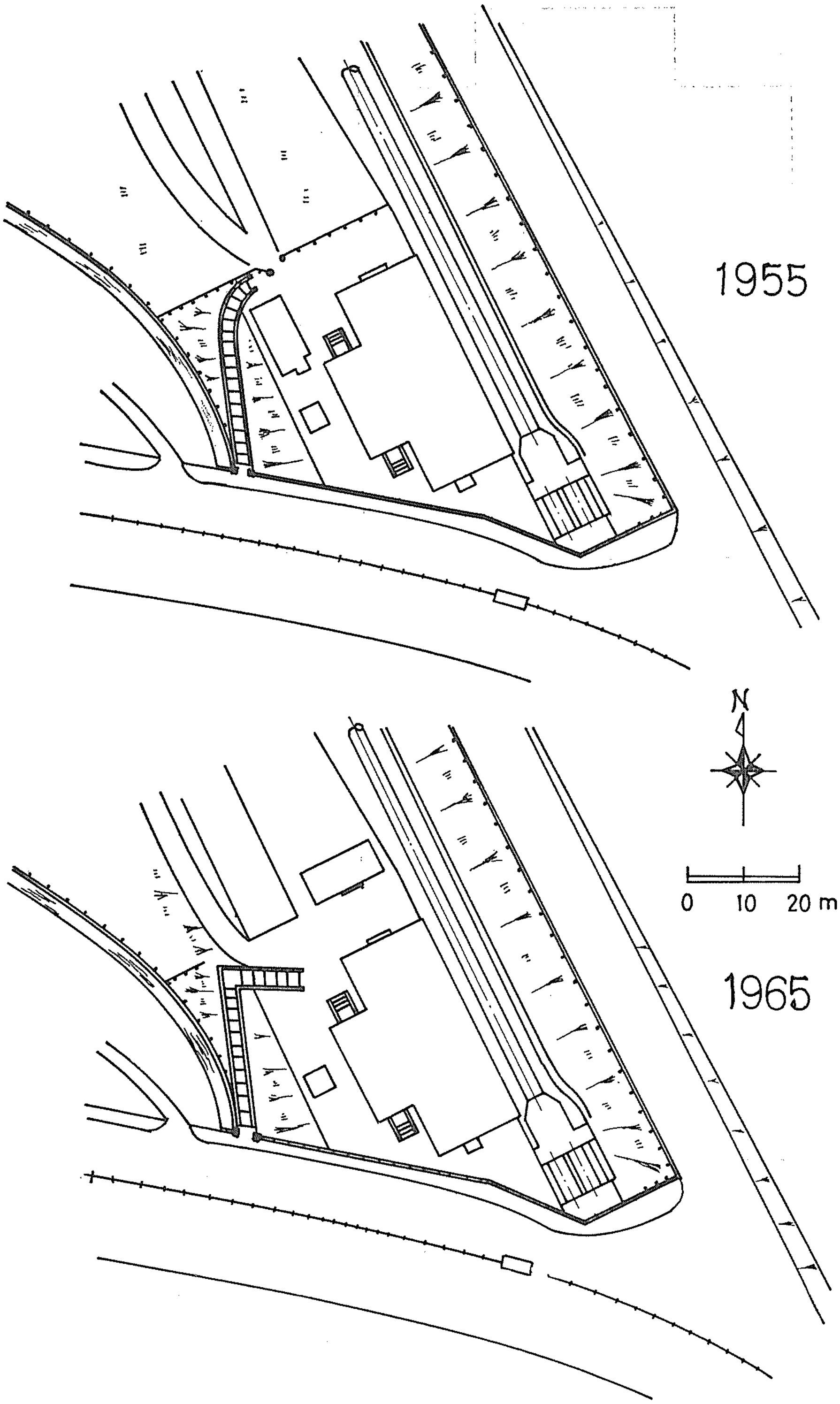

Fig. 2-2. Sketch map of the site and building, old and new.

operation, library, counting and a nuclear plate processing, and were completed in the beginning of 1960. The laboratory took shape and the research works on nuclear physics were commenced.

In 1961, two rooms were provided on the first basement, one for the beta-ray spectrometer and the other for target preparation. From this year until now, no change was made in the arrangement of the laboratory, except that an accessory wooden house was rebuilt in 1965 owing to the extension of the electric power plant of Kansai Electric Power Co. Inc. (Fig. 2-2).

3. FACILITIES AND TECHNIQUE DEVELOPMENT

The design, the specifications and the performance of the cyclotron are described in ref. [61-10], so here we introduce briefly the development of laboratory techniques and facilities equipped since 1960, and other things not described in ref. [61-10]. Numbers in the brackets indicate the references listed in section 6.

3-1. Acceleration of Heavy Ions with the Cyclotron

Co-operating with the members of the Department of Nuclear Engineering, Faculty of Engineering, the acceleration of heavy ions has been tried since 1963. [64-2] [64-7] [65-11] [65-15]. Since the frequency of r.f. oscillation of the cyclotron was fixed, the ions were accelerated by the third subharmonic period of the dee voltage. By this method, 10 MeV double charged carbon ions were extracted from the cyclotron. In Fig. 4-9-1, nuclear transmutations caused by carbon ions are cited. These phenomena were observed by nuclear plates made by Konishiroku Photo Industries Co. Recently, triple charged nitrogen ions were extracted from the cyclotron by the same method. In the case of carbon ions, as the extracted beam current was not so intense to use them immediately for nuclear physics experiment, the charge exchange experiments have been done. However, in the case of nitrogen ions, the beam intensity was about 10^{-9}A or greater, and the Coulomb excitation researches are attempted. Various improvements to facilitate heavy ion experiments are now under way.

3-2. Beam Transport System

Quadrupole lens magnets were installed in the beginning of 1956 and have been used to focus the extracted beam since 1960. Its aperture is 12 cm and maximum field gradient is 500 gauss/cm. Detailed descriptions will be published in this Bulletin. At the same time, a beam energy defining magnet was constructed and came to operation since 1958 coupled with a reaction analyzer magnet. The beam energy analyzer magnet has a gap of 45 mm and the maximum field is 12 kilogauss. Its deflection angle is 70° and vertical focussing of ion trajectory is obtained by the oblique entrance method. When the source point width is 1 mm and the image point width is limited to 0.76 mm the energy resolution is better than 0.1%. Detailed descriptions will appear in this Bulletin.

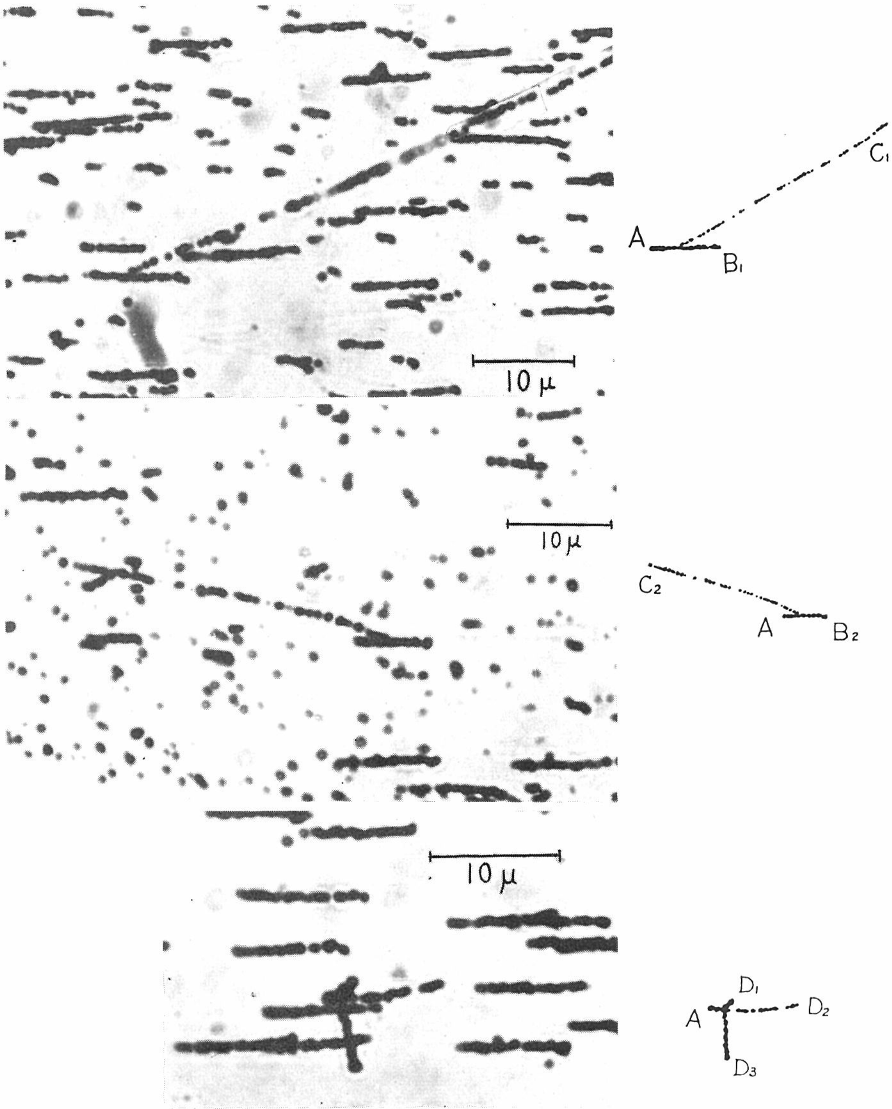

Fig. 3-1-1. Heavy ion reactions induced by the interactions of 10 MeV carbon ions with light nuclei in nuclear emulsion. A, B and C's are incident ions, reaction products and emitted light particles respectively. D's show fragments caused by a break up reaction. The carbon ions are introduced from left to right.

Finally, a beam switching magnet was built and installed in the beginning of 1965. It has a pole gap of 60 mm and could deflect the extracted beam from the cyclotron by 30° to the left or the right direction. Present day beam handling system is shown in Fig. 3-2-1.

3-3. Reaction Analyzer Magnet

A Browne-Buechner type broad range magnetic analyzer for the investigation of nuclear reactions was designed and constructed in 1958. Effective radius of the

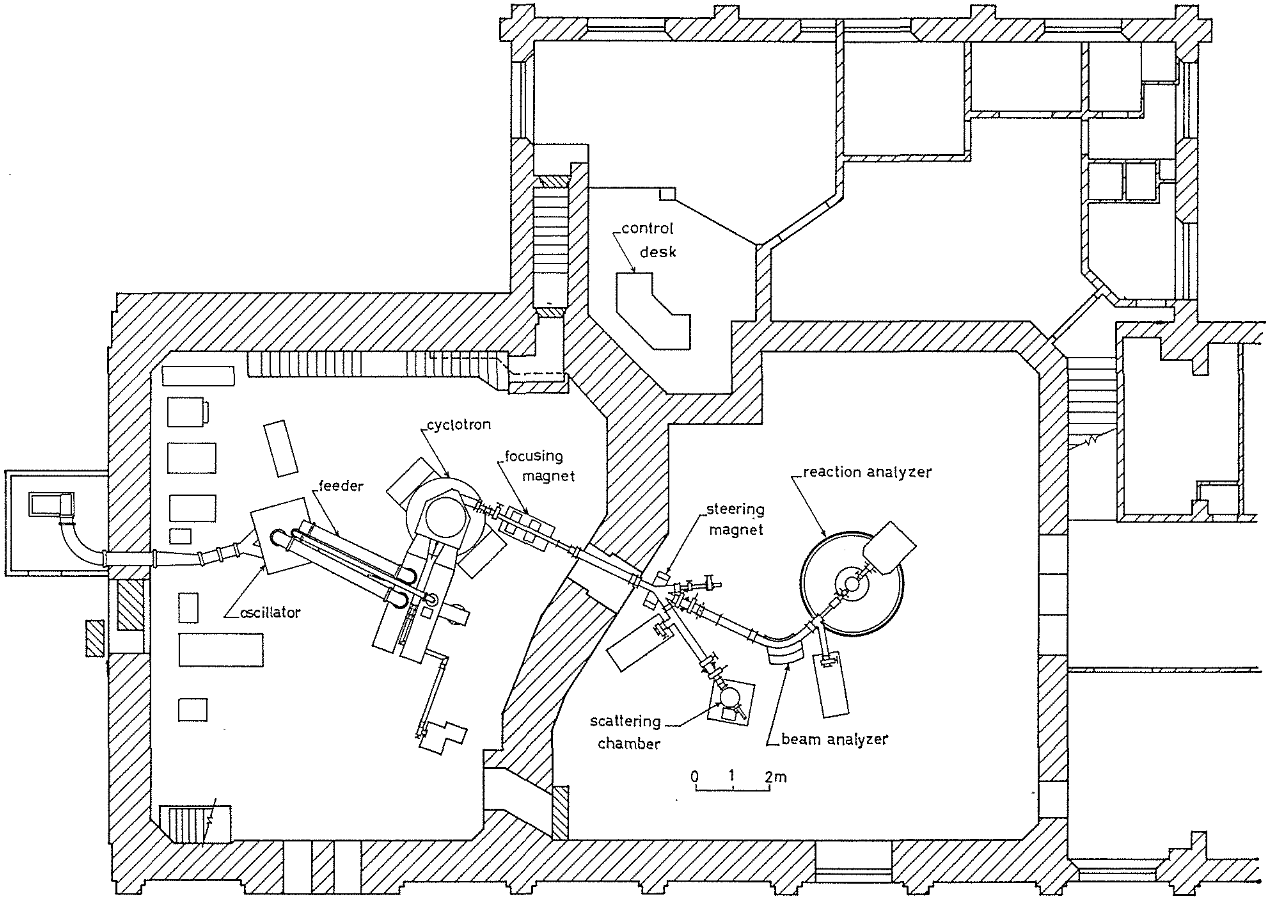

Fig. 3-2-1. Lay-out of the beam transport systems.

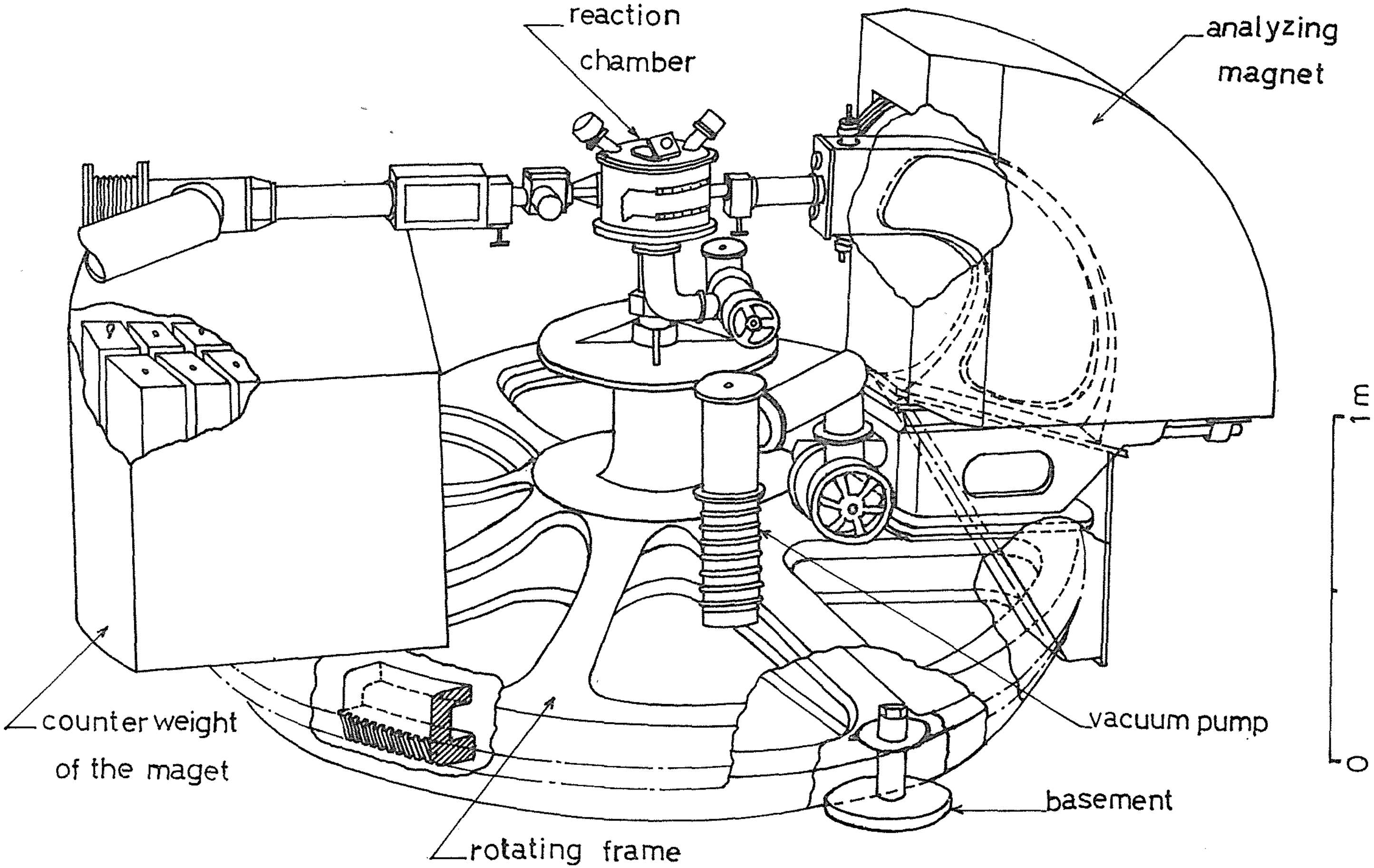

Fig. 3-3-1. Cut-away view of the broadrange magnetic analyzer.

magnet pole was designed as 67 cm, and the focal plane covered from the maximum energy to half its energy. The gap of the magnet is 20 mm and the maximum magnetic field strength is over 18 kilogauss. The analyzer magnet is mounted on a frame which can rotate about the axis of a reaction chamber centered on a fixed frame. The reaction chamber has two horizontally spread windows covered with sliding membranes and a vacuum duct connects the reaction chamber with the analyzing magnet. Detailed descriptions of the reaction analyzer will be published in this Bulletin. In Fig. 3-3-1, a cut-away view of this analyzer is shown.

3-4. Magnetic Thin Lens Type Beta-ray Spectrometer

In 1955, a thin lens type beta-ray spectrometer was designed by Jun KOKAME and Ryutaro ISHIWARI and installed in this laboratory in 1956. This beta-ray spectrometer had dual purposes, one was to assign the radioactive isotopes produced by the cyclotron beam irradiation and the other was to detect the gamma rays following nuclear reactions. Therefore the design principle was laid upon the luminosity of the spectrometer rather than the high resolution of beta-ray spectrum. Several reasons prevented the completion of this spectrometer and quite recently, in 1964, beta-ray spectrum was first obtained. [65-18]. As the recent development of the solid state detector lessened the feasibility of the magnetic type beta-ray spectrometer, this spectrometer may be of little use in future in the field of research

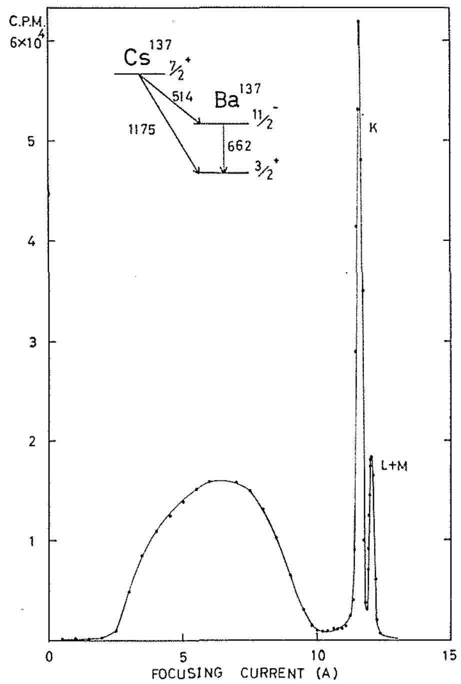

Fig. 3-4-1. Beta-ray spectrum of Cs^{137} obtained by the thin lens spectrometer.

works, but still of great use to identify the radioactivity of some kind. The beta-ray spectrum of Cs^{137} obtained by this apparatus is shown in Fig. 3-4-1.

3-5. Vacuum Technique.

Vacuum techniques in this laboratory were developed mainly by Yoshiaki UEMURA. The 40 cm diameter oil diffusion pump of the cyclotron was designed by him and has worked well in the past decade. This diffusion pump was a long nozzle type and was a first one in Japan without a baffle. He and his co-workers contributed the laboratory in many ways other than the pump designing, that is, the technique of leak hunting of a large scale evacuating system, the technique of ion source of the cyclotron, the design of a vacuum evaporation apparatus, the design of the vacuum gate valves, flanges, ducts and other components of vacuum system and so on.

The leak hunting of a large scale system is, as is well known, very tedious and time consuming, but an inevitable task to succeed in the accelerator operation. UEMURA and others established the technique of leak hunting in three steps. First, they measured the de-sorption of gasses from various metal surfaces and found the method to estimate the quantity of gas leakage from outside the vacuum system of which the volume and the inner surface area are known. [54-1]. Then they studied the substitution sensitivity factor of helium and propane gasses for single ionization vacuum gauge. [61-2]. In the third step, they measured the volume of bubbles in a unit time which escape from inside of the vacuum system when pressurized air filled the vessel. By these three methods, i.e., estimation of leakage from a build up of pressure in the vessel, estimation of leakage from a volume of extruded air bubbles from a vessel, and finally hunting of leaking position by blowing down propane gas and by watching the corresponding ion current increase of the ionization gauge, leak hunting labour became a very easy task to handle. Detailed descriptions are given in [54-1], [54-2], [56-1], [56-2], [58-4], [61-1] and (61-2). Propane gas is now widely used in Japan as a leak hunting probe gas, after the basic technique developed in this laboratory.

3-6. Target Preparation

In low energy nuclear physics, target preparation is an essential step to achieve the experiments. The required thickness of targets is nearly 1 mg/cm^2 or less in the energy range investigated in our laboratory, so techniques to produce thin films of desired material are very important.

Targets thus far used in our laboratory are, d, He, Be, B, C, N, O, F, Ne, Na, Mg, Al, Si, S, P, Cl, K, Ar, Ti, Co, Ni, Cu, Ag, Cd, Sn and Au.

Among these materials, gaseous substances are used in forms of gas targets, as usual in every nuclear physics laboratory. Materials which required special cautions are described in the following.

Be: Natural Be metal were used as raw material of Be films. Thin films of Be were made by vacuum evaporation on a deck glass coated beforehand with a thin layer of nitrocellulose, and then stripped off from the glass in acetone. Be is very toxic, so evacuated gases from the vacuum coating apparatus are exhausted to the open air through a duct.

B: To make thin film of boron metal, vacuum furnace heated by bombardment with electrons is used. This vacuum evaparation apparatus was designed by Y. UEMURA. Boron film is made on a deck glass, and stripped off in water.

C: Self-supporting film of carbon is made by two ways. One way is thermal cracking method, which was developed by H. TAKETANI, now at the Tokyo Institute of Technology. The other way is vacuum evaporation method. When backing glass is coated with thin film of poly-styrene, or soaked beforehand in dilute solution of KOH, the carbon film is easily stripped off in benzen or in water.

F: Thin film of Teflon (or Japanese commercial name, Daiflon) is used as F target. Teflon film is made by the following procedure.

Aqueous dispersion of Daiflon powder are coated on Ta plate then dried and heated to a temperature where the linkage of Daiflon powder begins, and then the Daiflon film is stripped off from Ta plate in water.

Na: Thin layer of Na_2CO_3 powder was used as Na target. Na_2CO_3 powder was sedimented in alcohol or in water on a mylar film.

Mg: Natural Mg foil was got by vacuum evaporation method. When separated isotopes were needed, Au foil was used as a backing plate, and the Mg isotopes separated by Kyoto University mass separator was attached onto this backing foil.

Si: In the early stage of experiments, thin film of SiO_2 made by blown up method was used. Recently, silicon thin film could be produced by evaporation method in a apparatus designed by UEMURA.

S: SH_2 gas was used as a S target. Inner surface of the gas target vessel and the pipings of the gas target were coated with melamin varnish to prevent from corrosion of metals by SH_2 gas.

P: Thin layer of red phosphorous powder was got by sedimentation method. As the dispersion medium, ethyl alcohol was used. Water was not suitable.

Cl: Chlorine gas was used as Cl_2 gas target. Cautions were needed to prevent from corrosion of metallic vessel of the gas target.

K: Thin layer of K_2CO_3 powder sedimented on a mylar film was used as a K target.

Ar, Ti, Co, Cu, Ag, Cd, Sn and Au: Explanations are omitted.

Ni: Thin film of Ni metal was obtained by electroplating on a stainless steel. The foil can be stripped off from the base plate mechanically.

4. RESEARCH IN NUCLEAR PHYSICS

As was mentioned in section 1, experimental research of nuclear physics began since 1960. Here we survey the problems and results on nuclear physics research taken up in our laboratory until now.

There are two main streams of research. One is concerned with the excitation of nuclei by the inelastic scattering of charged particles and the other with the problems of rearrangement nuclear reaction. In most cases, nuclides investigated are limited within light and medium weight nuclei, and among these, light nuclei were studied by the members of the Kéage Laboratory, and medium weight ones by the members of the Department of Physics.

In the following paragraphs, researches in nuclear physics are summarized with respect to each problem, and are not described in chronological order.

4-1. Elastic Scattering of Protons

The Kyoto University Cyclotron produces 7.5 MeV protons. The proton energy can be varied if the position of the shorting condenser is changed, but until now this method has not been used. Contrarily, stacked foils are inserted at the focal point of the quadrupole magnet, and the proton energy is degraded down to 6 MeV by changing the thickness of the foils. The stacked foil method is used in cases of protons and alpha particles, but is not used in the case of deuterons because of the high level back ground produced by the foils.

In the proton energy range from 6 to 7.5 MeV, the energy dependence of elastic scattering from light nuclei was investigated. Target nuclei are:

Be^9 : [61-7], [63-5],
B^{11} : (96.7% enriched) [62-1], [63-5], [65-3],
Mg^{25}: (96% enriched) [65-3],
Al^{27} : [62-1], [63-5], [65-3],
P^{31} : [62-1], [65-3],
Cl : (natural abundance) [65-3],
Co^{59} : [62-1],
Cu : (natural abundance) [62-1].

Odd mass number nuclei were the main subject of the investigation. In cases of light even nuclei, as is well known, the elastic scattering of protons are violently energy dependent when the incident proton energy is below 10 MeV, but the elastic scattering of protons from odd mass nuclei are relatively energy independent in the energy range studied as seen in Fig. 4-1. The main reason of this difference was attributed to the difference of excitation energy of compound system and the elastic scattering of protons from odd-A nucleus seems to be essentially caused by some type of optical potential, and the contribution from the compound elastic process is rather small. (see ref. [62-1]).

4-2. Inelastic Scattering of Protons

Excitation of Be^9, B^{11}, C^{13}, F^{19}, Mg^{25}, Al^{27}, P^{31} and Cl^{35} nuclei have been studied

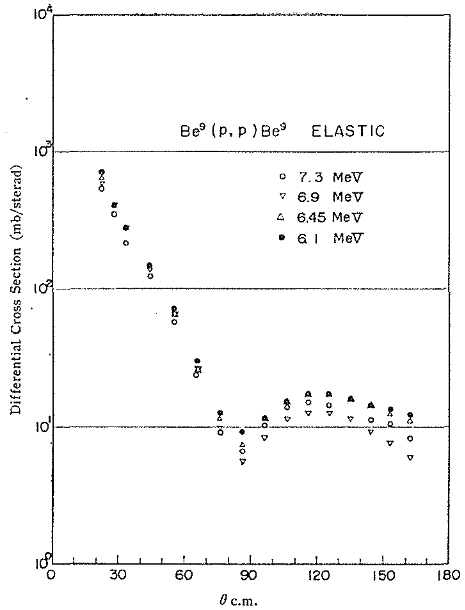

(a)

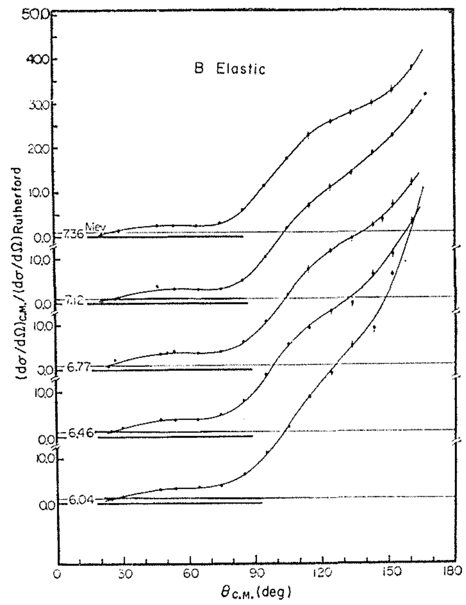

(b)

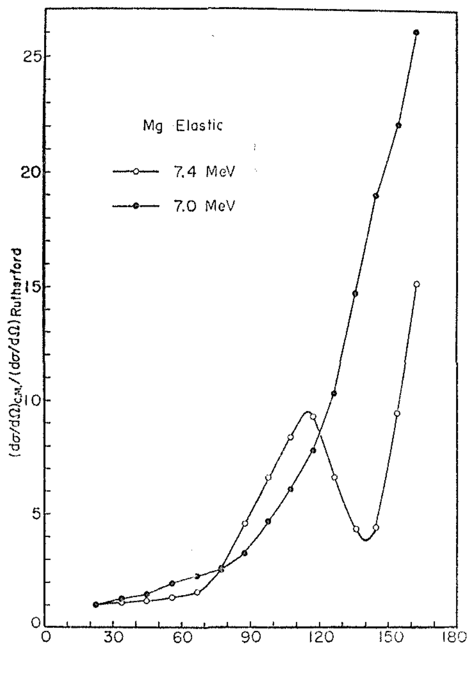

$Al^{27}(p, p_4')\ Al^{27*}$
Q = −2.731 MeV.

(c)

Fig. 4-1.

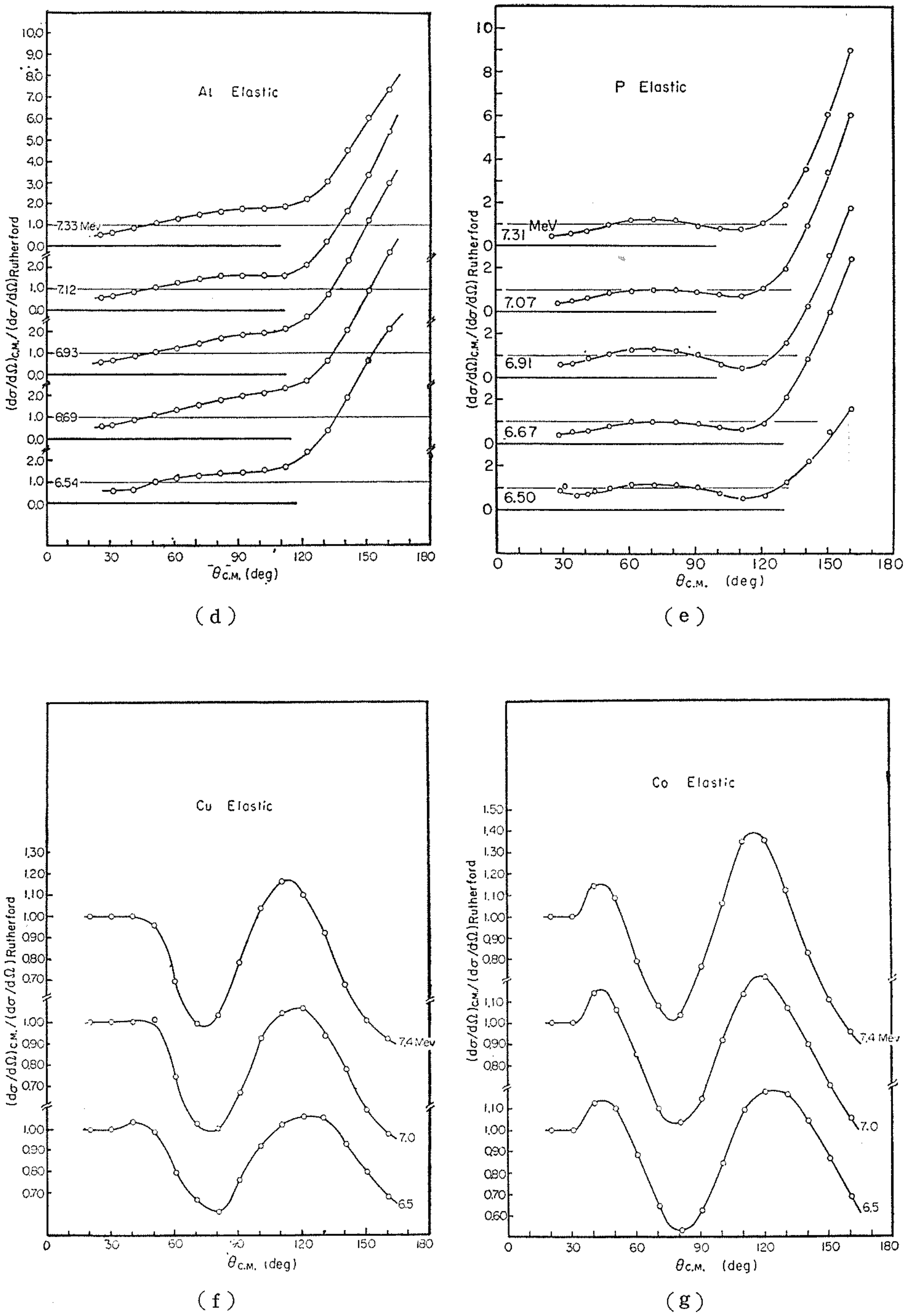

Fig. 4-1. Angular distributions of protons elastically scatterred from several elements. (a) Be^9, (b) B^{11}, (c) Mg, (d) Al, (e) P, (f) Co, and (g) Cu. Energies cited in the figures are incident proton energy in the laboratory system.

with the inelastic scattering of about 7.5 MeV protons. Levels investigated are the following:

Be^9 : 1st, 2nd and 3rd [61-7]
B^{11} : 1st [61-4] [63-5] [65-3]
C^{15} : 1st, 2nd and 3rd [65-3]
F^{17} : ground+1st+2nd, 3rd+4th+5th, 6th [61-4] [65-3]
Mg^{25}: 1st, 2nd, 3rd, 4th, 5th, 6+7th, 8+9th [64-1] [65-3]
Al^{27} : 1st+2nd, 3rd, 4th, 5+6th, 7th [61-7] [63-5] [64-1] [65-3] [65-8]
P^{31} : 1st, 2nd [61-7] [63-5] [65-3]
Cl^{35} : 1st [65-3].

Among these nuclei, excitations of Be^9, B^{11}, Al^{27} and P^{31} have also been investigated with 8 to 14 MeV protons, using a cyclotron of the Institute for Nuclear Study, University of Tokyo. [63-5].

Problems of interest taken by the members in our laboratory have been:

1) Whether collective level excitation is enhanced in light nuclei as well as in heavy nuclei or not.

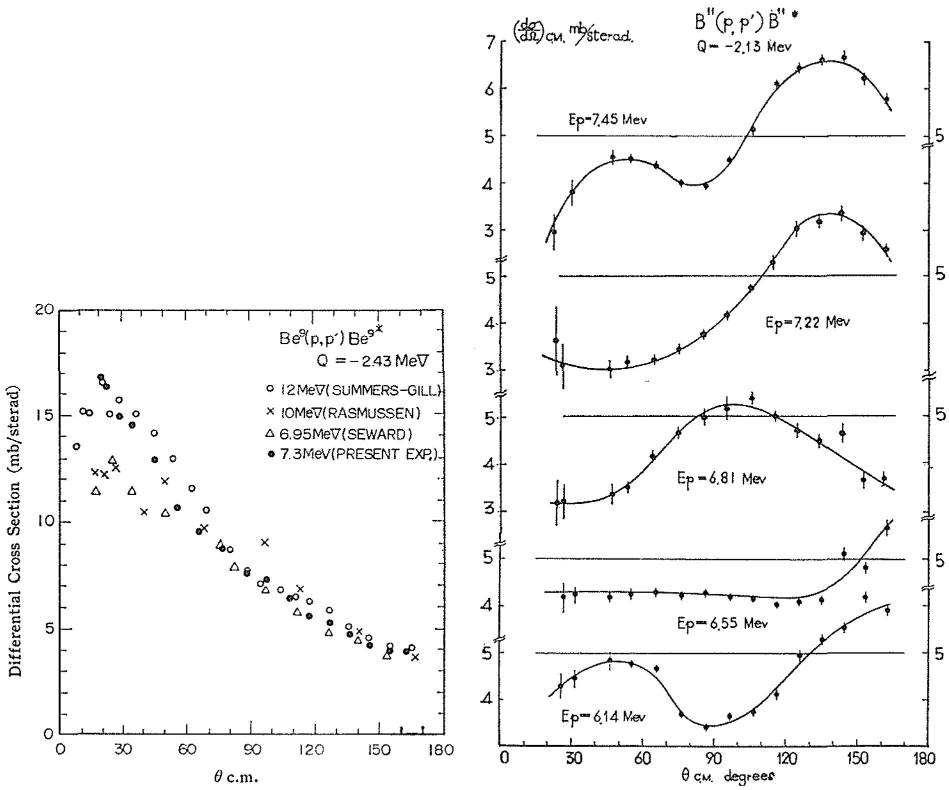

(a) (b)

Fig. 4-2-1.

2) Relation between the relative intensity of scattered protons from different levels and the nuclear structure.

3) How occurs mixing of the excitation mode of two extreme cases; direct process and compound nuclear reaction process.

Angular distributions of inelastically scattered protons were studied with changing the incident proton energy, and the results obtained were discussed by the authors of references as follows.

1) The energy dependence of the (p,p′) scattering from odd-mass number nuclei is not so strong as of the (p,p′) scattering from even-even nuclei in the energy range studied.

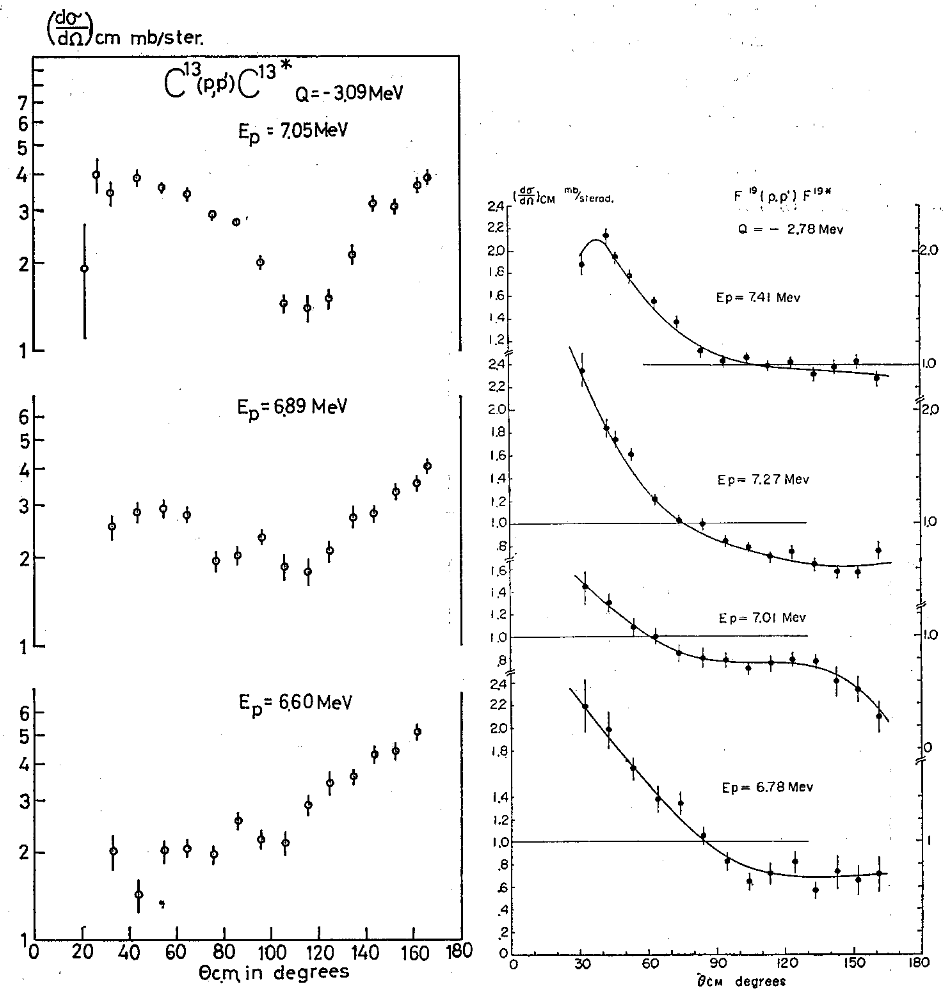

(c) (d)

Fig. 4-2-1. Angular distributions of protons scattered inelastically from several odd-A elements. (a) Be^9, 2.43 MeV state. (b) B^{11}, 2.13 MeV state. (c) C^{13}, 3.09 MeV state and (d) F^{19}, 2.78 MeV state.

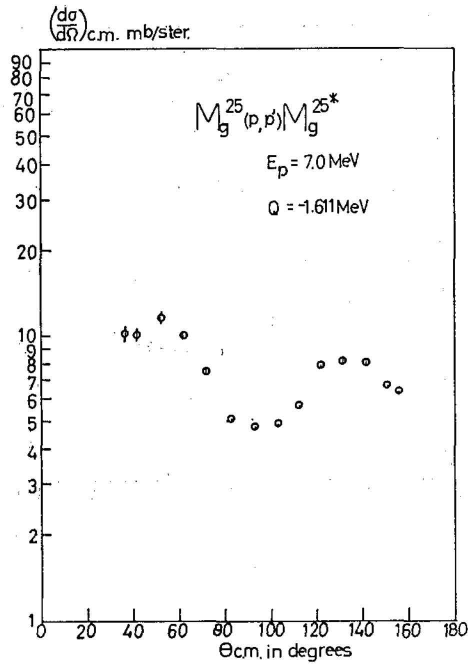

(a)

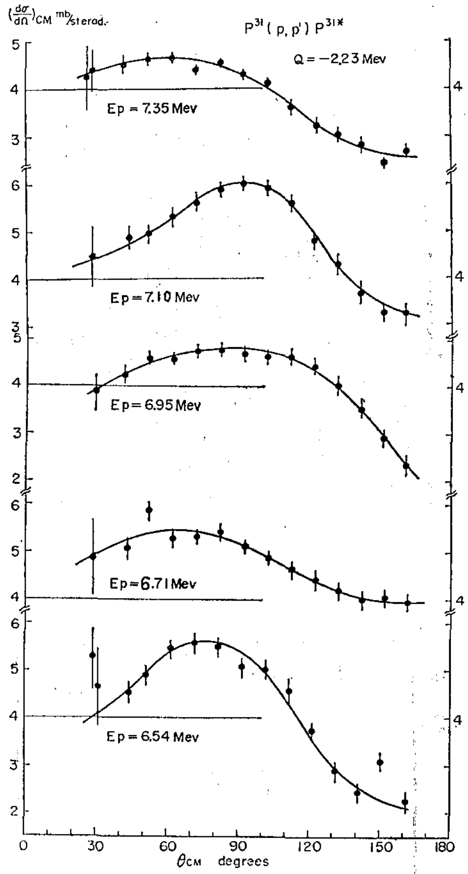

(b)

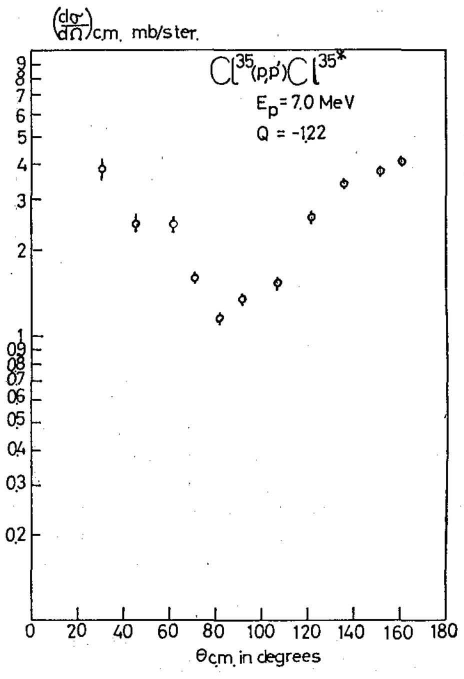

(c)

Fig. 4-2-2. Continuation of the preceeding figure. (a), Mg^{25}, 1.61 MeV state. (b), P^{31}, 2.23 MeV state and (c), Cl^{35}, 1.27 MeV state.

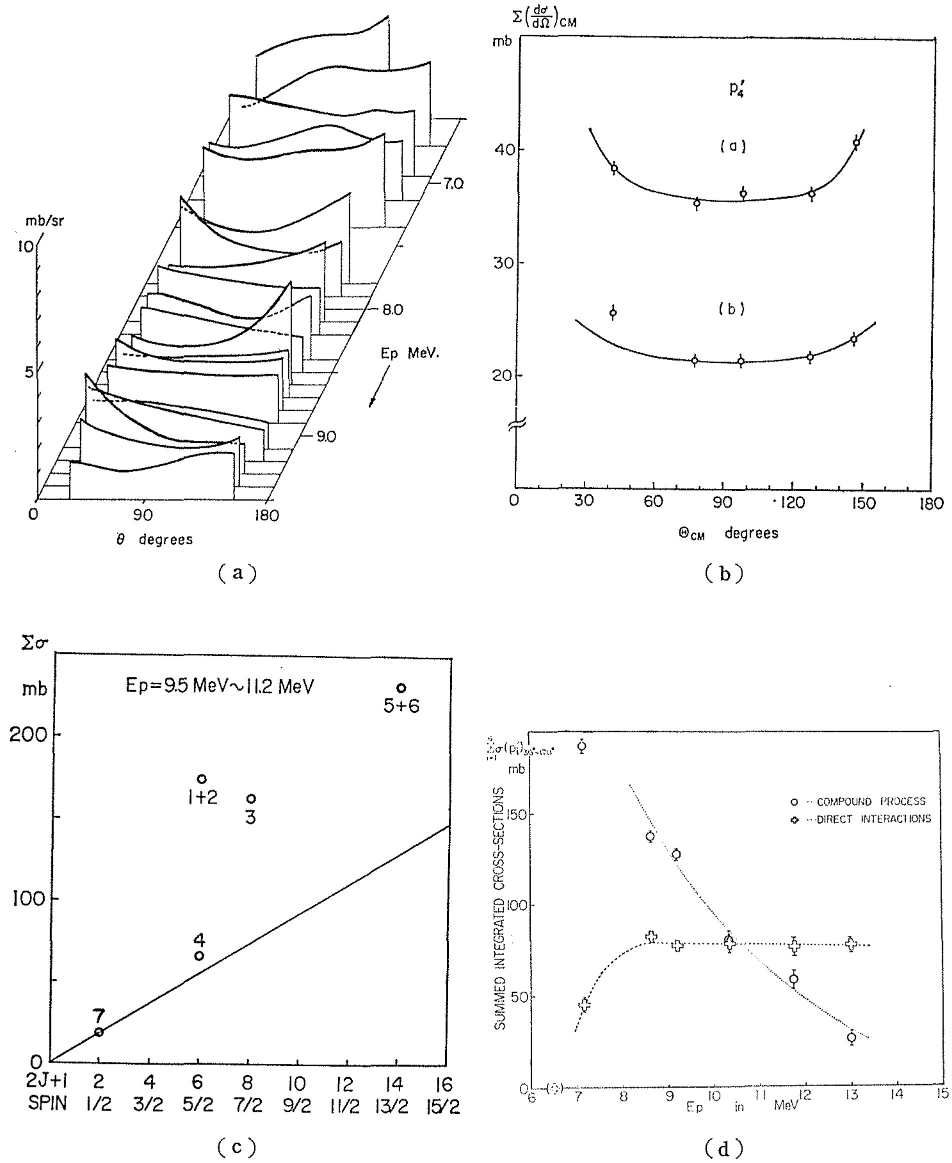

Fig. 4-2-3. Inelastic scattering of protons from 6 to 14 MeV by Al^{27}. (a) Energy dependence of angular distributions of protons (p_4') inelastically scattered from Al^{27}, $Q=-2.731$ MeV. (b) summed angular distributions of p_4'. Symbol (a) in the figure shows the results in the incident proton energy from 6 to 6.9 MeV. Symbol (b) shows the results from 8.5 to 11.2 MeV. Solid curves in the figure are 90° symmetric curves arbitrarily drawn. (c) integrated cross sections of proton groups inelastically scattered from Al^{27} as a function of $2J+1$. The line from the origin is a border line proportional to $2J+1$, below this line the yield is considered to be due to compound nuclear process. (d), estimated direct- and compound-reaction. The differential cross sections were integrated over 30° to 170°C. M., and summed up from the first to sixth levels. The incident energy was an averaged one over some suitable range and represented in abscissa. The low energy side of the graph (≤ 8 MeV) has some ambiguity.

2) The mode of collective state excitation shows resemblances to that with inelastic scattering of alpha particles.

3) Nilsson model of deformed nucleus can give fairly good explanation of the excitation of odd mass number nuclei.

4) In the inelastic scattering of 6∼7.5 MeV protons, the formation of compound nucleus plays an important role, and the rate of mixing of compound process and direct process varies from nucleus to nucleus according to the structure of target nuclei, character of the levels, and the existance of other reaction channels than (p,p′) scattering.

The most thorough investigation of the elastic and inelastic scattering of protons is described in ref. [65-8]. Kokame *et al.* performed the experiment on the proton scattering from Al^{27} in the energy range from 6 to 14 MeV. They analyzed the results comparing with the Ericson's fluctuation theory, $2J+1$ rule and compound nuclear theory, and estimated the mixing of C. N. and D. I. processes.

Examples of the inelastic scattering of protons are cited in the figures.

4-3. Elastic and Inelastic Scattering of Polarized Protons

Utilizing p-α scattering, one can get a beam of polarized protons. An experiment was performed in our laboratory to study the asymmetry of the scattering of polarized protons by Be and Al. [65-1]. The apparatus is shown in Fig. 4-3-1, and the results obtained are shown in Fig. 4-3-2. Polarized proton beam was obtained from recoiled protons by 28.5 MeV alpha particles at 50° and 25° in the laboratory system. Their energies were 7.0 MeV and 12.3 MeV respectively.

From these figures, it may be seen that the asymmetry of the elastic scattering of polarized protons is rather energy independent. The author of ref. [65-1] discusses further, the excitation of Be^9 may be explained when the structure of Be^9 is assumed to be two alpha particles in a core and an outer neutron.

4-4. Elastic and Inelastic Scattering of Deuterons

The study of elastic and inelastic scattering of deuterons began rather recently. Nuclei picked up as targets of deuteron beam were, deuterons, Be^9, C^{12}, N^{14} and O^{16}. The experimental results are not yet published, so here we give a brief introduction.

Deuteron-deuteron elastic scattering is interesting from the standpoint of obtaining interaction potential. The experimental result is shown in Fig. 4-4-1. The interference between the Coulomb force and the nuclear force is not observed in the d-d scattering in the angular range thus far investigated.

One more thing to be noticed is the fact that in the d-d scattering elastic channel and the break up channel are almost equally opened. Detailed analysis of these phenomena by Hidehiko Itoh are now in progress and will appear soon.

Elastic and inelastic scattering of deuterons from Be^9, C^{12}, N^{14} and O^{16}, were

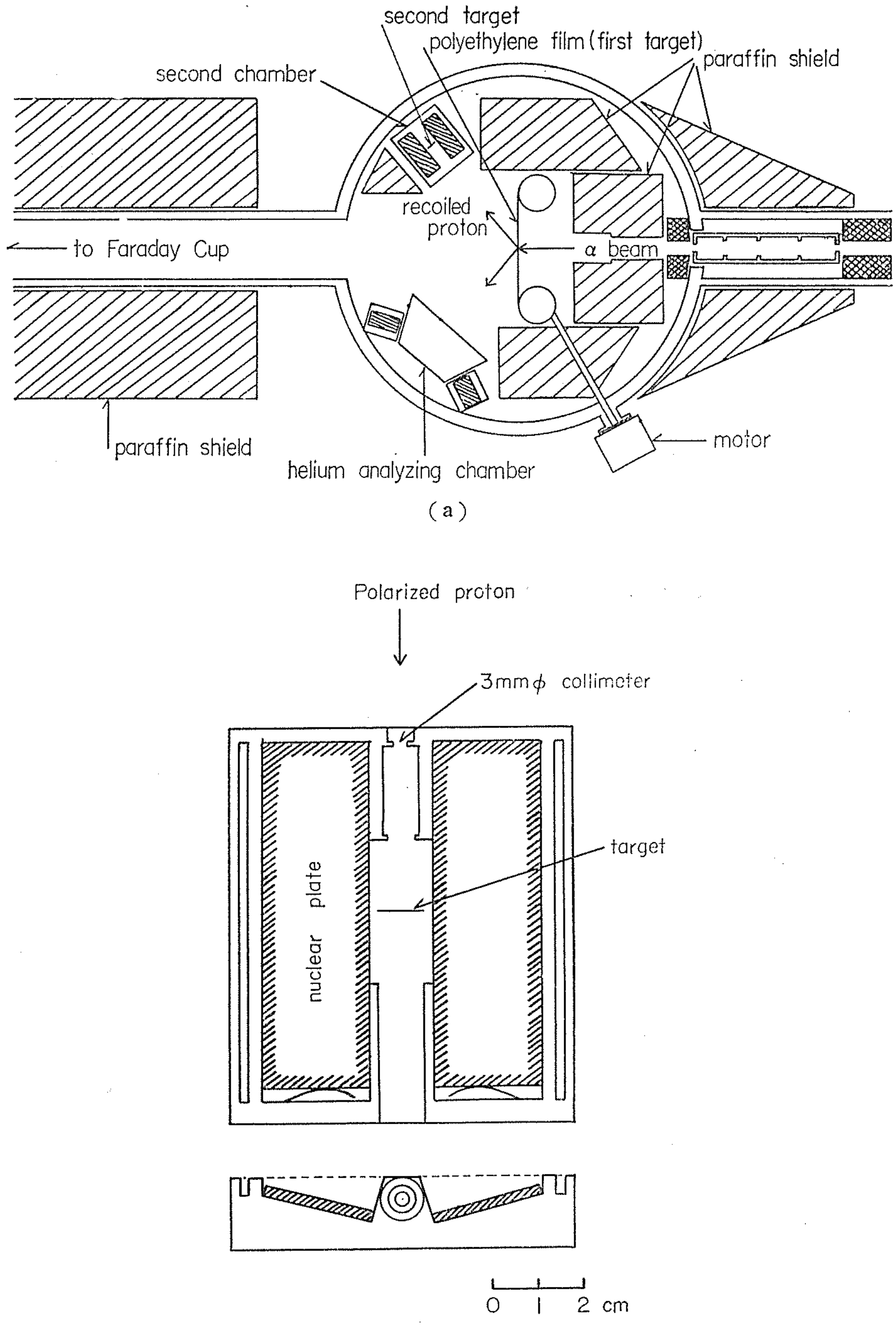

Fig. 4-3-1. Schematic drawings of the experiment on the scattering of polarized protons. (a), experimental set up and (b), details of the second scattering chamber.

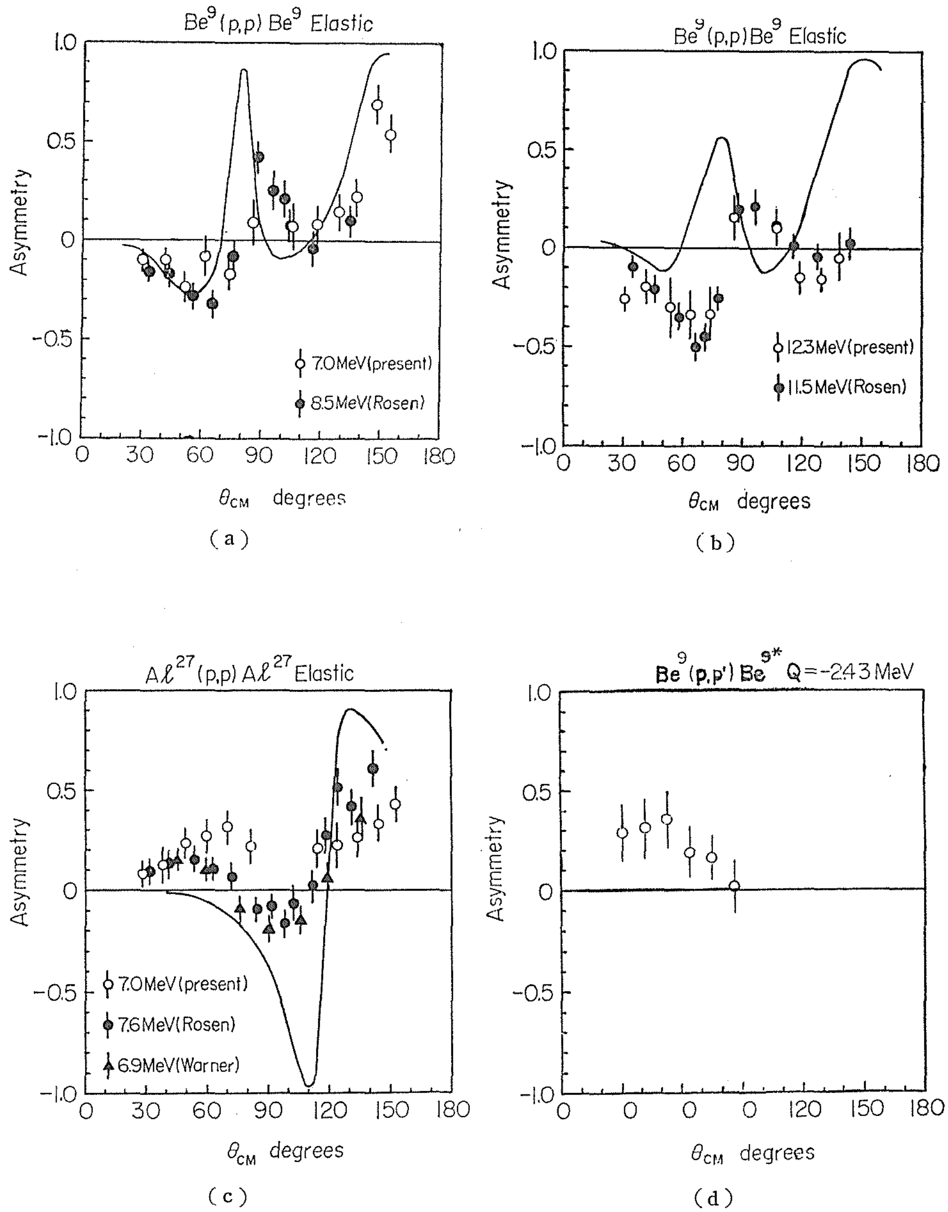

Fig. 4-3-2. Angular dependence of the polarization in the elastic and inelastic scattering of protons by Al^{27} and Be^9. (a) from Be^9, E_p=12.3 MeV. Solid curve is after Rosen. (c), from Al^{27}, E_p= 7.0 MeV. Solid curve is after Rosen. (d), asymmetry of the inelastically scattered protons by Be^9. The Q-value is −2.43 MeV and the E_p= 7.0 MeV.

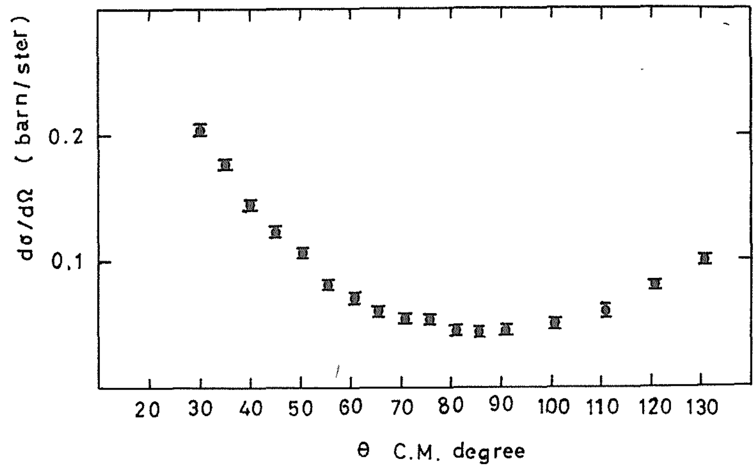

Fig. 4-4-1. Differential cross sections of d-d elastic scattering at 14.11 MeV.

studied by Dai-Ca NGUYEN. Part of the results are shown in Fig. 4-4-2. In general, elastic scattering of deuterons are fairly well interpreted by optical model analysis. But the mode of nuclear excitation by deuteron inelastic scattering contains some difference from that of protons or alpha particles. These facts may be caused by the spreading of the deuteron wave, the difference of transparency of nucleus for protons, deuterons and alpha particles, and the difference of particle width in nuclei among protons, deuterons and alpha particles. Detailed discussion will appear soon.

4-5. Elastic Scattering of Alpha Particles

Elastic scattering of alpha particles from various elements such as He^{4}, Be^{9}, B^{11}, C^{12}, C^{13}, O^{16}, Ne^{20}, Mg^{24}, Al^{27}, Si^{28}, P^{31}, S^{32}, Ar^{40}, Ti^{48}, Co^{59}, Ni^{58}, Ni^{60}, Cu, Ag, Cd and Sn have been investigated intensively. The α-α scattering experiment was performed mainly to estimate the precise phase shift of G-wave so as to obtain informations on α-α potential. Regarding the scattering experiments with Be^{9} to Ar^{40}, there were two different aims. One was to clarify the characteristic behavior of the elastic scattering of alpha particles from odd mass nuclei, and the other was to ascertain the character of even-even or, so to say, 4n type nuclei. For Ti^{48} and heavier, the experiments were done by the members of the Department of Physics, and the aim of the experiments was to obtain most reliable parameters of optical potential for 28 MeV alpha particles.

References relating to each target material are as follows.

He^{4} : [61-8]
Be^{9} : [64-8]
B^{11} : [65-4]
C^{12} : [65-4]

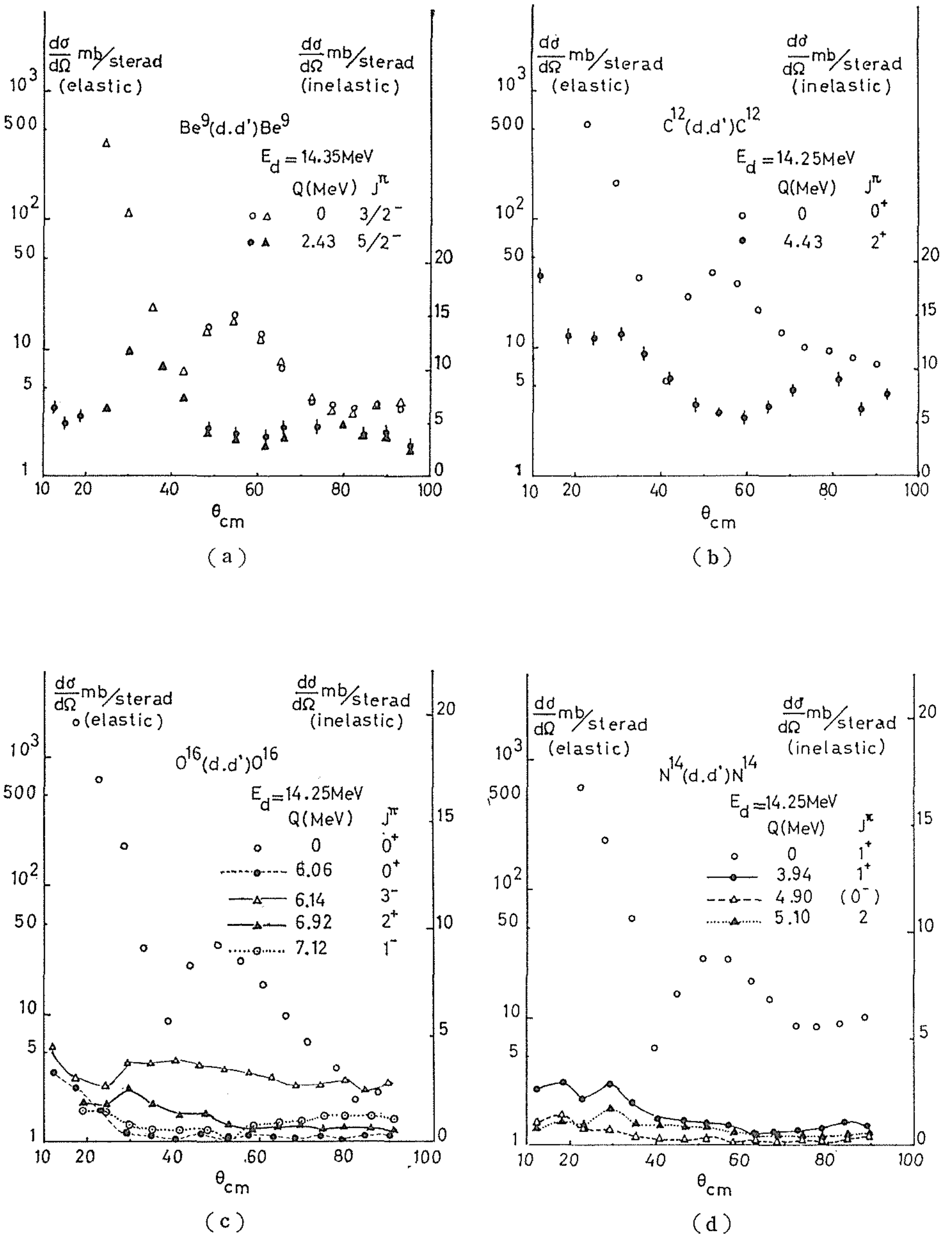

Fig. 4-4-2. Angular distributions of deuterons elastically and inelastically scattered from several elements. (a) from Be^9. Open and solid circles are data obtained with magnetic spectrograph. Open and solid triangles are the data obtained with a solid state detector. (b), from C^{12}. (c), from N^{14} and (d), from O^{16}.

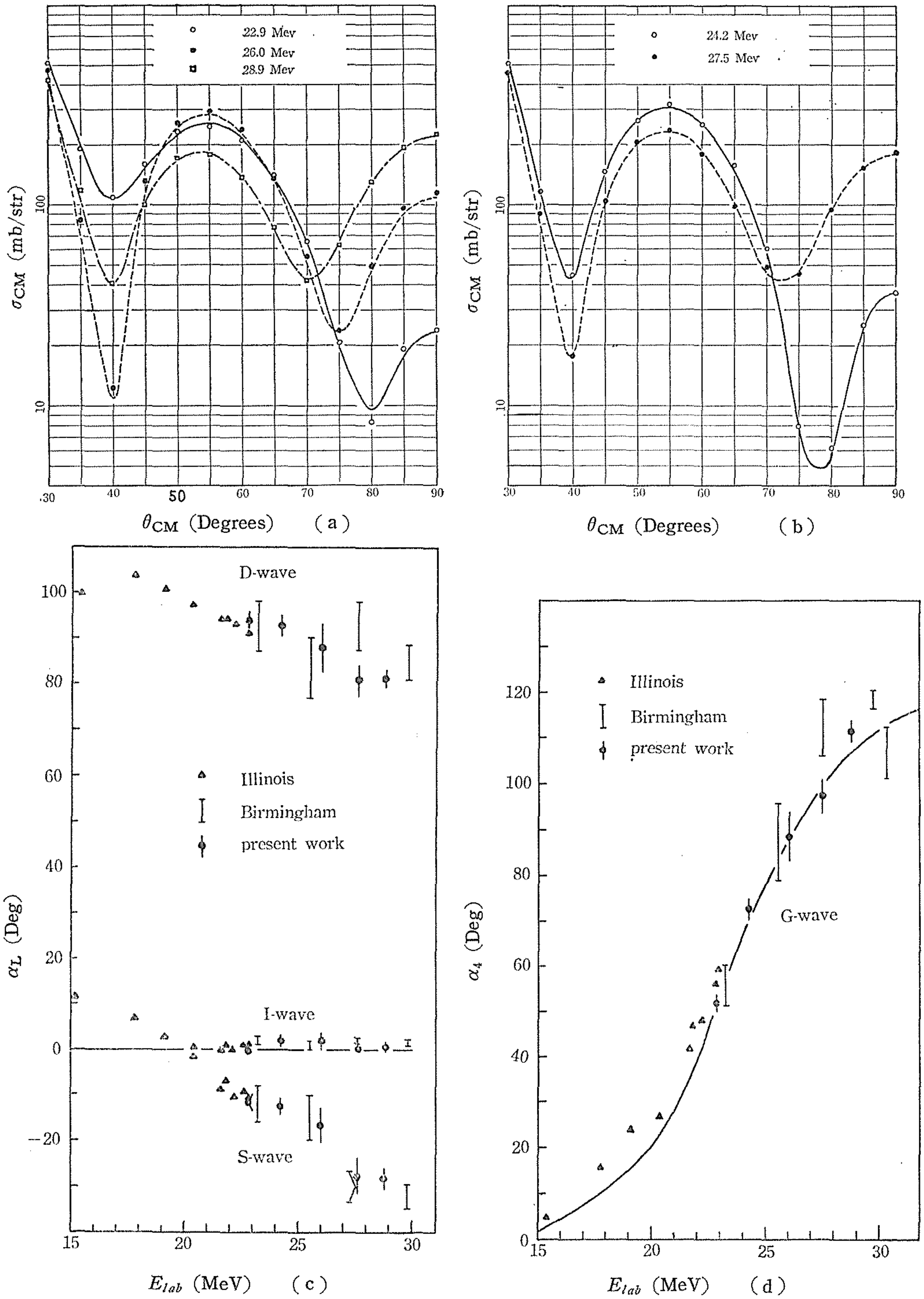

Fig. 4-5-1. Differential cross sections and phase shifts of alpha-alpha scattering at several incident energies. (a) at 22.9, 26.0 and 28.9 MeV. (b), at 24.2 and 27.5 MeV. Curves in (a) and (b) show the computed ones with the best phase shifts obtained from this work. (c) shows the experimentally obtained S-, D- and I-wave phase shifts, and (d), the G-wave phase shifts obtained from the single-level dispersion theory with a hard-core radius of $3{,}5\times10^{-13}$ cm, a reduced width of 3.5 MeV and a resonance energy of 12,5 MeV,

Table 4-5-1 (after Kozo MIYAKE)
Differential cross sections for alpha-alpha scattering.

$E_{lab}=22.9\pm0.3$ MeV			$E_{lab}=24.2\pm0.3$ MeV		
$\theta_{C.M.}$ degree	$\frac{d\sigma}{d\Omega}_{meas.}$ * mb/sterad.	$\frac{d\sigma}{d\Omega}_{cal.}$ ** mb/sterad.	$\theta_{C.M.}$ degree	$\frac{d\sigma}{d\Omega}_{meas.}$ * mb/sterad.	$\frac{d\sigma}{d\Omega}_{cal.}$ ** mb/sterad.
30	514.4±12.0	524.0	30	502.0±12.0	505.9
35	189.9± 4.0	193.3	35	115.5± 4.1	107.4
40	107.4± 1.6	107.2	40	44.4± 1.4	44.4
45	158.0± 3.1	156.0	45	145.5± 3.5	145.6
50	234.2± 3.9	228.1	50	261.2± 4.2	268.2
55	246.5± 4.3	253.0	55	314.3± 3.3	307.9
60	210.9± 3.4	214.1	60	249.3± 5.4	255.4
65	145.2± 3.3	138.2	65	157.8± 3.3	152.8
70	63.1± 2.3	64.0	70	57.9± 2.4	57.8
75	20.5± 1.0	19.9	75	7.0± 0.7	8.1
80	7.9± 0.7	9.8	80	6.1± 0.5	5.8
85	19.4± 0.9	17.8	85	25.6± 0.9	25.5
90	23.6± 0.9	23.4	90	35.9± 0.8	36.5
95	18.8± 0.9	17.8	95	24.6± 1.0	25.5
100	8.5± 1.0	9.8	100	6.2± 0.6	5.8
105	20.4± 1.2	19.9	105	8.7± 1.0	8.1
110	68.6± 3.4	64.0	110	61.2± 2.6	57.8
115	137.1± 5.1	138.2	115	153.0± 4.4	152.8
Best set of phase shifts. (degree)		$\alpha_0=-11.6\pm1.7$ $\alpha_2=+94.2\pm1.4$ $\alpha_4=+51.7\pm2.0$ $\alpha_6=+\ 0.7\pm0.6$	Best set of phase shifts. (degree)		$\alpha_0=-12.6\pm1.9$ $\alpha_2=+93.0\pm2.3$ $\alpha_4=+72.5\pm2.5$ $\alpha_6=+\ 2.1\pm1.0$

* $\frac{d\sigma}{d\Omega}_{meas.}$ denotes the measured differential cross sections.

** $\frac{d\sigma}{d\Omega}_{cal.}$ denetes the differential crors sections calculated by using the best set of phase shift.

Table 4-5-1. (Continued).

$E_{lab}=26.0\pm0.3$ MeV			$E_{lab}=27.5\pm0.3$ MeV		
$\theta_{C.M.}$ degree	$\frac{d\sigma}{d\Omega}_{meas.}$ * mb/sterad.	$\frac{d\sigma}{d\Omega}_{cal.}$ ** mb/sterad.	$\theta_{C.M.}$ degree	$\frac{d\sigma}{d\Omega}_{meas.}$ * mb/sterad.	$\frac{d\sigma}{d\Omega}_{cal.}$ ** mb/sterad.
30	474.0±13.0	465.7	30	455.0±14.0	462.1
35	83.0± 7.0	67.0	35	88.9± 4.8	87.2
40	12.2± 0.7	10.3	40	17.6± 0.4	17.1
45	130.2± 3.7	123.1	45	102.6± 2.8	101.6
50	250.9± 4.7	244.9	50	203.0± 3.5	199.8
55	290.5± 4.1	287.2	55	235.5± 3.3	229.7
60	236.1± 5.0	234.4	60	179.9± 3.6	182.8
65	132.4± 4.7	135.1	65	99.1± 2.7	102.6
70	54.3± 2.2	51.9	70	48.3± 1.8	46.3
75	23.3± 0.9	23.8	75	44.5± 1.5	46.4
80	49.8± 2.4	48.0	80	93.0± 3.0	94.7
85	96.2± 3.5	89.7	85	156.0± 3.5	152.5
90	113.5± 3.0	109.3	90	179.7± 2.3	177.6
95	91.0± 7.0	89.7	95	147.5± 3.7	152.5
100	48.3± 2.2	48.0	100	94.6± 3.1	94.7
105	24.9± 2.4	23.8	105	46.4± 2.2	46.4
110	55.8± 3.4	51.9	110	49.6± 2.0	46.3
115	139.2± 5.0	135.1	115	95.0± 3.9	94.7
Best set of phase shifts. (degree)		$\alpha_0=-16.5\pm4.2$ $\alpha_2=+88.0\pm6.0$ $\alpha_4=+89.1\pm6.0$ $\alpha_6=+\ 2.4\pm2.0$	Best set of phase shifts. (degree)		$\alpha_0=-28.8\pm4.2$ $\alpha_2=+81.1\pm3.3$ $\alpha_4=+97.7\pm4.5$ $\alpha_6=+\ 0.4\pm1.0$

* $\frac{d\sigma}{d\Omega}_{meas.}$ denotes the measured differential cross sections.

** $\frac{d\sigma}{d\Omega}_{cal.}$ denotes the differential cross sections calculated by using the best set of phase shifts.

Table 4-5-1. (Continued).

$E_{lab}=28.9\pm0.3$ MeV		
$\theta_{C.M.}$ degree	$\frac{d\sigma}{d\Omega}_{meas.}$ * mb/sterad.	$\frac{d\sigma}{d\Omega}_{cal.}$ ** mb/sterad.
30	418.0±13.0	424.2
35	119.9± 5.7	106.3
40	40.7± 0.8	40.8
45	99.6± 2.2	100.2
50	170.4± 1.6	168.8
55	176.9± 2.6	182.4
60	137.0± 2.6	138.0
65	77.7± 1.8	75.5
70	42.2± 1.1	42.9
75	64.0± 1.7	64.1
80	129.3± 2.8	126.9
85	196.6± 4.3	192.2
90	227.4± 4.1	219.6
95	188.4± 4.0	192.2
100	123.1± 4.1	126.9
105	60.3± 1.8	64.1
110	44.5± 1.5	42.9
115	82.4± 2.7	75.5
120	135.4± 3.5	138.0
Best set of phase shifts (degree)	$\alpha_0=-28.2\pm1.4$ $\alpha_2=+81.1\pm1.4$ $\alpha_4=+11.5\pm3.0$ $\alpha_6=+\ 0.4\pm0.6$	

* $\frac{d\sigma}{d\Omega}_{meas.}$ denotes the mseaured differential cross sections.

** $\frac{d\sigma}{d\Omega}_{cal.}$ denotes the differential cross sections calculated by using the best set of phase shifts.

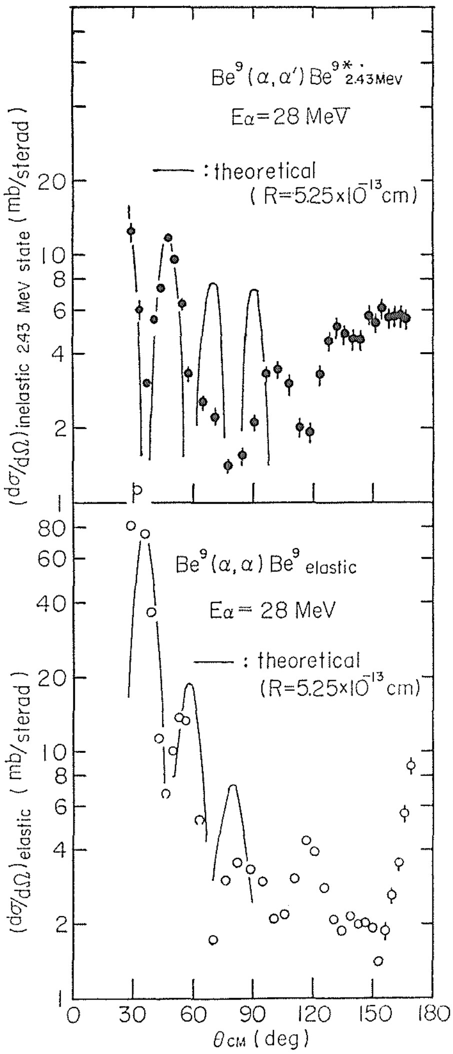

Fig. 4-5-2. Angular distributions of alpha particles elastically and inelastically scattered from Be^9. The solid curve present the theoretical fit with the Blair's formula.

C^{13} : [65-4]
O^{16} : [64-4] [65-4] [65-7]
Ne^{20} : [64-4] [65-4] [65-7]
Mg^{24} : [64-4] [65-4] [65-7]
Al^{27} : [65-2] [65-4]
Si^{28} : [64-4] [65-4] [65-7]
P^{31} : [65-4]
S^{32} : to be published
Ar^{40} : to be published
Ti^{48} : [64-3]
Co^{59} : [64-3]
Ni^{58} : [64-3]
Ni^{60} : [64-3]
Cu : [65-20]
Ag : [65-20]
Cd : [65-20]
Sn : [65-20]

Except the cases of He^4 and Be^9, elastic scattering of alpha particles from other elements closely relate to the inelastic scattering phenomena, so we present here the results of elastic scattering of alpha particles from He^4 and Be^9 only.

The α-α elastic scattering was measured with alpha particles from 22.9 to 28.9 MeV. The phase shift analysis were performed up to L=6. Angular distributions and the best sets of calculated phase shifts are shown in Fig. 4-5-1. The author of ref. [61-8] discusses the results and concludes that the serial levels of Be^8, ground (0^+), 3.1 MeV (2^+) and 12.5 MeV (4^+) states are most likely consist of two alpha particle states. This conclusion is very interesting in relation to the (α, 2α) reaction experiment described later. The numerical values of α-α scattering cross sections are not published until now, so the results are presented here in Table 4-5-1.

Elastic scattering of alpha particles from Be^9 are interesting from the standpoint of alpha clustering in the Be^9 nucleus. The elastic and inelastic scattering angular distributions are shown in Fig. 4-5-2. The reader should pay attention to the sharp rise of cross sections at extremely backward angles. These phenomena seem to be caused by exchange reactions between the incident and the quasi alpha particles in Be^9.

4-6. Inelastic Scattering of Alpha Particles

Levels investigated by means of inelastic scattering of alpha particles from nuclei are the following.

Be^9 : 1st (undistinguished) 2nd [64-8]
B^{11} : 1st, 2nd, 3rd, 4th+5th, 6th [65-4]

C^{12} : 1st. [65-4]
C^{13} : 1st, 2nd+3rd, 4th, 5+6+7th [65-4]
O^{16} : 1st, 2nd, 3rd, 4th, 5th, 6th, 7th, 8th [64-4] [65-4] [65-7]
Ne^{20} : 1st, 2nd, 3rd, 4th, 5th [64-4] [65-4] [65-7]
Mg^{24} : 1st, 2nd, 3rd, 4th, 6th, 6th [64-4] [65-4] [65-7]
Al^{27} : 1st, 2nd, 3rd, 4th, 5th, 6th [64-3] [65-2] [65-4]
Si^{28} : 1st, 2nd, 3rd, 4th, 5th, 6th [64-4] [65-2] [65-4] [65-7]
P^{31} : 1st, 2nd [65-4]
S^{32} : 1st, 4th, 6th (to be published)
Ar^{40} : 1st, 4th (to be published)
Ti^{48} : 1st, 3rd, 5th [64-3] [65-12] [65-20]
Co^{59} : 3rd, 15th [64-3] [65-12]
Ni^{58} : 1st, 4th [64-3] [65-12]
Ni^{60} : 3rd, 5th [64-3] [65-12]
Cu : natural. 1st to 7th. [65-20]
Ag : natural. 2nd to 6th [65-20]
Cd : natural. 1st to 7th [65-20]
Sn : natural. 1st to 5th [65-20]

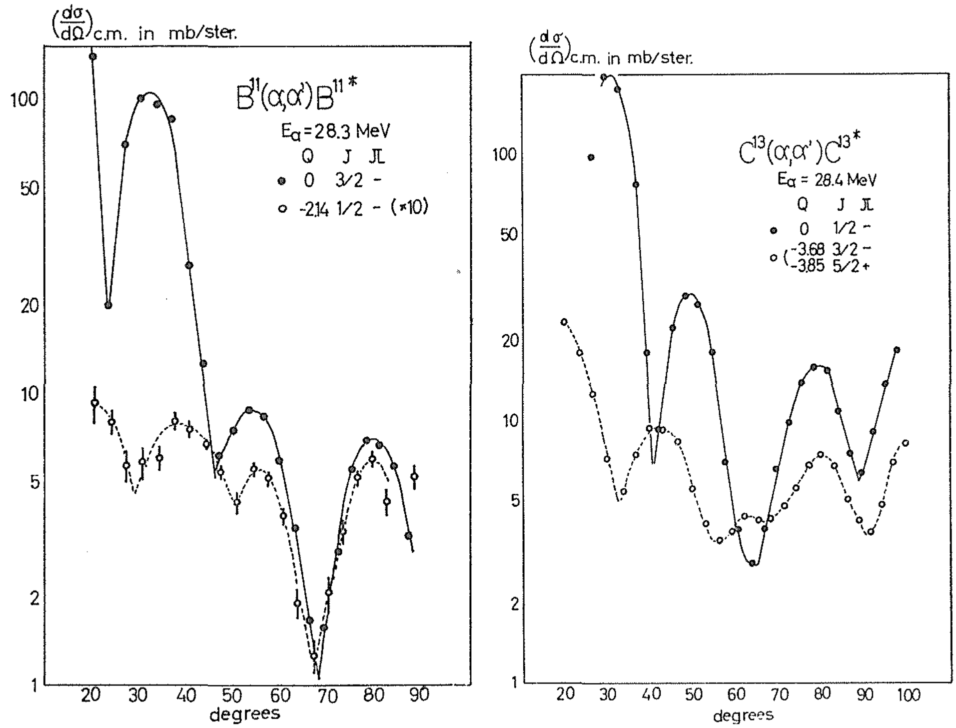

(a) (b)

Fig. 4-6-1.

Angular distributions of elastic and inelastic scatterings of alpha particles from B^{11}, C^{13}, Al^{27} and P^{31} are shown in Fig. 4-6-1. The results of C^{12}, S^{32} and Ar^{40} in Fig. 4-6-2, of O^{16}, Ne^{20}, Mg^{24} and Si^{28} in Fig. 4-6-3 and of Ti^{48}, Co^{59}, Ni^{58} and Ni^{60} in Fig. 4-6-4, and finally from Cu, Ag, Cd and Sn are shown in Fig. 4-6-5. These figures do not cover the whole experimental results, so the reader is requested to refer to each reference.

From these figures, no essential differences are found between inelastic scattering of alpha particles from odd mass nuclei and that from even mass nuclei. Blair's phase rule and the fact that the collective levels of nucleus are preferencially excited by inelastic scattering of alpha particles, hold at least qualitatively throughout the experiments thus far performed. The target nucleus seems to be black or almost

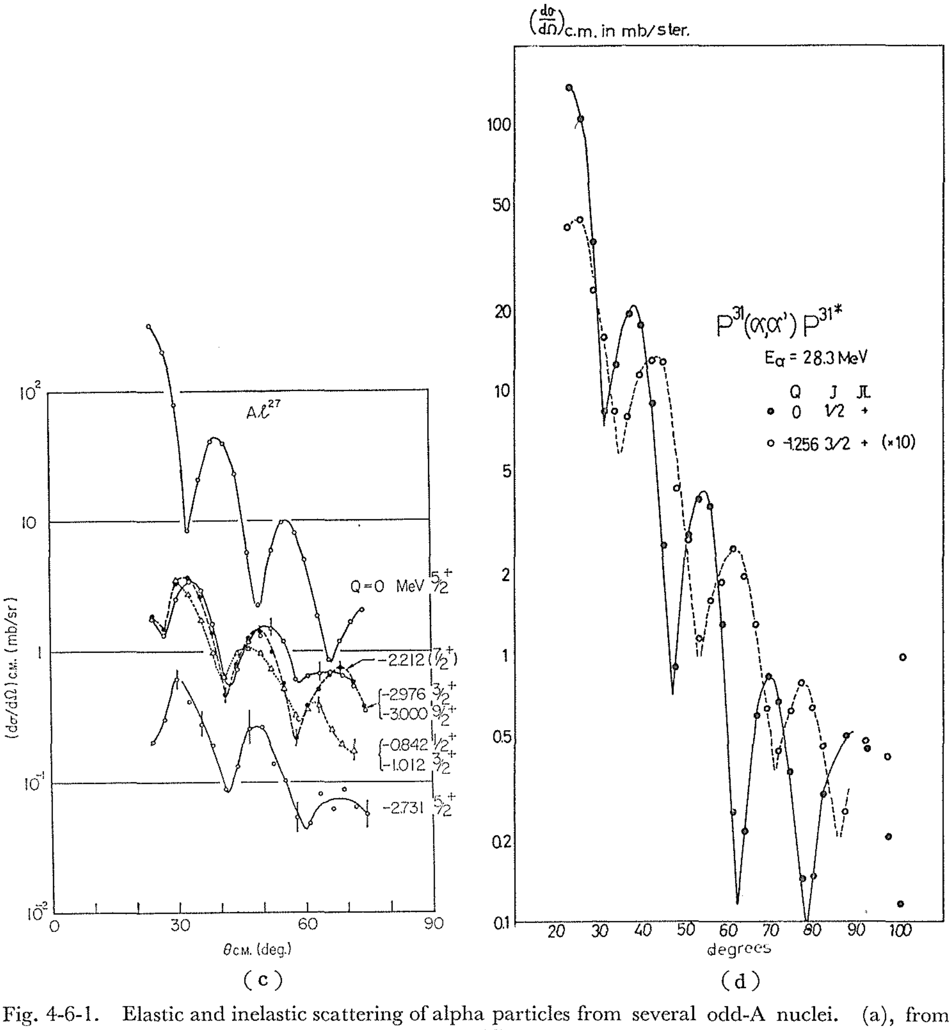

(c) (d)

Fig. 4-6-1. Elastic and inelastic scattering of alpha particles from several odd-A nuclei. (a), from B^{11}, (b), from C^{13}, (d), from Al^{27} and (d), from P^{31},. Solid lines in the figures are the smoothed curves of experimental points.

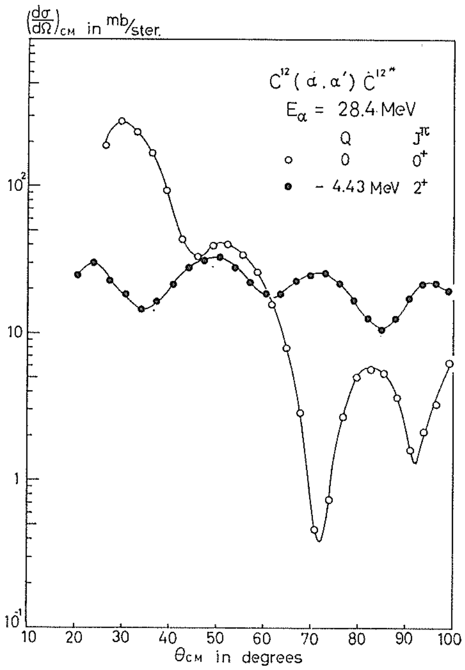

(a)

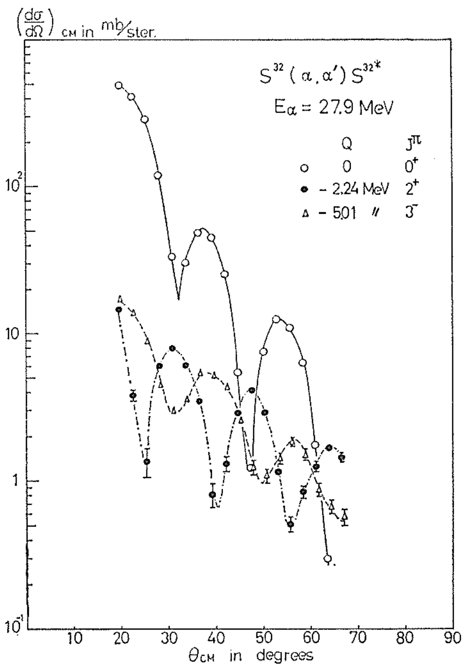

(b)

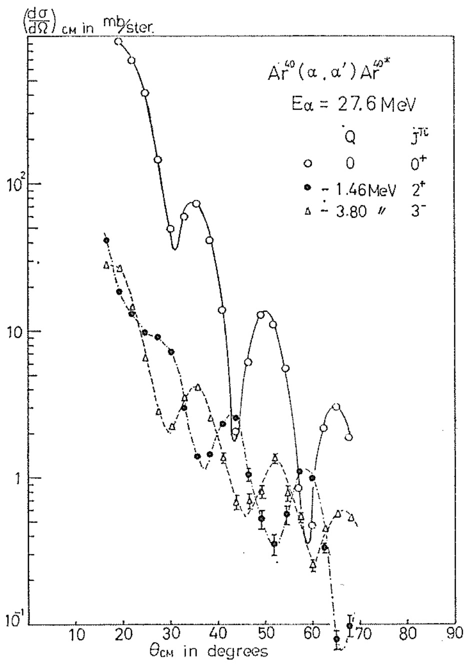

(c)

Fig. 4-6-2. Elastic and inelastic scattering of alpha particles from several even-A nuclei. (a), from C^{12}, (b) from S^{32} and (c), from Ar^{40}. Solid lines are the smoothed curves of the experimental points.

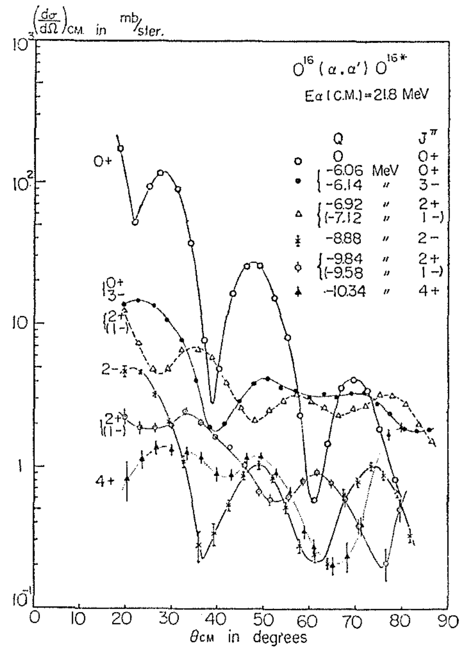
$\left(\frac{d\sigma}{d\Omega}\right)_{CM}$ in mb/ster.
$O^{16}(\alpha,\alpha')O^{16*}$
Eα (C.M.) = 21.8 MeV
Q J^π
0 0+
-6.06 MeV 0+
-6.14 " 3-
-6.92 " 2+
(-7.12 " 1-)
-8.88 " 2-
-9.84 " 2+
(-9.58 " 1-)
-10.34 " 4+
θcm in degrees

(a)

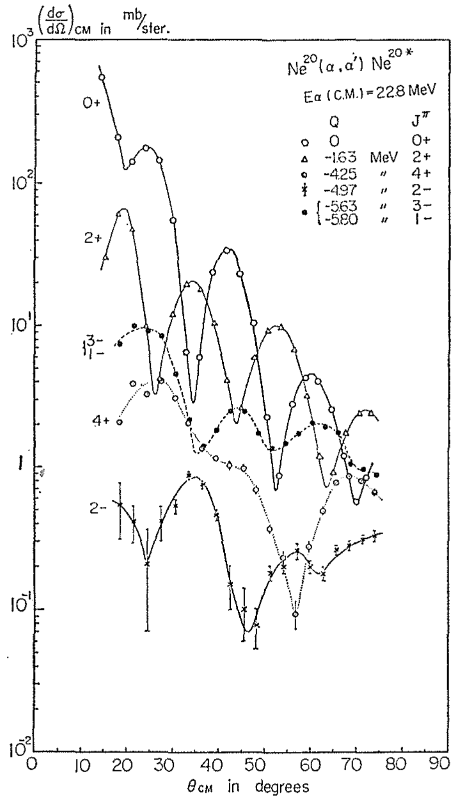
$\left(\frac{d\sigma}{d\Omega}\right)_{CM}$ in mb/ster.
$Ne^{20}(\alpha,\alpha')Ne^{20*}$
Eα (C.M.) = 22.8 MeV
Q J^π
0 0+
-1.63 MeV 2+
-4.25 " 4+
-4.97 " 2-
-5.63 " 3-
-5.80 " 1-
θcm in degrees

(b)

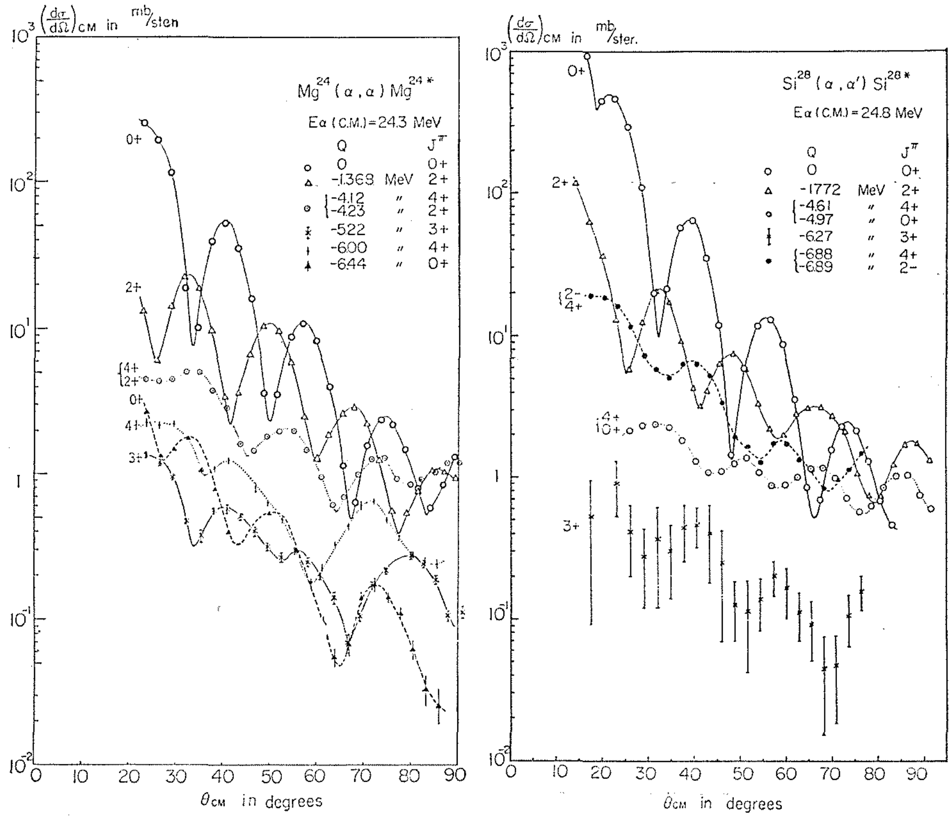

(c) (d)

Fig. 4-6-3. Continuation of the preceding figure. (a), from O^{16}, (b), from Ne^{20}, (c), from Mg^{24}. and (d), from Si^{28}. The solid lines are the smoothed curves of the experimental points.

black for incident alpha particles. The individual character of the target nucleus seems to play no important role. Especially, DWBA analysis of scattering of alpha particles from medium weight nuclei gives good agreement with experiments. [65-12]. But, when one thinks of it, it is interesting that light nuclei thus far investigated behave as a system of correlated many particle assembly as heavy nuclei do. Light nucleus also behaves as a source of optical potential and resembles collective excitation for the incident alpha particles.

Some topics must be added about inelastic scattering of alpha particles, these are, the core excitation in light nuclei and unnatural parity level excitation. The former problem was studied in the case of Al^{27}. [65-2]. The latter problem was studied in the cases of O^{16}, Ne^{30}, Mg^{24} and Si^{28}. [64-4].

Kokame *et al.* studied the inelastic scattering of alpha particles from Al^{27} up to 6th excited states and compared the results with that of the inelastic scattering from the first 1.77 MeV level of Si^{28}, and concluded that the inelastic scattering from

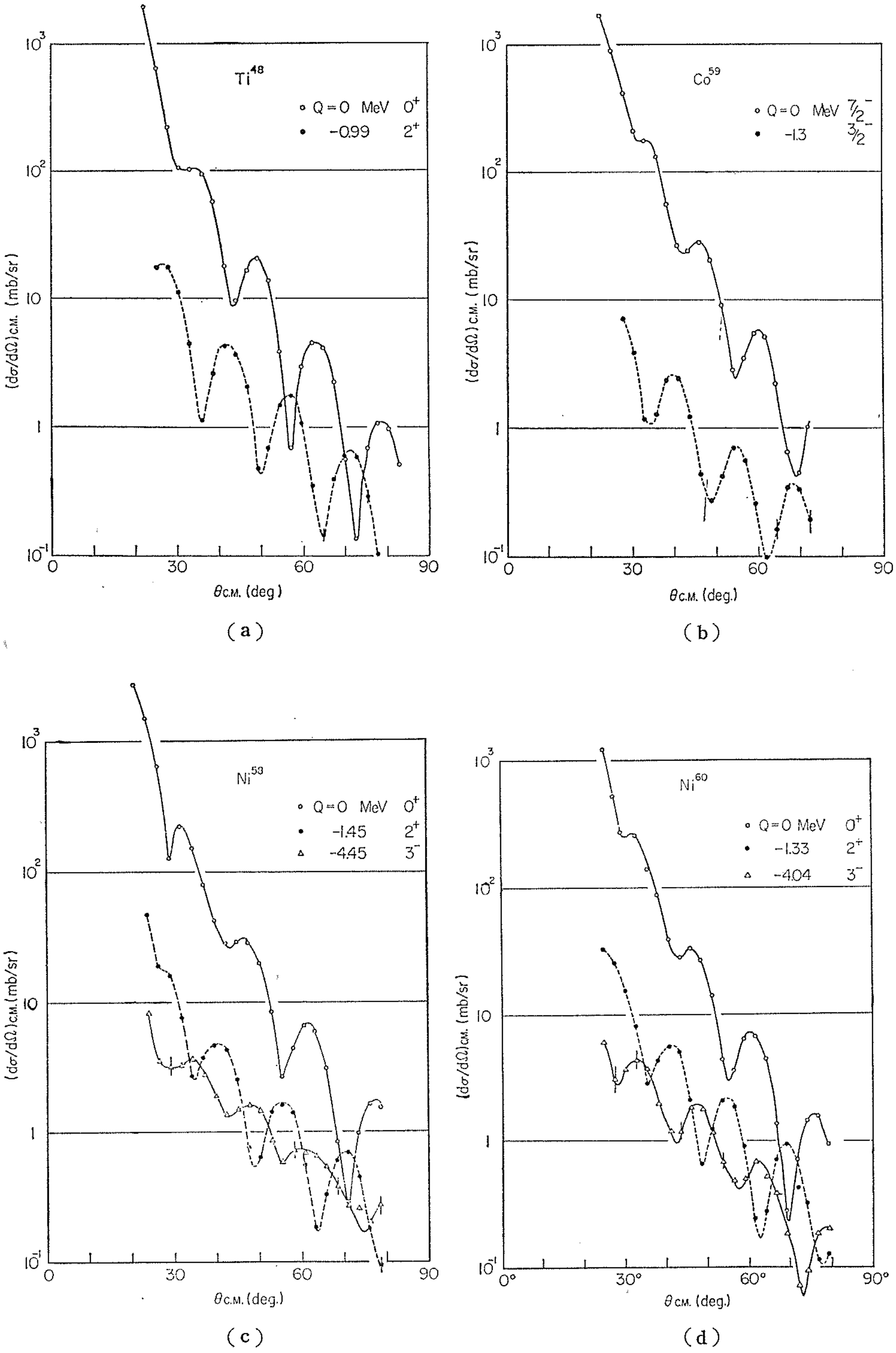

Fig. 4-6-4. Angular distributions of alpha particles scattered elastically and inelastically from several medium weight nuclei. (a), from Ti^{48}, (b) from Co^{59}, (c), from Ni^{56} and (d), from Ni^{60}. Solid or dotted lines are the smoothed curves of the experimental points.

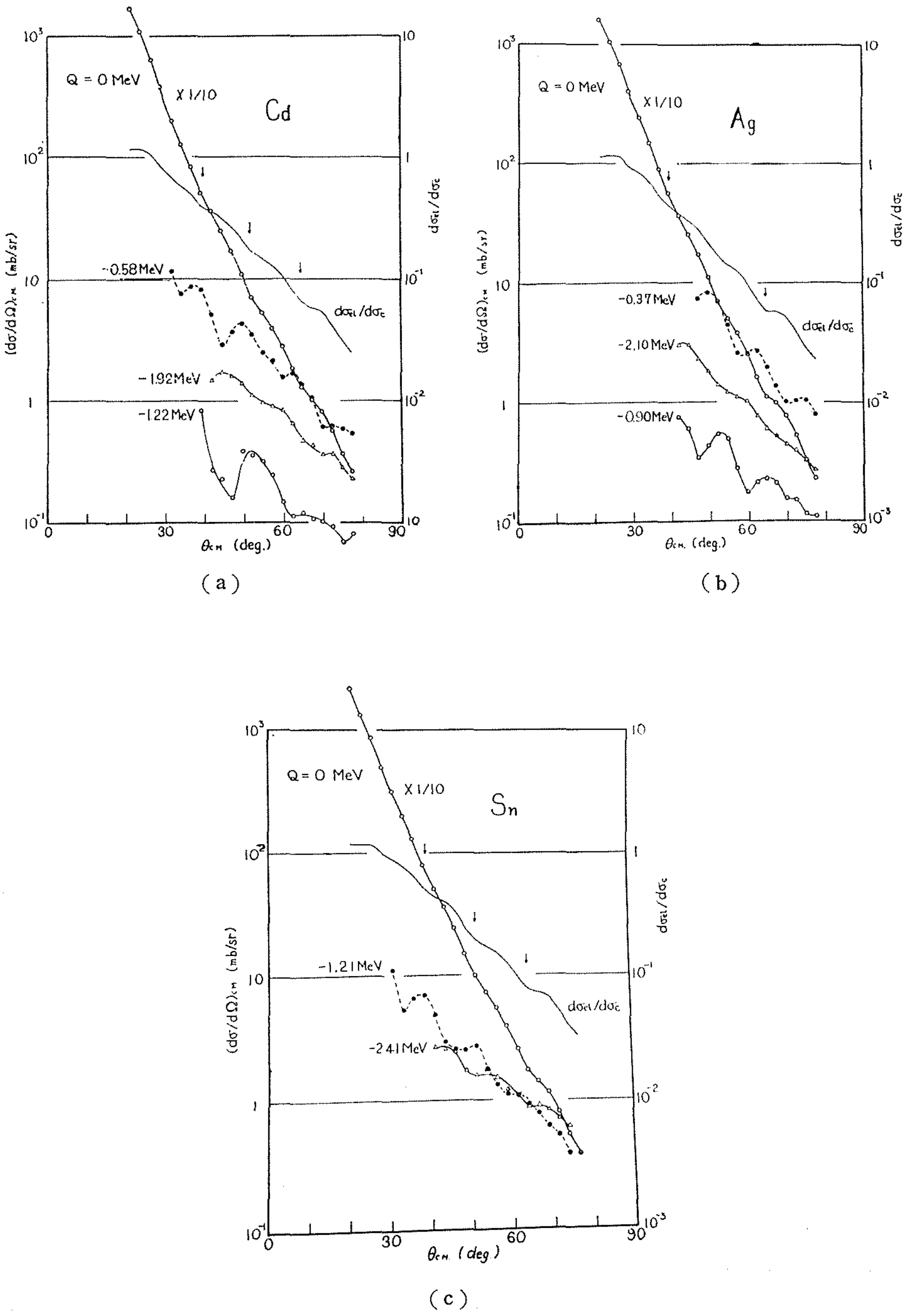

Fig. 4-6-5. Continuation of the preceding figure. (a) from Cd, (b), from Ag and (c), from Sn. *Solid or dotted lines are the smoothed curves of the experimental points.*

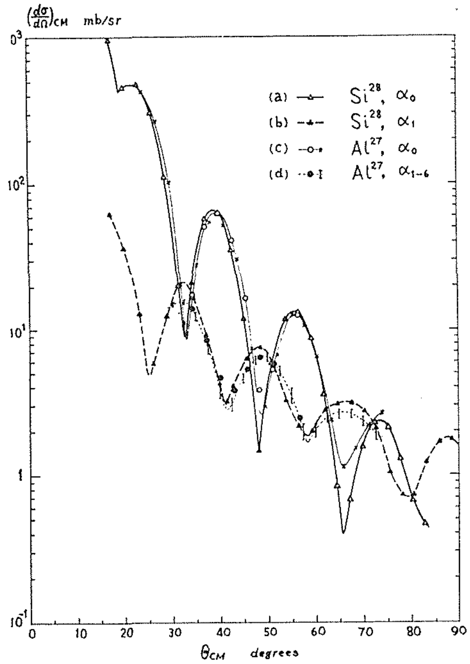

Fig. 4-6-6. Angular distributions of alpha particles showing resemblances between Al^{27} and Si^{28}. $E_{\alpha}=28.5$ MeV in both cases. (a), the elastic scattering from Si^{28}, (b), the inelastic scattering from the 1.77 MeV (2^+) level of Si^{28}, (c), the elastic scattering from Al^{27} and (d), the summed angular distributions of α_1 to α_6 from Al^{27}. The data in (c) and (d) were obtained from ref. [64-3]. All the data of Al^{27} are multiplied by a factor of 1.3 in this figure.

Al^{27} was mainly caused by the Si^{28} core excitation coupled to one proton hole. The same authors also investigated the excitation of the unnatural parity levels of above mentioned nuclei, O^{16} (2^-), Ne^{20} (2^-) Mg^{24} (3^+) and Si^{28} (3^+), and concluded that the reactions most probably took place through the exchange process and/or the successive multiple process. Experimental results are shown in Figs. 4-6-6 and 4-6-7.

4-7. Rearrangement Reactions Induced by Protons

In this and in the following paragraphs, we introduce the rearrangement reactions studied in our laboratory.

Rearrangement reaction is interesting from the standpoint of nuclear reaction mechanism and nuclear structure. About nuclear reaction mechanism, current conception is divided into two categories, i.e., direct interaction process and compound nucleus process. The former stands for the fast process, that is, all the

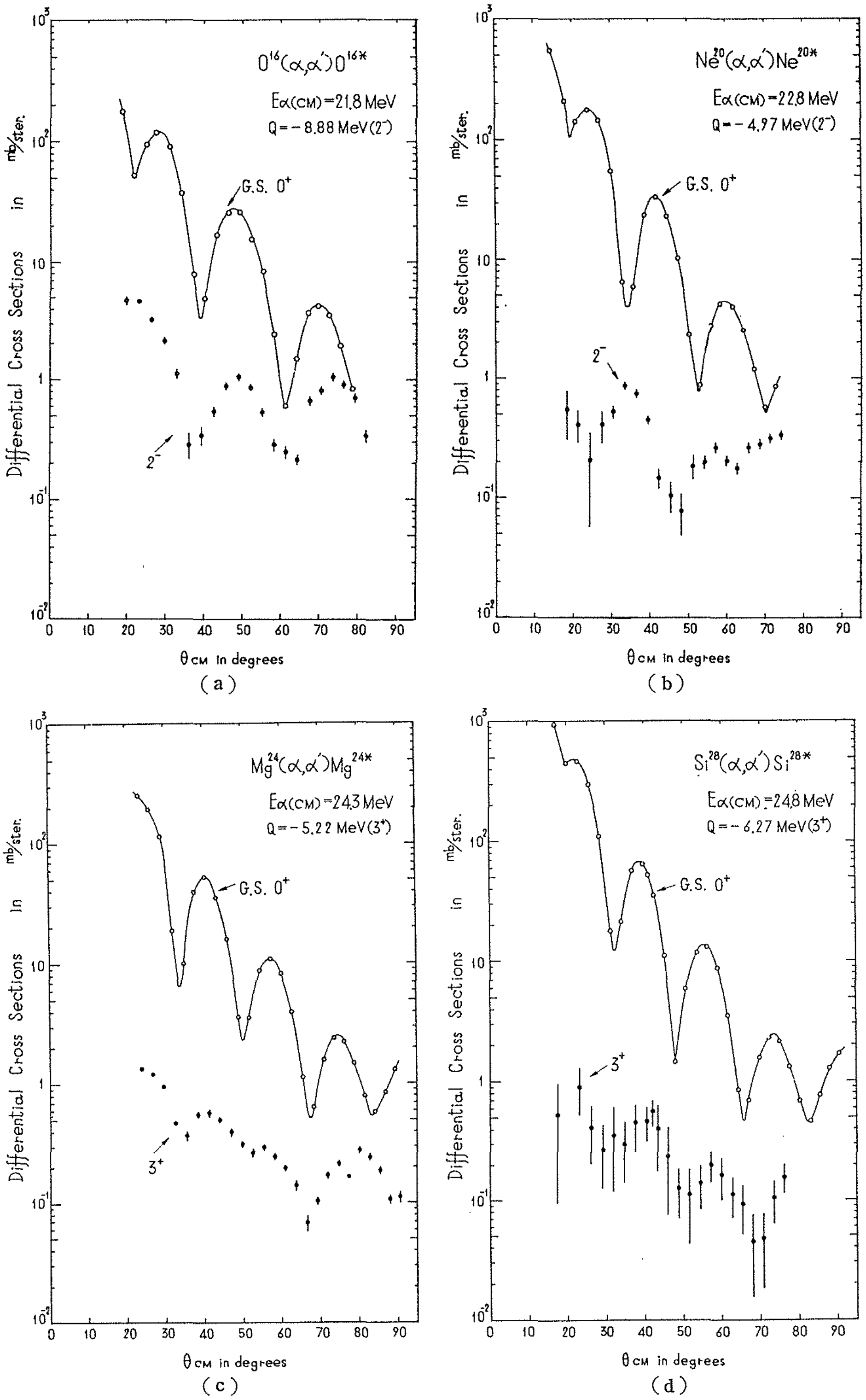

Fig. 4-6-7. Angular distributions of alpha particles leading to the unnatural parity levels of even nuclei. (a), O^{16} ground and 8.88 MeV (2^-) levels. (b), Ne^{20} ground and 4.97 MeV (2^-) levels. (c), Mg^{24} ground and 5.22 MeV (3^+) levels. (d), Si^{28} ground and 6.27 MeV (3^+) levels.

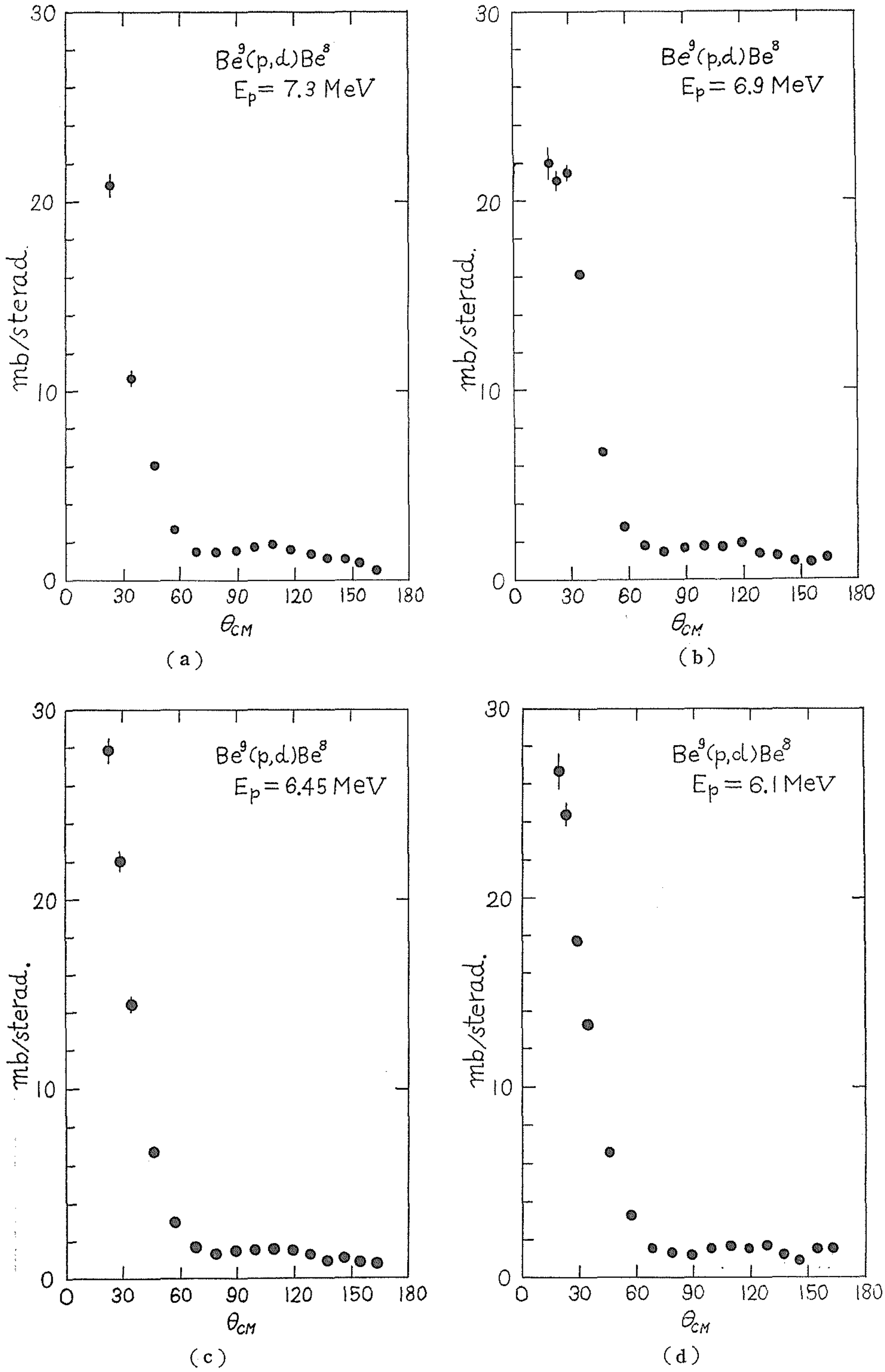

Fig. 4-7-1. Angular distributions of deuterons from the reaction Be^9 (p, d) Be^8g'nd. (a), $E_p=7.3$ MeV. (b), $E_p=6.9$ MeV. (c) $E_p=6.45$ MeV and (d), $E_p=6.1$ MeV. The data were obtained by ISHIWARI.

Table 4-7-1. (p, α) reaections.

Target	Residual	Resolved α	Reference
Be^9	Li^6	α_0, α_1	[64-7]
B^{10}	Be^7	α_0	[64-7]
B^{11}	Be^8	α_0	[64-7]
F^{19}	O^{16}	α_0	[61-6] [65-5]
Na^{23}	Ne^{20}	α_0, α_1	[62-3] [65-5]
Al^{27}	Mg^{24}	α_0, α_1	[61-6] [65-5]
P^{31}	Si^{28}	α_0, α_1	[61-6] [65-5]
K^{39}	Ar^{36}	α_0, α_1	[62-3] [65-5]

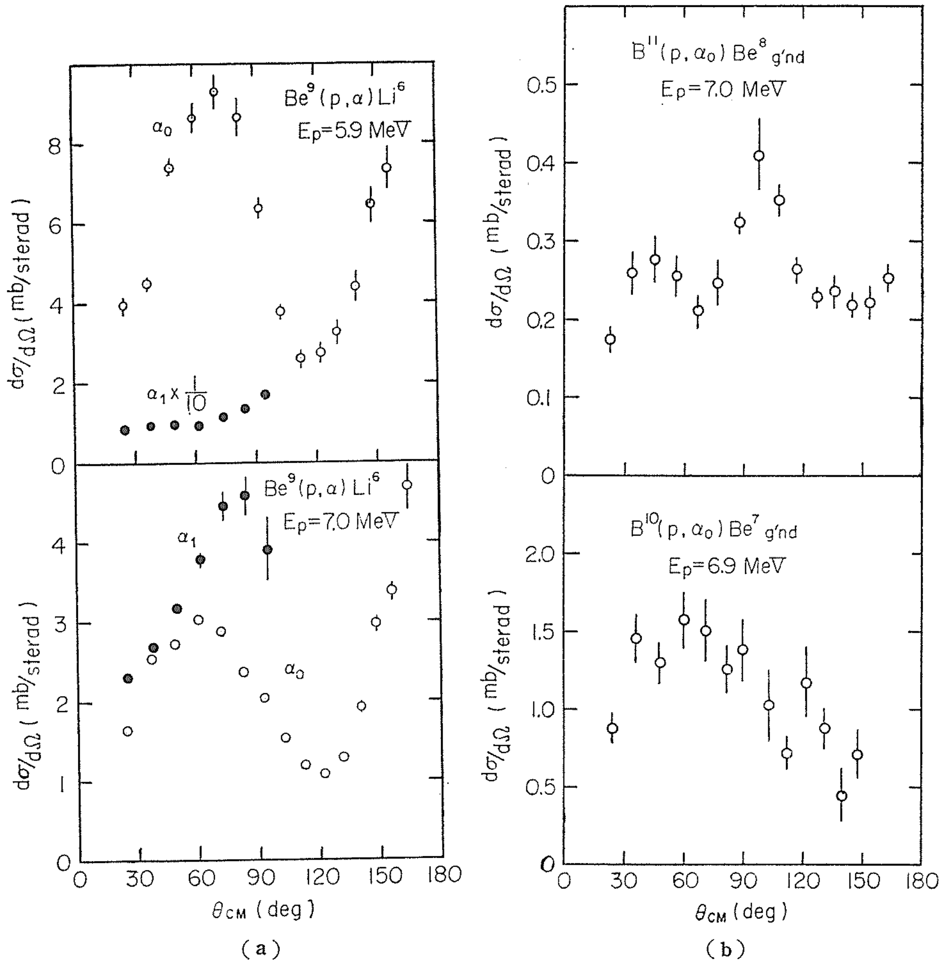

Fig. 4-7-2. Angular distributions of alpha particles from the (p, α) reaction on several elements. (a) Be^9 and (b), B^{10} and B^{11}.

reaction processes complete in time interval of the order of 10^{-22} sec, and the latter stands for the slow process, that is, the reaction process which needs 10^{-19} sec or longer. Real reaction mechanism should lie between these two extreme cases, or contain two kinds of processes simultaneously. In general, when the incident particle energy is high, the fast process is dominant, and if the energy is low, the slow process is dominant. The energies of protons, deuterons and alpha particles accelerated by the cyclotron in our laboratory, are neither so high nor so low, it is interesing to see what a characteristic behavior appears in the re-arrangement reaction induced by those particles. First the results obtained by protons are given.

(p,d) Reaction: The (p,d) reaction is not yet fully investigated in this labora-

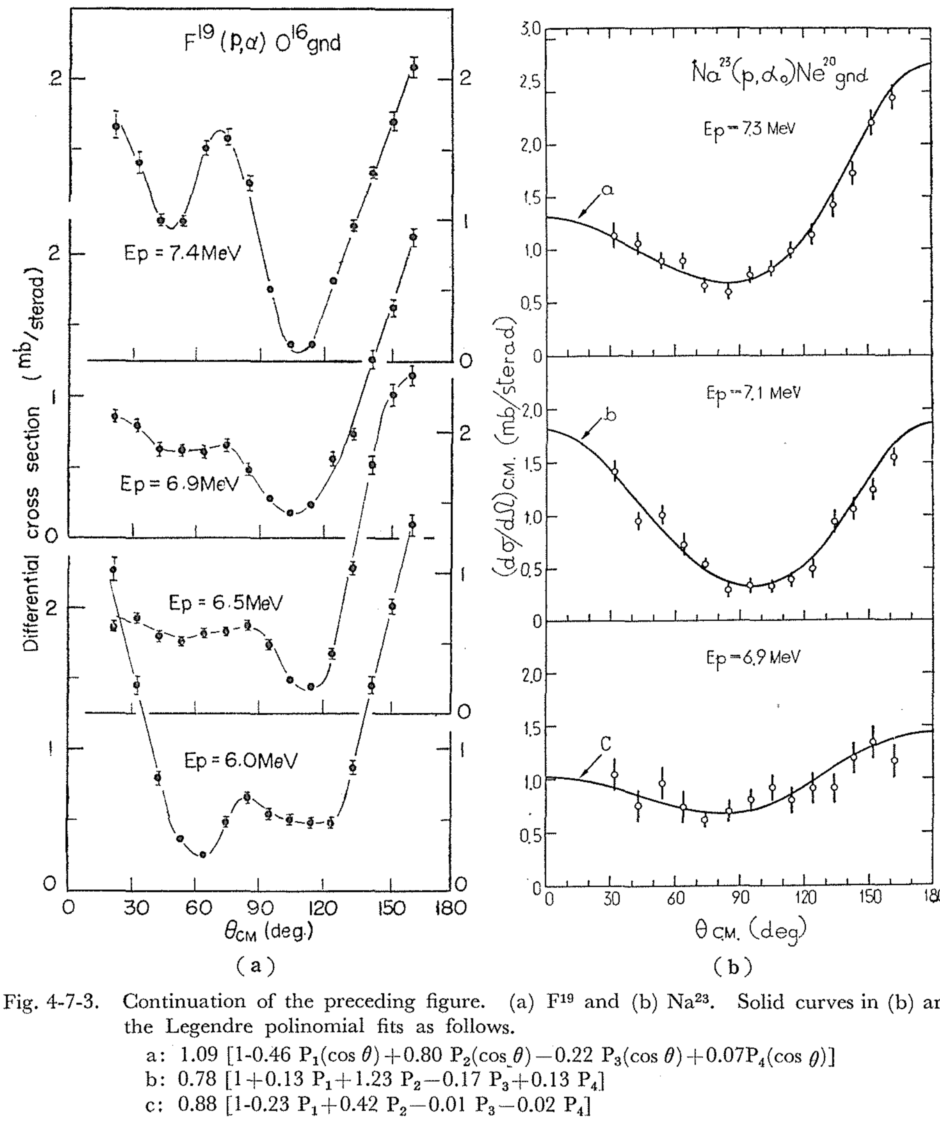

Fig. 4-7-3. Continuation of the preceding figure. (a) F^{19} and (b) Na^{23}. Solid curves in (b) are the Legendre polinomial fits as follows.

a: $1.09\ [1\text{-}0.46\ P_1(\cos\theta)+0.80\ P_2(\cos\theta)-0.22\ P_3(\cos\theta)+0.07P_4(\cos\theta)]$
b: $0.78\ [1+0.13\ P_1+1.23\ P_2-0.17\ P_3+0.13\ P_4]$
c: $0.88\ [1\text{-}0.23\ P_1+0.42\ P_2-0.01\ P_3-0.02\ P_4]$

tory, only Be^9 (p,d) Be^8 reaction were observed. [61-7] [64-8]. The angular distributions of deuterons at various proton energies are cited in Fig. 4-7-1. This reaction was mainly investigated by ISHIWARI.

(p, α) Reaction: The (p, α) reaction was investigated with target materials such as Be^9, B^{10}, B^{11}, F^{19}, Na^{23}, Al^{27}, P^{31} and K^{39}. Angular distributions of alpha particles leaving the residual nuclei in their low-lying states are given in Figs. 4-7-2 to 4.

Resolved states of residual nuclei and references are given in Table 4-7-1. From these results it may be seen that in the (p, α) reaction the individual character of the target nucleus plays an important role, that is,

a) Angular distributions of alpha particles from Na^{23} and K^{39} are almost 90° symmetry and independent on the incident proton energy.

b) Sharp rise of cross section in the backward direction is observed in cases

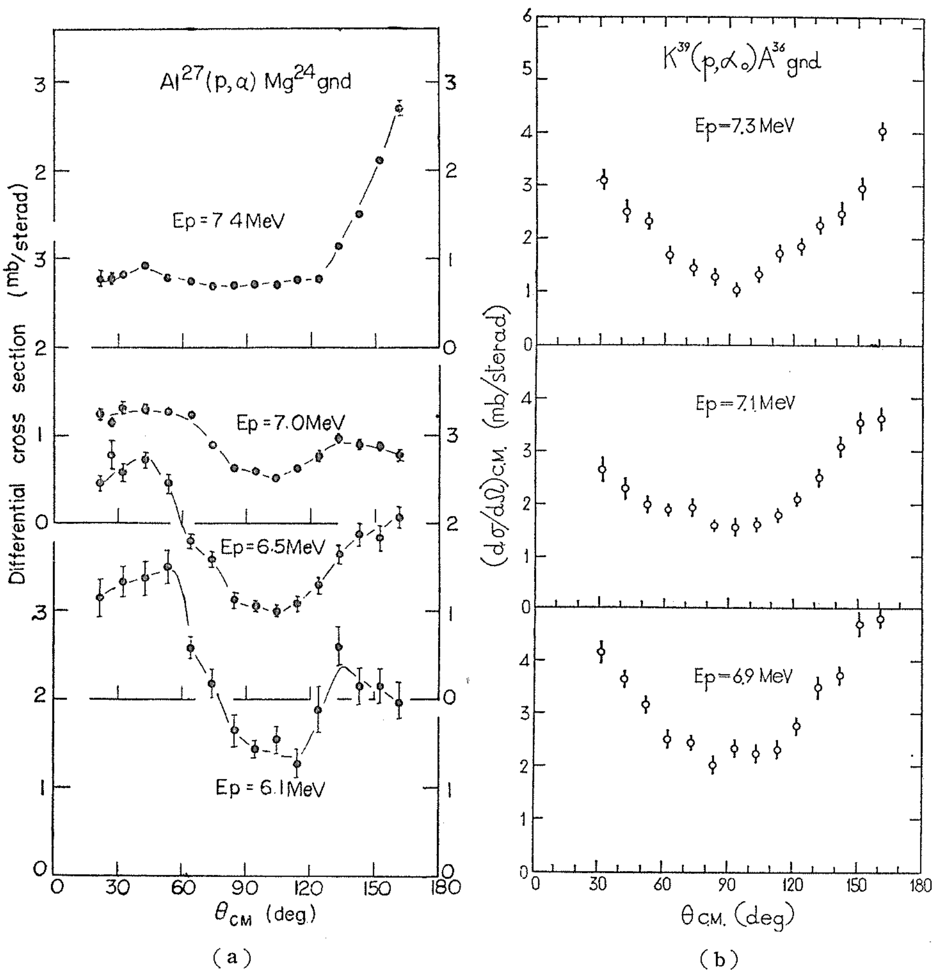

Fig. 4-7-4. Continuation of the preceding figure. (a), Al^{27} and (b), K^{39}. Solid lines are smoothed curves of the experimental points.

of Be^9 and F^{19} and this fact suggests the existence of alpha clusters in these target nuclei, and so on. These characteristics are of great interest to see the reaction mechanism in the medium energy range, and to investigate the nuclear structure. For detailed discussions, the reader should refer to each reference.

4-8. Rearrangement Reactions Induced by Deuterons

Variety of reactions can occur when a nucleus is struck by 15 MeV deuterons, but until now, only (d, α) reactions were investigated in our laboratory. Target materials used and the references are given in Table 4-8-1. Among those 12 materials, C^{12} (d, α) B^{10} and O^{16} (d, α) N^{14} reactions were studied not only by using the Kyoto University Cyclotron, but also by using the Institute for Nuclear Study Cyclotron.

Table 4-8-1. (d, α) reactions.

Target	Residual	Resolved α	References
Be^9	Li^7	α_0, α_1, α_2	[64-7]
B^{10}	Be^8	α_0, α_1	[64-7]
B^{11}	Be^9	α_0	[64-7]
C^{12}	B^{10}	α_0, α_1, α_3, α_4	[61-3] [61-5] [62-4] [65-5] [65-6]
N^{14}	C^{12}	α_0, α_1	[61-3] [61-5] [65-5]
O^{16}	N^{14}	α_0, α_2	[61-3] [61-5] [61-9] [62-4] [65-5] [65-6]
F^{19}	O^{17}	α_0, α_1, α_2, α_3, α_4	[62-5] [65-5]
Ne^{20}	F^{18}	α_0, α_1, α_2, α_3, α_4, $\alpha_5+\alpha_6+\alpha_7$	[62-5] [65-5]
Mg^{24}	Na^{22}	α_0	[62-5]
Al^{27}	Mg^{25}	α_0, α_1, α_2, α_3, α_4, $\alpha_5+\alpha_6+\alpha_7+\alpha_8+\alpha_9$	[62-6] [65-5]
P^{31}	Si^{29}	α_0	[62-5] [65-5]
S^{32}	P^{30}	α_0, α_1, α_2, α_3, α_4, $\alpha_5+\alpha_6+\alpha_7+\alpha_8+\alpha_9$	[62-5] [65-5]

Some of the results obtained are shown in Figs. 4-8-1 to 5. From these figures one can see that the (d, α) reactions are fairly dependent on the character of targets and the residual nuclei. In Fig. 4-8-6, the integrated cross sections of the (d, α_0) reactions are plotted as functions of target nucleus mass number. It is very interesting that 4n type nuclei show large cross sections of the (d, α) reaction. One more thing observed in the series of (d, α) reaction, is that cross sections at backward angles rise sharply in Be^9, B^{10}, B^{11}, C^{12}, O^{16} and Ne^{20}. So the (d, α) reactions on C^{12} and O^{16} were investigated with higher energy deuterons to see whether this backward rise is dependent on the incident deuteron energy. The variation of angular distributions are cited in ref. [62-5], and here the integrated cross sections are shown in Fig. 4-8-7 as functions of incident energy.

The (d, α) reaction is caused by a very complicated mechanism, but the deuteron or alpha particle clustering in the target and/or residual nuclei play an important role, and the reaction time needed to complete this reaction is just between the fast and the slow processes, this is our present day conclusion.

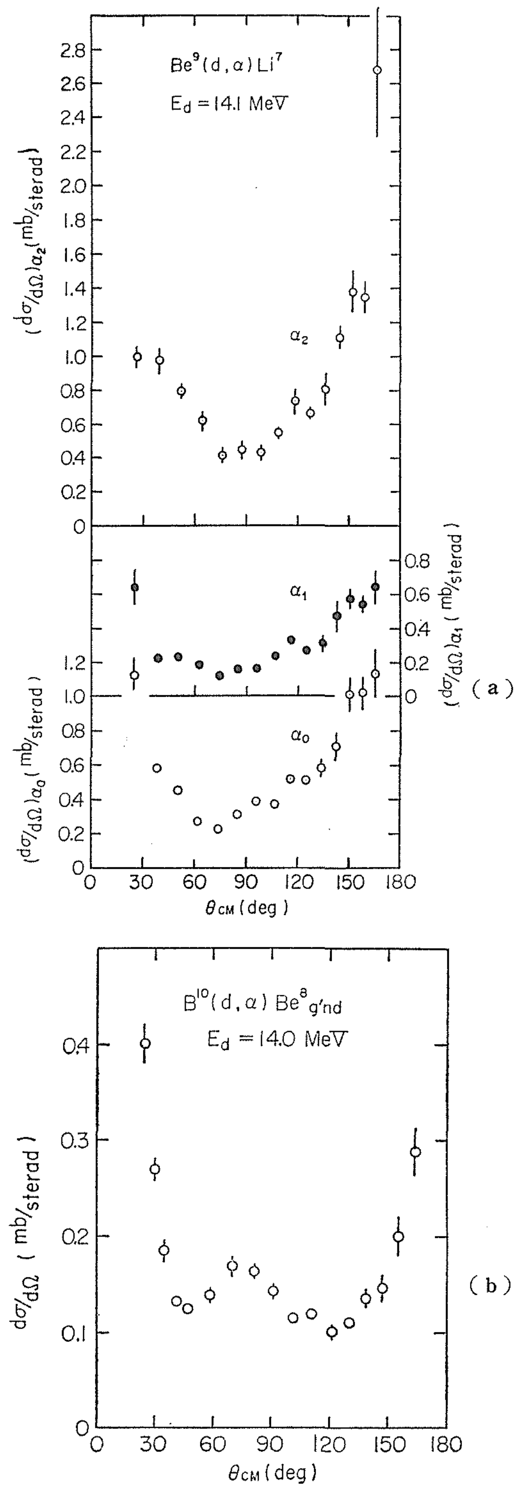

Fig. 4-8-1. Angular distributions of alpha particles from the (d, α) reaction on several elements. (a), Be^9 and (b), B^{10}.

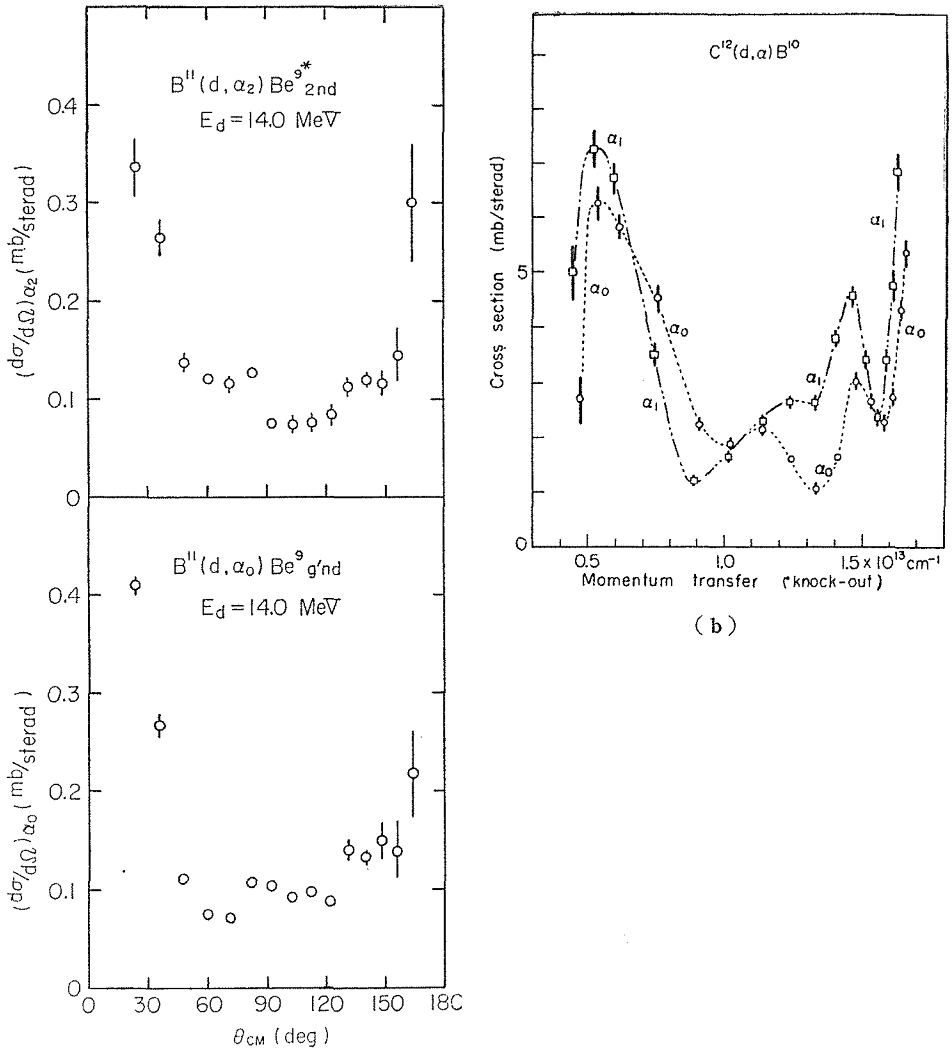

Fig. 4-8-2. Continuation of the preceding figure. (a) B^{11} and (b), C^{12}. In figure (b), the abscissa shows momentum transfer calculated from knockout process.

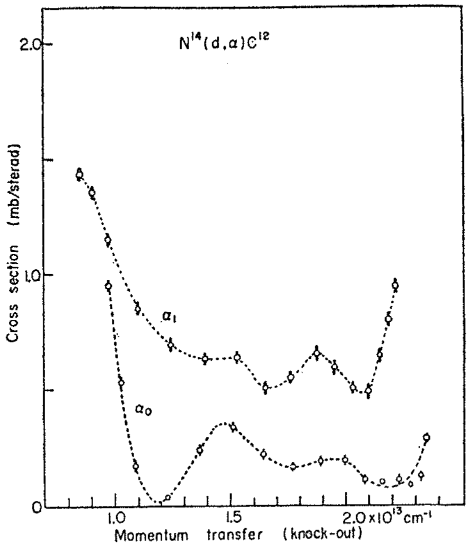

(a)

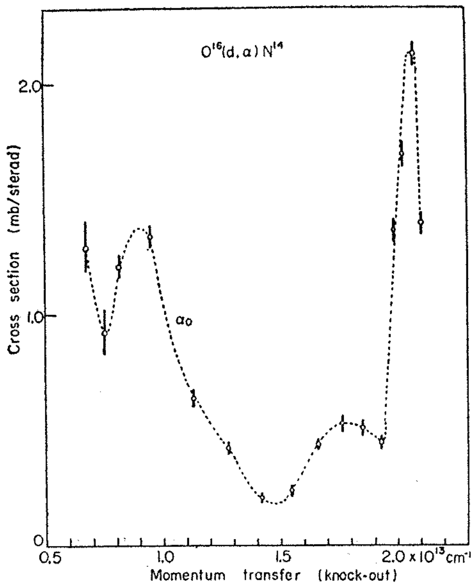

(b)

Fig. 4-8-3. Continuation of the preceding figure.
(a), N^{14} and (b), O^{16}.

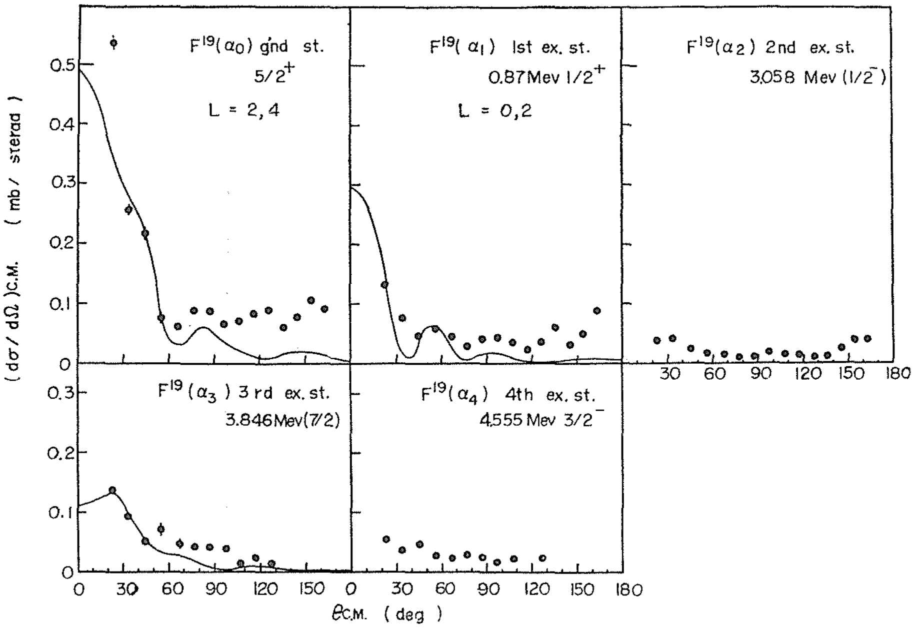

(a)

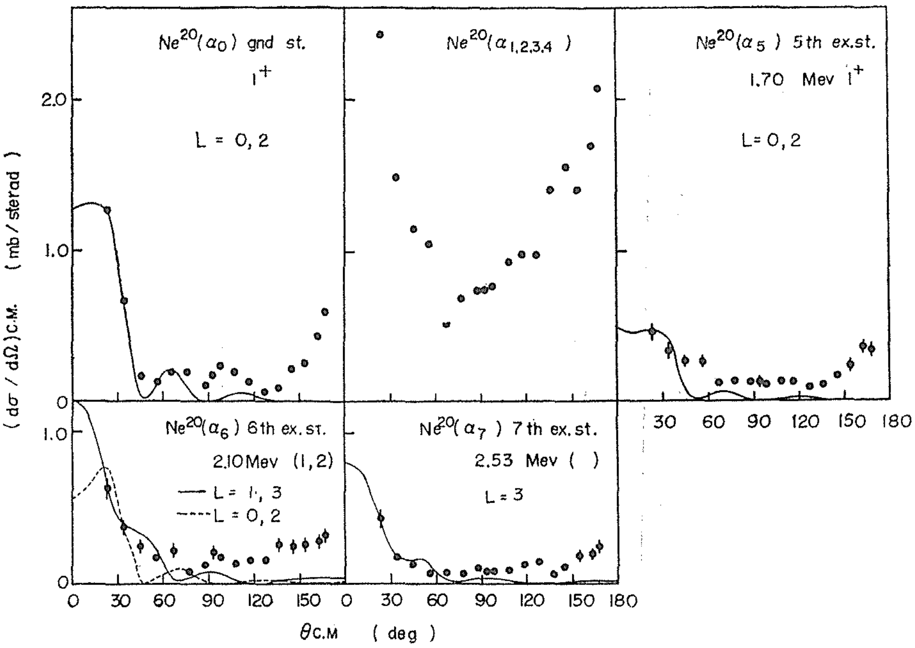

(b)

Fig. 4-8-4. Angular distributions of alpha particle groups from the reactions $F^{19}(d, \alpha)\, O^{17}$ and $Ne^{20}(d, \alpha)\, F^{18}$. (a), the case of F^{19}. Curves in the figure are; $F^2[0.41\, j_2^2(QR_0) + 0.53\, j_4^2(QR_0)]$ for α_0, $F^2[0.29\, j_2^2(QR_0) + 0.09\, j_4^2(QR_0)]$ for α_1, and $F^2[0.135 j_3^2(QR_0) + 0.1 j_5^2(QR_0)]$ for α_3, where F is the form factor and $R_0 = 5.0$ fm. (b), the case of Ne^{20}. Curves in the figure are the theoretical fits by spherical Bessel functions. See ref. [62-5].

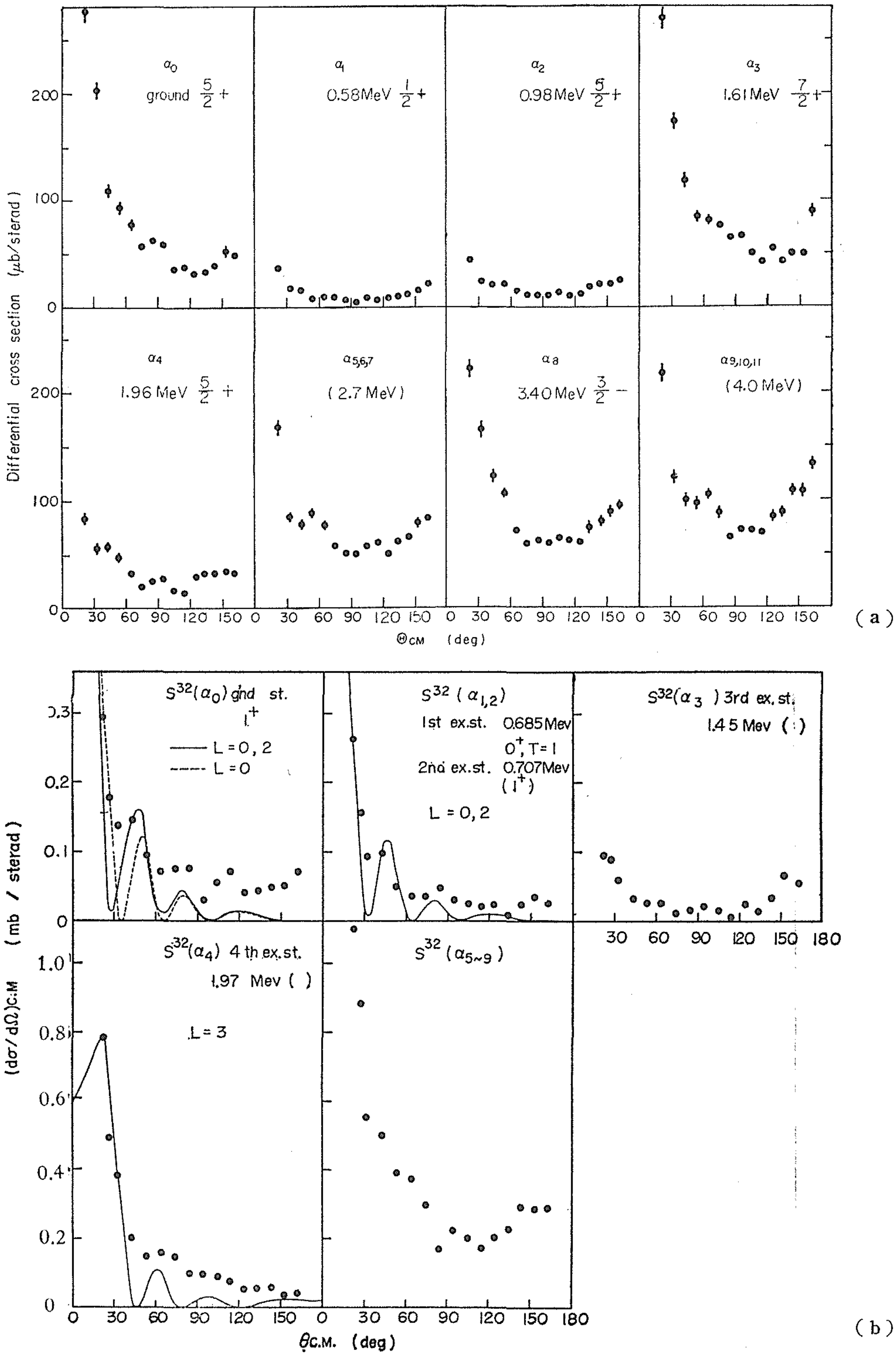

Fig. 4-8-5. Continuation of the preceding figure. (a), the ease of Al^{27} and (b), the case of S^{32}. For curves in the figure, see ref. [62-5].

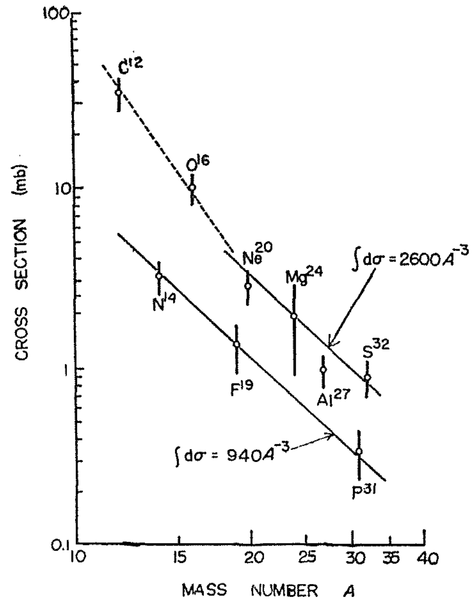

Fig. 4-8-6. Plots of integrated cross sections of the (d, α) reactions on several elements leading to the ground states of residual nuclei. The abscissa gives the mass number of target nuclei. The solid lines show,

$\int d\sigma = 2.6 \times 10^3 . A^{-3}$ (mb)

for the even-even nuclei and

$\int d\sigma = 0.94 \times 10^3 . A^{-3}$ (mb)

for the odd-odd and odd nuclei.

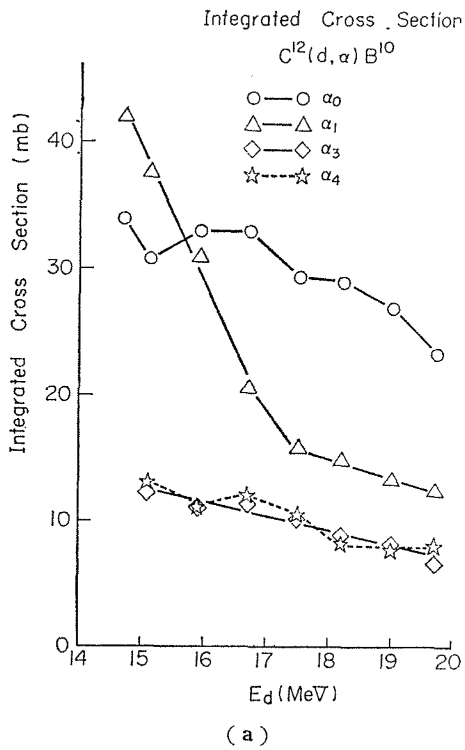

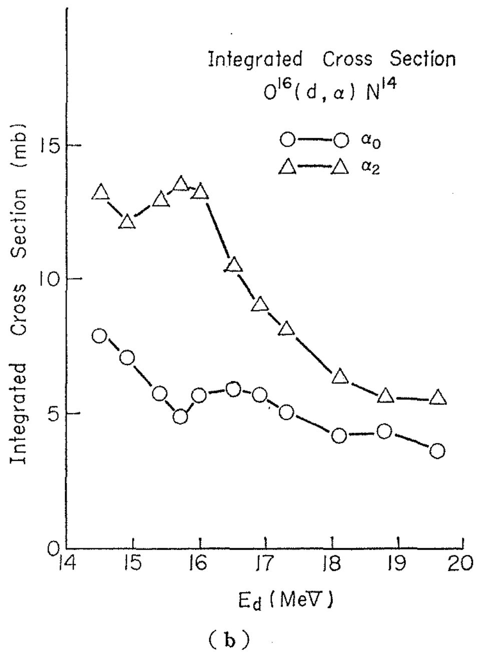

Fig. 4-8-7. Integrated cross sections of the reactions $C^{12}(d, \alpha) B^{10}$ and $O^{16}(d, \alpha) C^{12}$ as functions of incident deuteron energy. (a), C^{12} and (b), O^{16}.

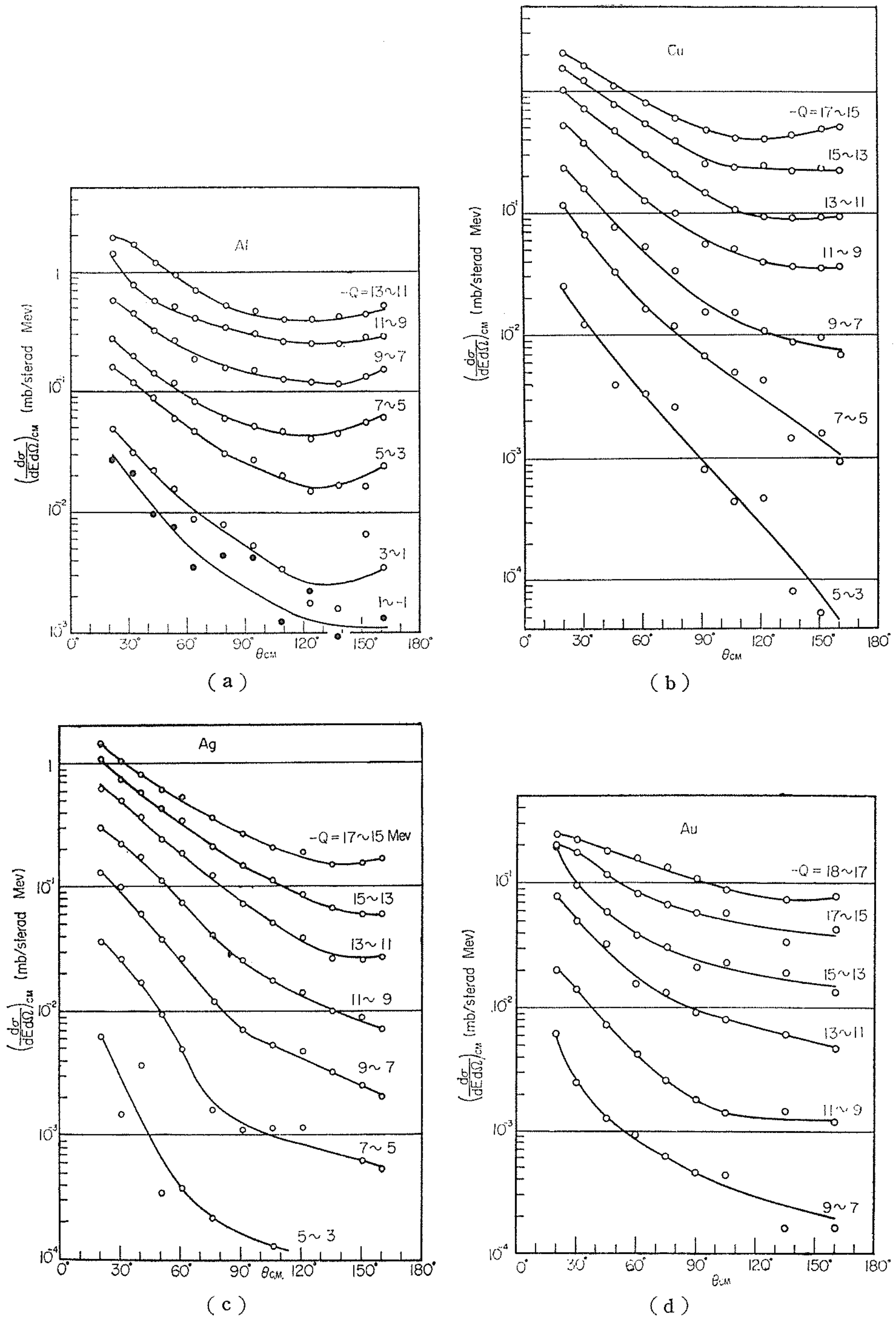

Fig. 4-9-1. Angular distributions of protons from the (α, p) reactions on several elements. E_α= 30 MeV and the solid lines are the smoothed curves of the experimental results. (a), in the case of Al. The experimental points give the averaged values over 2 MeV intervals cited in the figure. (b), in the case of Cu. The meaning of experimental points is the same to (a). (c), in the case of Ag and (d), in the case of Au.

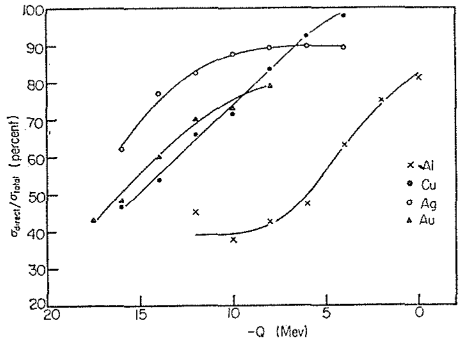

(a)

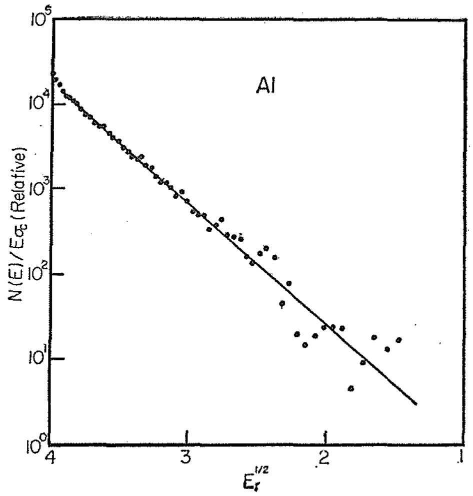

(b)

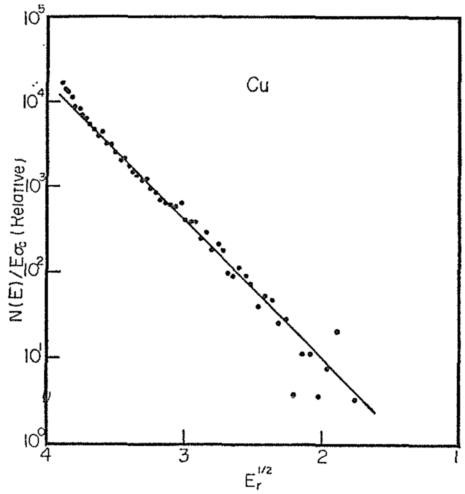

(c)

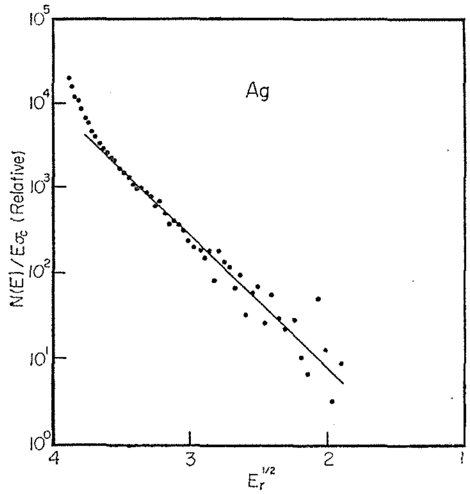

(d)

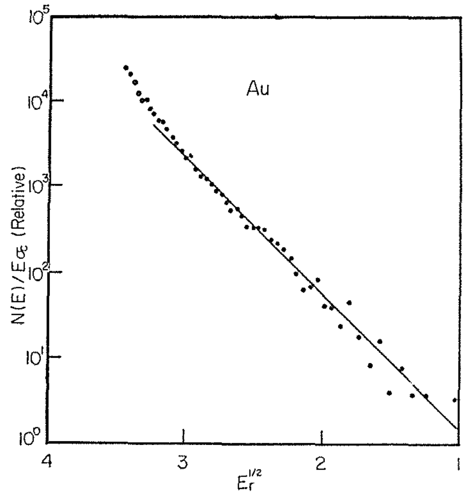

(e)

Fig. 4-9-2. (a). Ratios of the cross-sections caused by the direct process to the total cross-sections as functions of the (α, p) reaction Q-value. (b). The quantity N(E)/Eσ_c from the (α, p) reaction on Al as a function of $Er^{1/2}$. For detailed explanation, see ref. [62-7]. (c). The same as above in the case of Cu. (d), in the case of Ag, (e), in the case of Au.

4-9. Rearrangement Reactions Induced by Alpha Particles

Various kinds of rearrangement reactions can be induced also by 30 MeV alpha particles, but until now, only the following reactions were investigated in this laboratory, simply because we have not yet enough techniques to identify other particles.

Reactions studied and the references are:

(α, p) reactions on Al^{27}, Cu, Ag and Au [62-7],

(α, d) reactions on Be^9, F^{19} and Al^{27} [65-14],

(α ,t) reactions on Be^9, F^{19} and Al^{27} [65-14].

Protons from the (α, p) reactions were identified with a solid state detector with thick absorber to stop particles other than protons. Deuterons and tritons from the (α, d) and the (α, t) reactions were recorded by nuclear emulsions.

The aims of the investigation of the (α, p) reactions were to obtain information about the nuclear level densities in the continuum state and besides to estimate the hybridization of direct and compound nucleus processes.

Some of the results are shown in Figs. 4-9-1 and 2. KUMABE *et al.* [62-7] concluded from these results that the incident alpha particles most likely heated the peripheral region of the target nucleus and the nuclear temperature obtained from

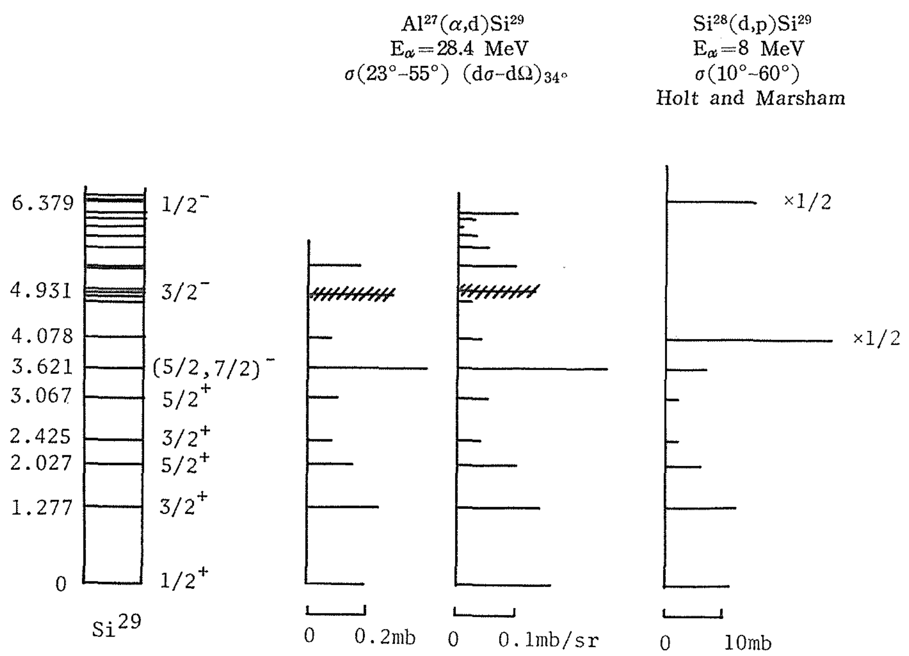

Fig. 4-9-3. Cross sections of the reactions $Al^{27}(\alpha, d)$ Si^{29} at 28.4 MeV and $Si^{28}(d, p)$ Si^{29} at 8 MeV. The length of a line represents the value of cross sections leading to the levels of Si^{29} cited in the figure. The (α, d) reaction is similar to the (d, p) reaction in the mode of relative excitation of the first five states which are well interpreted by the rotational model of Nilsson.

the (α, p) reaction was higher than the temperature obtained from the (n,n'), (n,p), (n, α), (p,p'), (p,n) and (p, α) reactions.

Investigation of the (α, d) and the (α, t) reactions were performed to see whether special type of levels of residual nucleus appears or not by one and two nucleon transfer reactions. Resemblances between the (α, d) and the (d, p) reactions and between the (α, t) and the (He^3, d) or the (d,n) reactions leading to the same residual nucleus were mentioned. Some of the results are shown in Fig. 4-9-3. Detailed analysis by KAKIGI are described in ref. [65-14].

4-10. Search for Alpha Particle Clustering in Nucleus

In a series of experiments of alpha emitting reactions such as (p, α), (d, α) and (α, α'), YANABU, YAMASHITA and others assumed that the alpha particle clustering played an important role in such reactions. Based on this working hypothesis, they tried to search for alpha clusters in nuclei and to find the direct evidence of a role of alpha cluster in a alpha emitting reaction.

The search was begun since 1962, in a way to estimate the pre-existence probability of alpha clusters by the quasi-free proton-alpha or alpha-alpha scattering. By the word quasi-free scattering, it is meant that the incident proton or alpha particle collides the alpha cluster in a target nucleus, and quasi-free scattering occurs between proton and alpha cluster or between alpha particle and alpha cluster. Alpha cluster in a nucleus is bound to residual nucleus with some binding energy, so this scattering is not pure elastic scattering. The angular correlation between the proton and the alpha cluster after the quasi-free scattering resembles the correlation in a pure elastic scattering if the binding energy of the alpha cluster in a nucleus is not so large comparing to the incident particle energy.

Up to the present, quasi-free proton-alpha scattering was examined by using a F. M. cyclotron of the Institute for Nuclear Study, University of Tokyo. Incident proton energy was near 55 MeV and the targets thus far studied were C, Al and Ni. Some of the results are described in refs. [63-4] and [64-9], but small yield of this phenomenon prohibit to draw a definite conclusion.

On the other hand, quasi-free alpha-alpha collisions were investigated by using the Kyoto University Cyclotron, and some definite results were obtained. [64-6], [65-10]. Fig. 4-10-1 gives the angular correlations of two alpha particles which are emitted simultaneously when Be^9 target was bombarded by 30 MeV alpha particles. Other than Be^9, C^{12} and O^{16} were used as targets of (α, 2α) reaction. The latter two elements are now in the way of investigation, but in the preliminary work, curious angular correlations between two alpha particles were observed in the case of C^{12}. [65-10].

The cluster structure of Be^9 relates some problems studied in our laboratory with one another. These are, the α-α elastic scattering by MIYAKE, [61-8], the asymmetry of polarized proton scattering from Be^9 studied by FUKUNAGA, [65-1], and the

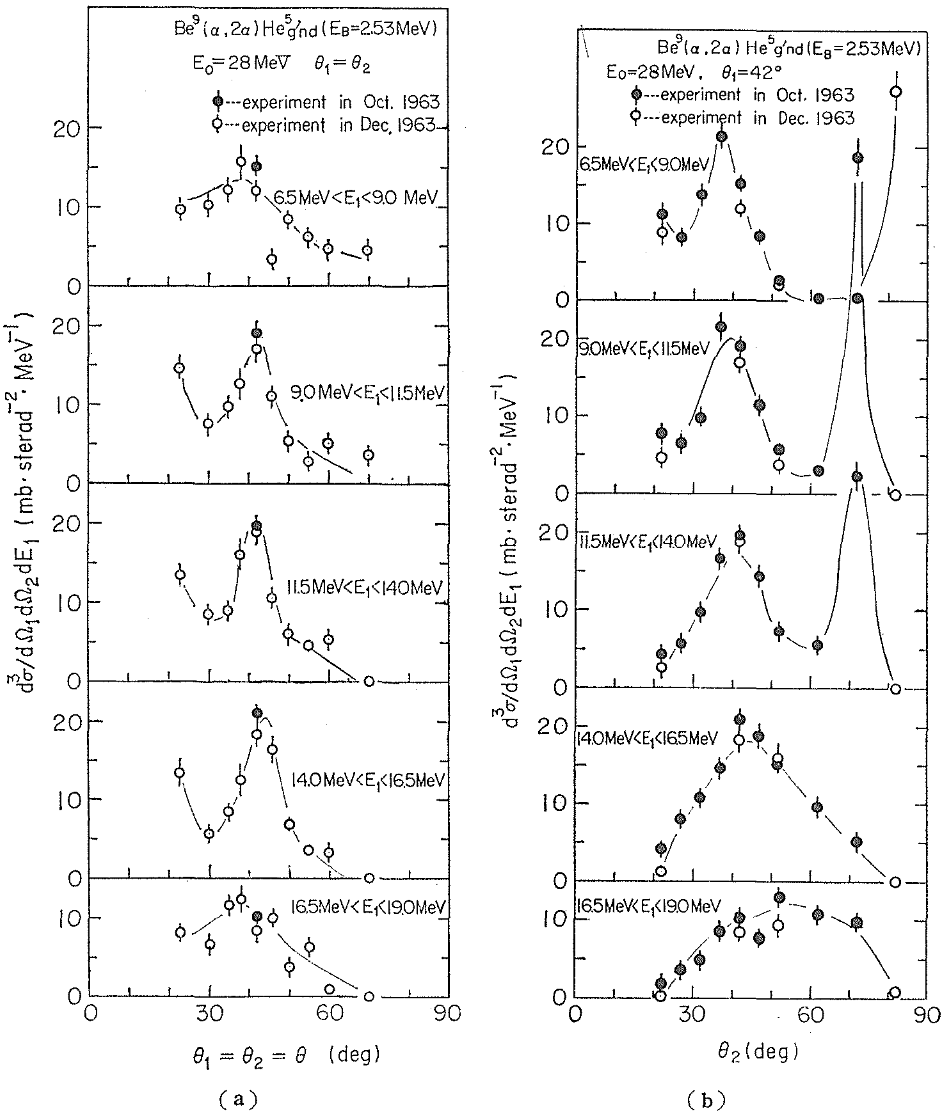

Fig. 4-10-1. Angular correlations of the alpha-particles from the reaction $Be^9(\alpha, 2\alpha)He^5{}_{g'nd}$ (E_B=2.53 MeV.) (a), results obtained when both alpha particle detectors were set symmetrically with respect to the incident beam. Those are shown for each interval of 2.5 MeV of the energy E_1 of the alpha particles entered into one of the detectors (b), the results obtained when one of the detectors was set at 42° and the other detector moved. E_1 is the energy of the alpha particles entered into the fixed counter.

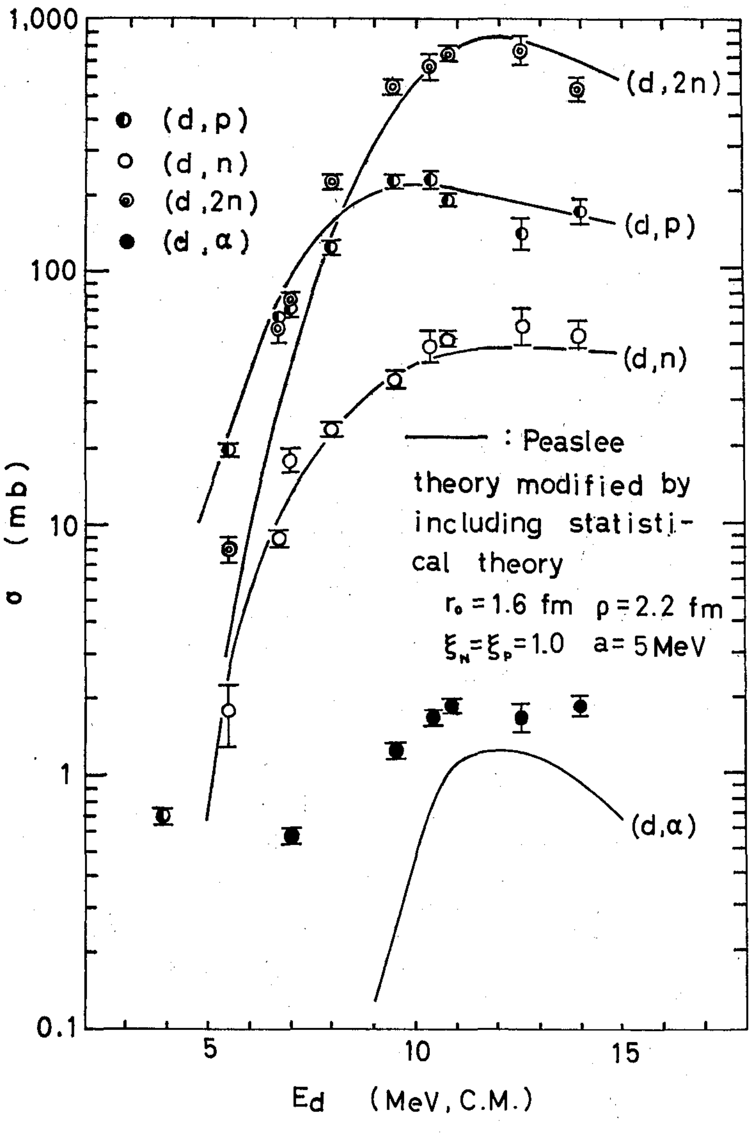

Fig. 4-12-1. Excitation functions of deuteron induced reactions on Ce^{142}. The results in low energy side of deuterons were obtained with the Osaka University Cyclotron and in high energy side were obtained with the Kyoto University Cyclotron. Solid lines in the figure represent calculated results by modified Peaslee theory. Detailed explanations appear in ref. [65-19].

alpha emitting reactions of Be^9. [64-8].

4-11. Energy Loss of Alpha Particles

Energy loss of charged particles in materials is the basic knowledge of nuclear physics, and more and more precise values of energy loss are needed for the promotion of radiation detection. The energy of the alpha particles from the Kyoto cyclotron lies just in the vacant region of the world wide feasibility, it may be our duty to measure precise values of energy loss of alpha particles in various materials. This project was planned by ISHIWARI since 1964 and the preliminary results are reported in ref. [65-15]. The project is now under way and the results will be published soon.

4-12. Research in Nuclear Chemistry

This subject seems inadequate to be introduced here, but the content of the research is in concordance with nuclear physics.

Recently, the laboratory members began their cooperation with Professor Nishi of the Engineering Research Institute, Kyoto University, and with Professor OTOZAI of the Department of Chemistry, Faculty of Science, Osaka University, in the field of nuclear chemistry. Their aim is to investigate the type of nuclear reaction by the method of radio-chemistry and to determine the excitation function as the incident projectile energy is changed. They picked up rare earth elements as the object of research. One of these elements was Ce^{142}, and the investigation of deuteron induced reactions on Ce^{142} have been performed in the energy range of deuterons from 5 to 14.2 MeV using the Osaka University Cyclotron and the Kyoto University Cyclotron. A part of results is shown in Fig. 4-12-1, and the complete article will appear soon in *Nuclear Physics*. [65-18]. They estimated the cross sections of Ce^{142} (d,p) Ce^{143}, Ce^{142} (d,n) Pr^{143}, Ce^{142} (d,2n) Pr^{142} and Ce^{142} (d, α) La^{140} reactions simultaneously as functions of deuteron energy, and concluded that Peaslee theory based on deuteron stripping reactions must be modified so as to include the fact that the entire absorption of deuterons by target nucleus is larger than expected. It is very fruitful to catch all open channel reactions by radiochemical technique for understanding the reaction mechanism.

5. RESEARCH IN RADIATION BIOLOGY AND RELATED PROBLEMS

To utilize the cyclotron as a tool for radio-isotope production, as a high intensity neutron source for radio-biological researches, was one of the main purposes of re-constructing a Kyoto University Cyclotron. The cyclotron in this laboratory was, as described in ref. [61-10], the resuscitation of the former cyclotron which was destroyed by the U. S. A. armed forces in 1945. The former cyclotron had an obligation, under the leadership of Professor B. ARAKATSU, to serve as a radioisotope production tool, in those days radio-isotopes became to be widely used in various fields of biology and biochemistry.

After the World War II, the development of neutron chain reactors lessened the usefulness of a cyclotron as a production apparatus of radio-isotopes, it still had great value as a high intensity neutron source, especially in Japan, to find the basis of the biological injuries caused by the atomic bomb of U.S.A.

5-1. Neutron Flux Distribution Around the Cyclotron

In 1957, soon after the radiation shielding walls and ceilings surrounding the cyclotron were constructed, neutron flux distributions around the cyclotron were measured by the following way.

As a neutron monitor, a set of In foil surrounded with paraffin block was prepared. This paraffin block was about $10\times10\times10$ cm^3 cubic form, and in the center of this cube located the In foil. A number of such neutron monitors were distributed around the cyclotron, and at one point, this neutron monitor and a commercial neutron fluxmeter NEMO, made by Nuclear Chicago Inc., were placed in the same position. Neutrons from the cyclotron were produced by the deuteron beam bombardment on a Cu target placed inside the acceleration chamber of the cyclotron. After the operation of the cyclotron stopped, induced activities of In foils were estimated and converted to the neutron flux intensity after the calibration by NEMO. This commercial neutron monitor could detect fast and slow neutron flux separately, so the standard neutron monitor was calibrated in two cases, that was, In foil plus paraffin block and In foil plus paraffin block plus Cd cover. The result showed that the slow neutron flux was nearly equal to the fast neutron flux.

Fig. 5-1-1 gives the distribution of fast neutron fluxes normalized by deuteron beam current. Gamma rays, of course, were generated heavily, but the distribution of gamma ray fluxes was not measured. It was estimated roughly, however, by using NEMO and ionization gamma-ray dosimeter simultaneously, that the gamma dose were of the same order of the neutron dose.

5-2. Neutron Irradiation on Various Living Things and Substances

After the measurement of neutron flux distribution was completed, we proposed to the members of the Kyoto University to utilize neutron irradiation on various things in their way of research. The number of applications was about 25, and a lecture meeting was held at the Research Institute of Fundamental Physics, Kyoto University, on September 18th, 1957, on the results obtained by neutron irradiation. In Table 5-2-1, the program of this lecture meeting is introduced to see what kind of works can be done with the cyclotron.

5-3. Biological Researches by the Cyclotron

Most of the experiments appeared in Table 5-2-1, were rather of preliminary nature, so, few articles have been published since then. But biological researches got some definite conclusions and their results are published as seen in section 6.

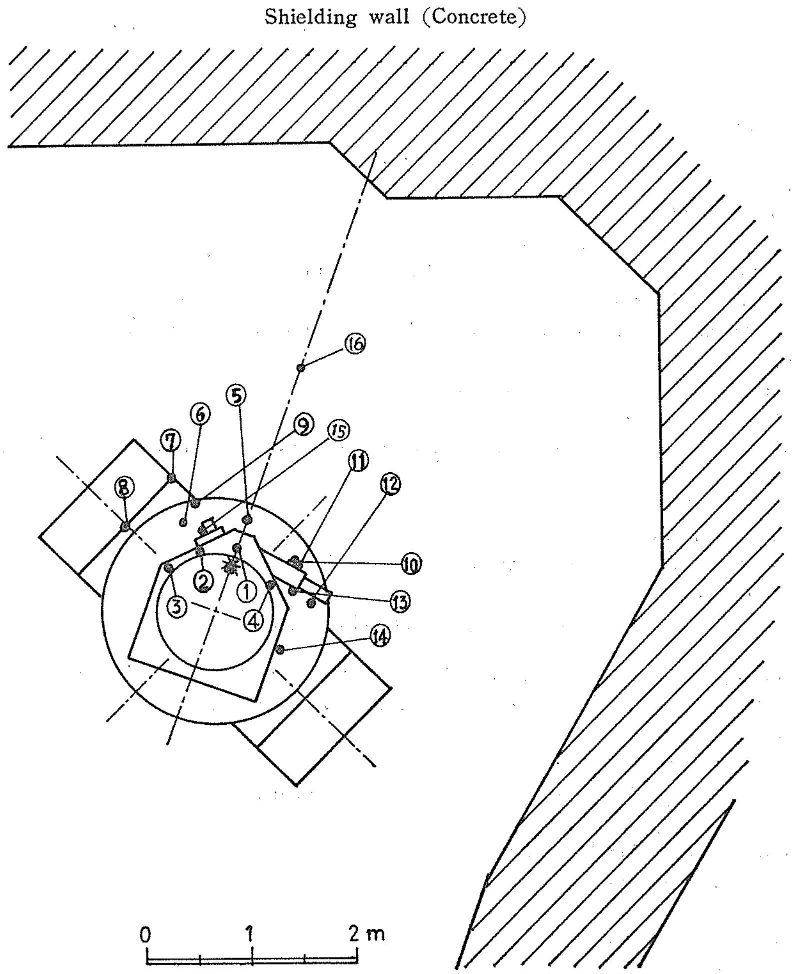

Fig. 5-1-1. Fast neutron flux distributions around the cyclotron. Neutron intensities in n/cm² 100 μA of deuterons to Cu target are as follows,

* Source point of neutrons
1) (at the top of accel. chamber) 9.23×10^{7}
2) (ditto) 3.45×10^{7}
3) (ditto) 1.41×10^{7}
4) (ditto) 3.66×10^{7}
5) (at median plane) 2.19×10^{7}
6) (ditto) 2.00×10^{7}
7) (ditto) 1.01×10^{7}
8) (ditto) 8.21×10^{6}
9) (at the top of coil tank) 8.48×10^{6}
10) (at the median plane) 1.24×10^{7}
11) (at the top of coil tank) 1.17×10^{7}
12) (ditto) 1.86×10^{7}
13) (at the median plane) 2.61×10^{7}
14) (ditto) 7.33×10^{6}
15) (at the top of coil tank) 1.99×10^{7}
16) (at the median plane) $9.52\ 10^{5}$

Table 5-2-1. Program of the Lecture Meeting on Neutron Irradiation.

1. Biological effects of neutrons from a cyclotron in mice.
   G. MIYAKE, G. WAKISAKA and T. MORII.
   Faculty of Medicine.
2. Estimation of nucleic acids in the internal organs of neutron irradiated rats.
   G. MIYAKE, G. WAKISAKA and T. HIRAI.
   Faculty of Medicine.
3. Hematoscopy of neutron irradiated rats.
   T. FUKUDA, F. TUTUMI, H. MURANAKA and T. IGARASHI.
   Faculty of Medicine.
4. Effect of neutrons on the metabolism of nucleic acids and on the histological breathing of the internal organs of rats.
   T. FUKUDA, T. TANAKA and G. YOKOTA.
   Faculty of Medicine.
5. Histological studies on the hematopoietic organs of mice irradiated with high doses of neutron.
   S. AMANO and M. HANAOKA.
   Faculty of Medicine.
6. Radiation effects on enzymes.
   S. TANAKA, H. HATANO and S. TAKANO.
   Faculty of Science.
7. Effect of neutron irradiation on the silicate glass and phosphate glass.
   S. SAKUHANA
   Institute for Chemical Research.
8. Formation of radicals in the organic solvents by neutron irradiation.
   S. FUTAMI
   Faculty of Engineering.
9. Production of isotope ^{18}F by $^{5}Li\ (n, \alpha)T$, $^{16}O(T,n)\ ^{18}F$ reaction.
   T. OKADA, T. NISHI and I. FUJIWARA.
   Engineering Research Institute.
10. Activation analysis of Hf in Zy.
    T. OKADA, T. NISHI and T. MATSUMOTO.
    Engineering Research Institute.
11. Radiation effect on alkali-hallide crystal.
    Y. UCHIDA and K. FUKUDA.
    Faculty of Science.
12. Erosion of stainless steels by uranyl salt.
    T. SANO
    Faculty of Science.
13. Neutron irradiation effect on scintillating phospher.
    R. FUJIMURA and Y. YANO.
    Faculty of Engineering.
14. Studies on the crop nutrition using ^{42}K as a tracer.
    A. OKUDA, Z. KASAI, H. NAKADA, K. ASADA and Y. YAMADA.
    Research Institute for Food Science.
15. Neutron flux attenuation in water measured from induced activity of In.
    T. HYODO
    Faculty of Engineering.
16. Studies on the abrasion of piston-rings radio-activated by neutron irradiation.
    M. KATO, N. TSUDA, G. TAKAI and A. UMEHA.
    Mitsubishi Oil Industry.

Here the contents of these articles are introduced briefly.

HANAOKA and others studied the radiation effect on experimental animals mainly with the aim to clarify the pathological findings of acute and subacute atomic bomb injuries of the human being. Male mice were irradiated by about 1.7×10^{11} fast neutrons/cm^2, and observed hematological and histological changes of the peripheral blood hematopoietic organs and other tissues of the whole body of mice for 3 to 72 hours following the irradiation. [58-1], [59-4], [64-5]. They then concluded that the blood cells and others were destroyed in two steps, the primary destruction being prominent in erythroblasts and lymphocytes, epithelial cells of small intestine, and spermatogonia etc., while the secondary one, in other mature leucocytes. They also discussed that the primary destruction was due to the direct effect of the radiation, on mitotic cells and the secondary destruction was due to the indirect influence of the substances such as peroxide and others accumulated in the blood after the primary destruction. Fig. 5-3-1 and the figure captions are cited from ref. [58-1]

Fig. 5-3-1. Hostological changes of neutron-γ-ray irradiated mice. Paraffin section, hematoxylin-eosin staining.

1～3, Small intestines.

1: Numerous cell debrises appear in the intestinal gland. The distribution of destructed cells agree with that of actively dividing cells which are observed in non-irradiated mice after colchicinization. Paneth's cells are intact. 3 hours later.

2: 18 hours later, some mototic cells are observed.

3: The atrophic profile of small intestine. 72 hours later.

4: Liver, 18 hours later. The cytoplasm of liver cells becomes to be the cord-like appearance. Venous is filled with hyaline clot.

5～12, Bone marrows.

5: Punched out structures are distributed in the bone marrow, 3 hours later.

6: Higher magnification of punched out structure which are composed of reticulum cells and cell debrises derived from actively dividing erythroblast during exposure, 3 hours later.

7: Enlarged punched out structure. 6 hours later.

8: The destruction of mature leucocytes are prominent and their distribution is sparse around the enlarged venous sinus. On the other hand, in the area nearby the beam of bone, the leucocytes with immature type are densely distributed. 18 hours later.

9: Leucocytes with degenerative ones remained around arteriolus, 24 hours later.

10: All remaining leucocytes are destructed.

11: Blood plasma fill the medullary cord, 48 hours later.

12: Aplastic marrow, 96 hours later.

13: Cell debrises in lymph follicle of spleen, 6 hours later.

14: Both of white and red pulp of spleen are constituted with the mesh of reticulum cells, 24 hours later.

15: Cell debrises are prominent in germinal center and phagocytized by reticulum cells, 6 hours later.

16: Many intact lymphocytes are distributed in the lymph node, but in same mouse splenic lymphocytes disappear almost completely, 18 hours later.

17: Numerous cell debrises appear in the cortex of thymus, 3 hours later,

18: Aplastic lymphatic tissue of ileum.

1 2

3 4

5 6

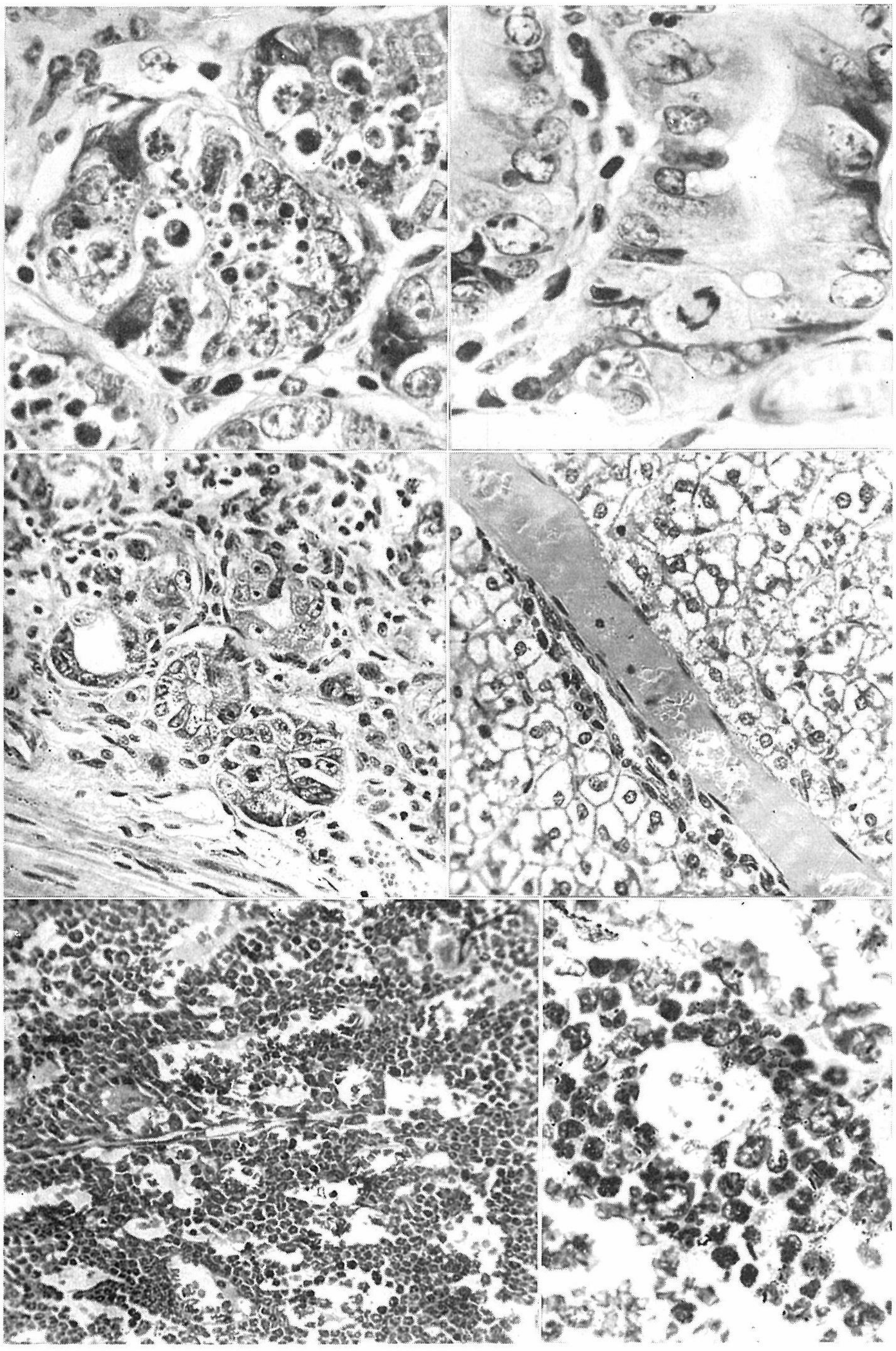

Fig. 5-3-1.

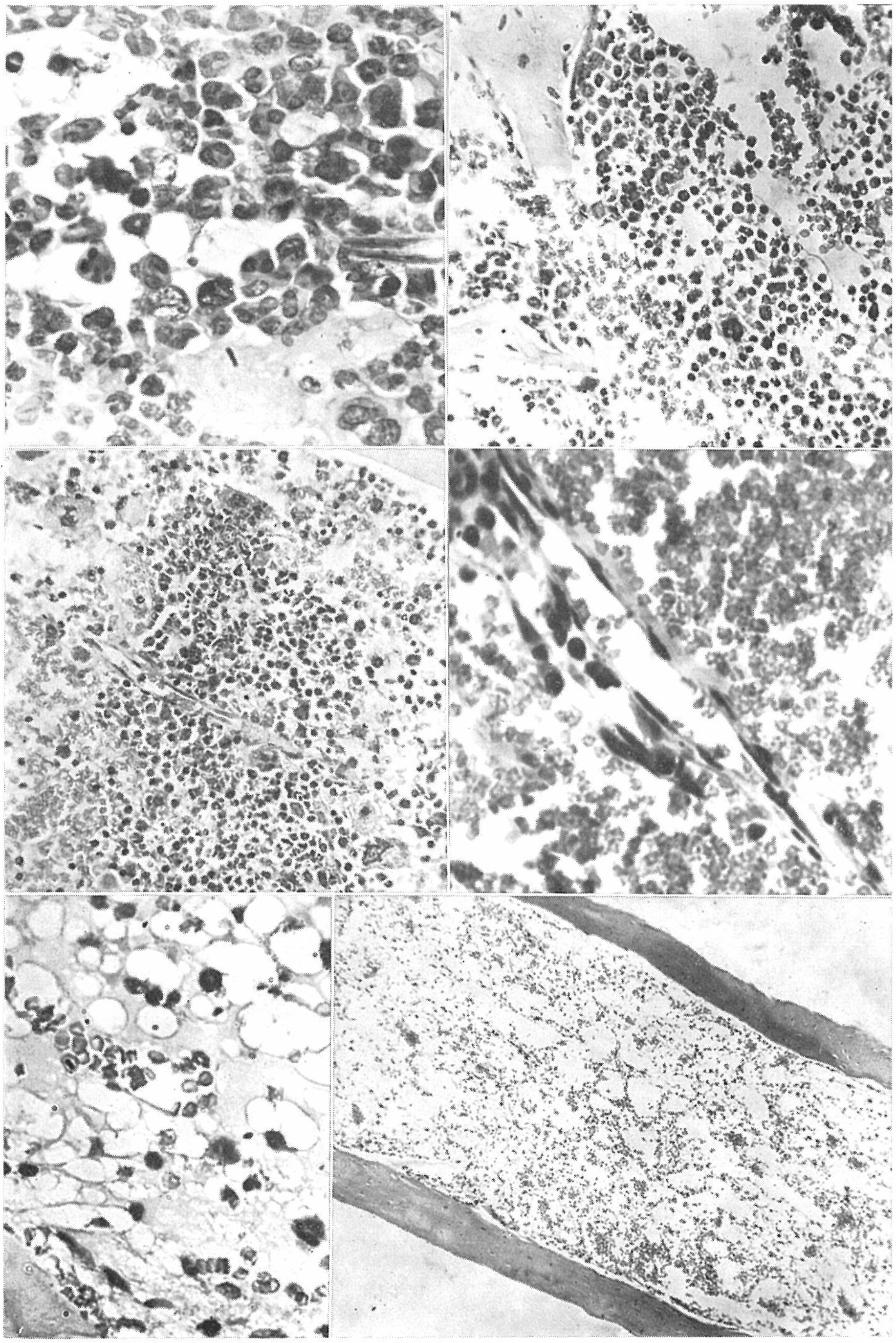

7 8 9 10 11 12

Fig. 5-3-1. (Continued).

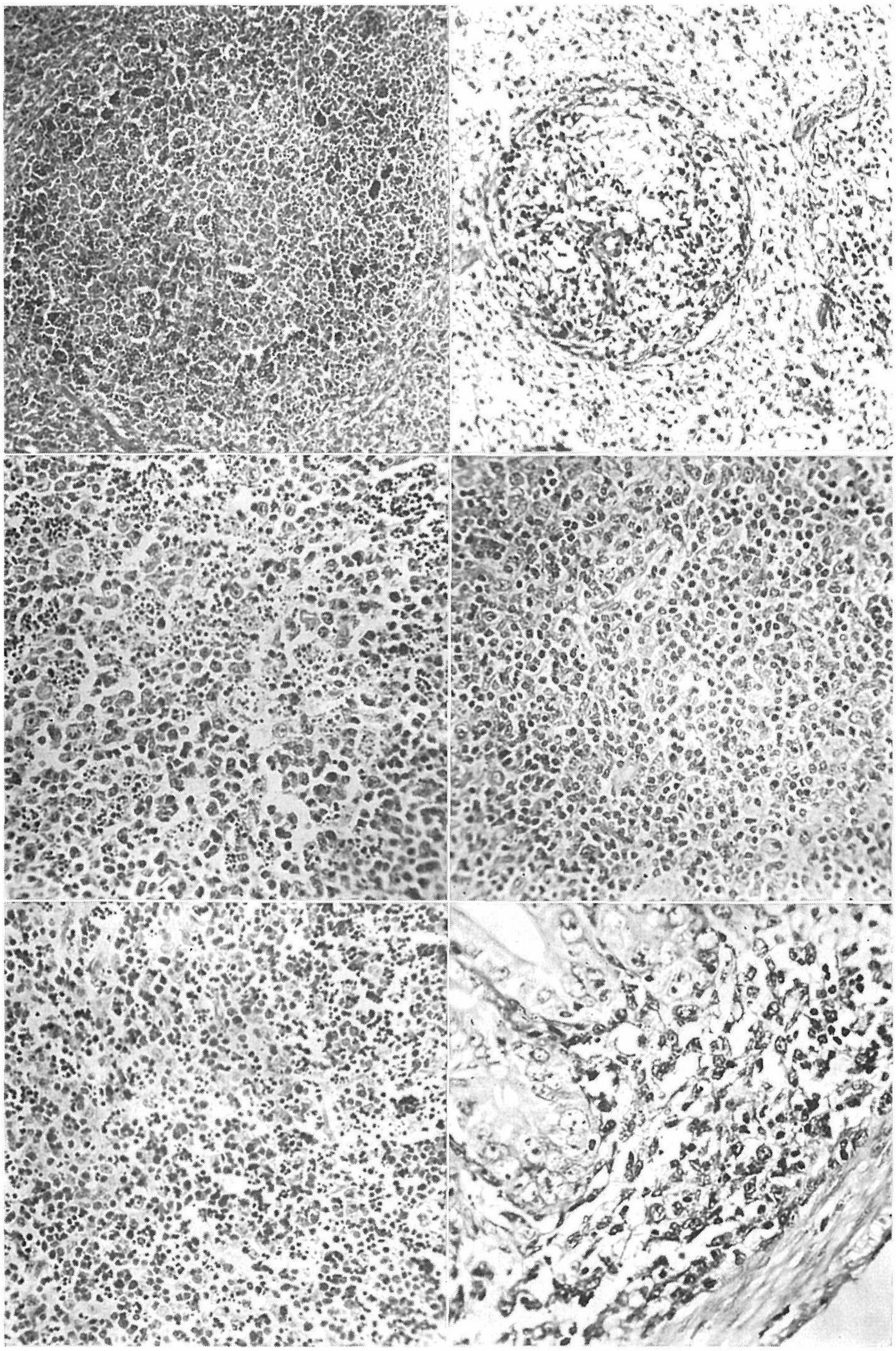

13 14 15 16 17 18

Fig. 5-3-1. (Continued).

by courtesy of Professor M. HANAOKA.

MORII and others let mice to be irradiated by neutrons (including gamma-rays) and observed the changes of the body weight, peripheral blood picture and histological findings through 18 weeks after irradiation, and found three modes of radiation effects as the followings:

1. In the group 1 given 1.1×10^{11} neutrons/cm^2, severe intestinal damage and leukopenia were observed and all died in the mean survival time of $3\frac{1}{8}$ days. These deaths were probably due to the "acute intestinal radiation death" and the radiation dose was thought to be equal to the supralethal range.

2. In the group 2 given neutrons in the dose between the groups 1 and 3, radiation effects were most severe on the third or fifth day after the irradiation and all mice of sm-strain died on about the seventh day. Leukopenia and infection seemed to play an important role in the cause of death. The radiation dose was thought to be equal to the midlethal range.

3. In the group 3 given 4.7×10^{10} neutron/cm^2, gross findings recovered by the 4th week, but when examined precisely, long continued radiation effects were observed. The radiation dose was thought to be equal to the sublethal range.

They then concluded from these observations that the radiation effects of neutrons are almost the same as that of the other ionizing radiation. For detailed discussions, see refs. [59-1], [59-2] and [59-3].

5-4. Application of Radio-active Isotopes

Besides neutron irradiation, the production of short life radio-isotopes has been performed when necessary. Among works contained in Table 5-2-1, biological studies were done by YAMADA *et al.* They used K^{42} as a tracer, and investigated the distribution of K^{42} absorbed by the tobacco plant precultured with standard

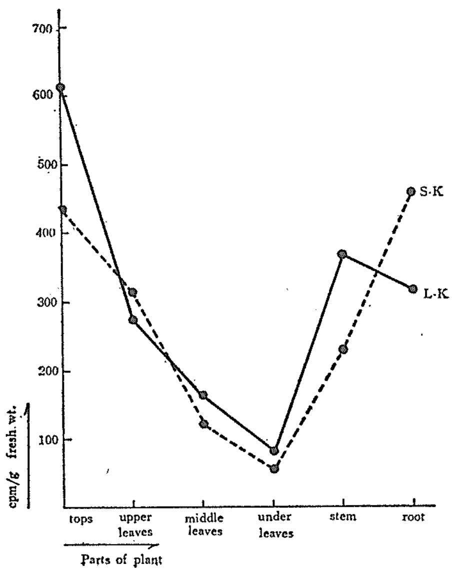

Fig. 5-4-1. Distributions of K^{42} in the tobacco plant. S-K means the plant precultured with standard level K (40 ppm), and L-K means the plant precultured with low level K (4 ppm).

level of potassium (S-K, 40 ppm) and with low level potassium (L-K, 4ppm). K^{42} was produced by K^{41} (d,p) K^{42} reaction, when a KCl single crystal plate was bombarded by the deuteron beam from the cyclotron. Detailed descriptions are given in refs. [58-3] and [62-2], so here the results are shown briefly in Figs. 5-4-1 and 2. These figures indicate that the percentages of K^{42} translocated to the shoot are greater on the plant in low K level than on the plant in standard K level.

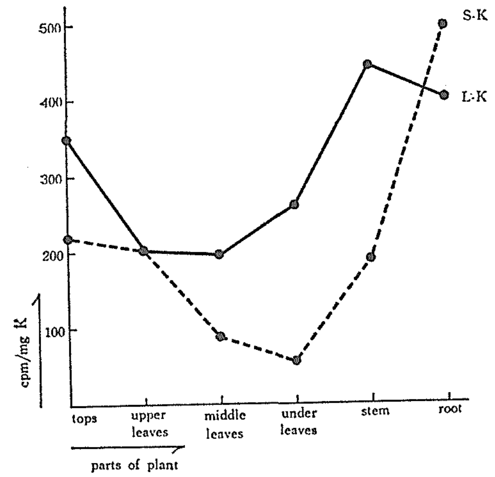

Fig. 5-4-2. Distribution of K^{42} absorbed in tobacco plant. (cpm/mg K). S-K and L-K in the figure are the same with those in Fig. 5-4-1.

Other problem such as the study of abrasion of metals by using the activation of metal surfaces is an important application of radio-isotpes, but because the dosimetry of neutrons and the uniform irradiation are difficult in the case of cyclotron, few investigations have been done since 1955.

6. PUBLICATIONS

In this section, the papers published in the period from 1954 to 1965 are compiled. In compilation, following criteria are adopted.

1) Seientific articles written by members of this laboratory and done in this laboratory.

2) Scientific articles of works done by using the Kyoto University Cyclotron.

3) Scientific articles of works done by members of this laboratory with the use of a cyclotron of the Institute for Nuclear Study, University of Tokyo.

4) Review articles written by the members of this laboratory.

Results are listed in the following table. In the table, first column indicates the reference numbers cited in this report, second column the names of authors, third column the titles of articles and the fourth column the names of journals in which the articles appeared.

Table 6-1. List of Publications.

Ref. No.	Author	Title	Journal
54-1	Yoshiaki UEMURA Jun KOKAME Hidetsugu IKEGAMI	Release of Adsorbed Gasses from Metallic Surfaces in a Vacuum System. (in Japanese)	Shinku-Gijutsu (Vacuum Technique) **5** 199 (1954)
54-2	Yoshiaki UEMURA Jun KOKAME Hidetsugu IKEGAMI	Characteristic Behavior of Propane and Butan Gasses used as Leak Hunting Probes. (in Japanese)	Shinku-Gijutsu (Vacuum Technique) **5** 212 (1954)
54-3	Sakae SHIMIZU Akira KATASE Hidekuni TAKEKOSHI Kenji TAKUMI Eiko TAKEKOSHI	On the Short-Circuiting Condenser in Kyoto Cyclotron.	Bull. Inst. Chem. Res. **32** 214 (1954)
56-1	Yoshiaki UEMURA	Vacuum Techniques applied to a 105 cm Cyclotron of Kyoto University. (in Japanese)	Sinku-Kogyo (Vacuum Engineering) **3** 14 (1956)
56-2	Yoshiaki UEMURA Jun KOKAME Hidetsugu IKEGAMI	Evacuation of a Cyclotron of Kyoto University. (in Japanese)	Shinku-Gijutsu (Vacuum Technique) **7** 229 (1956)
56-3	Jun KOKAME Sukeaki YAMASHITA	Electrostatic Deflection of a Cyclotron Ion Beam.	J. Phys. Soc. Japan **11** 332 (1956)
56-4	Ryutaro ISHIWARI Sukeaki YAMASHITA Kazunori YUASA Kozo MIYAKE	On the Ionization-Energy Relation for Alpha Particles.	J. Phys Soc. Japan **11** 337 (1956)
58-1	Masao HANAOKA Yasuo ICHIKAWA Hiroshi FUJI	Histological Studies on the Hematopoietic Organs of Mice Irradiated with High Doses of Neutrons (including Gamma Rays) from the Cyclotron. (in Japanese)	Acta Haem. Japonica **21** 1 (1958)
58-2	Kiichi KIMURA Jun KOKAME Sukeaki YAMASHITA	Observation of the Deflected Ion Beam Trajectory from a Cyclotron.	Rev. Sci. Inst. **29** 142 (1958)
58-3	Azuma OKUDA Zenzaburo KASAI Hitoshi NAKADA Kozi ASADA Yasuyuki YAMADA	Studies on the Crop Nutrition, Using Radioactive Potassium as a Tracer.	Memoirs of the Research Institute for Food Science, Kyoto University **15** 16 (1958)
58-4	Yoshiaki UEMURA Atsushi FUJINAGA Masayuki GOTOH Masami MICHISHIMA	Lectures on Vacuum Techniques. (in Japanese)	Shitsuryo-Bunseki (Mass Spectroscopy) **11** 100 (1958)
59-1	Tadashi MORII	Studies on the Biological Effects of Neutrons and Co^{60} γ-Rays in Mice I. Biological Effects of Neutrons in Mice. (in Japanese)	Japanese Archives of Internal Medicine **6** 453 (1959)
59-2	Tadashi MORII	Studies on the Biological Effects of Neutrons and Co^{60} γ-Rays in Mice II. Biological Effects of Co^{60} γ-Rays in Mice. (in Japanese)	Japanese Archives of Internal Medicine **6** 520 (1959)
59-3	Tadashi MORII	Studies on the Biological Effects of Neutrons and Co^{60} γ-Rays in Mice III. Modification of Radiation Injury in Mice. (in Japanese)	Japanese Archives of Internal Medicine **6** 585 (1959)

Table 6-1. (Continued).

Ref. No.	Author	Title	Journal
59-4	Masao HANAOKA	Histological Studies on the Mice Irradiated with Neutron-Gamma-Ray. The Primary and Secondary Injuries in the Acute Radiation. (in Japanese)	Symposia of the Society for Cellular Chemistry. **9** 201 (1959)
61-1	Yoshiaki UEMURA Jun KOKAME	Experimental Studies on the Air Test Method for Leak Detection. (in Japanese)	Shinku (Vacuum) **4** 20 (1961)
61-2	Yoshiaki UEMURA Hirokazu FUJITA	Measurements of the Substitution Sensitivity Factor to Propane and Helium Gases for the Leak Hunting. (in Japanese)	Shinku (Vacuum) **4** 30 (1961)
61-3	Takuji YANABU	(d, α) Reaction. (in Japanese.)	Genshikaku-Kenkyu. (circular in Japanese) **6** 165 (1961)
61-4	Jun KOKAME	Inelastic Scattering of Protons from Several Light Odd-Even Nuclei in the Energy Range from 6.0 MeV to 7.5 MeV.	J. Phys. Soc. Japan. **16** 2101 (1961)
61-5	Takuji YANABU	(d, α) Reactions on O^{16}, N^{14} and C^{12} by 14.7 MeV Deuterons.	J. Phys. Soc. Japan **16** 2118 (1961)
61-6	Sukeaki YAMASHITA	Angular Distributions of Alpha-Particles from F^{19}, Al^{27} and P^{31} bombarded with Protons.	J. Phys. Soc. Japan **16** 2378 (1961)
61-7	Ryutaro ISHIWARI	Elastic and Inelastic Scattering of Protons by Be^9 in the Energy Region from 6.1 to 7.3 MeV.	Bull. Inst. Chem. Res., Kyoto Univ., **39** 287 (1961)
61-8	Kozo MIYAKE	The Phase Shift Analysis on Alpha-Alpha Scattering in the Energy Range from 22.9 to 28.9 MeV.	Bull. Inst. Chem. Res., Kyoto Univ., **39** 313 (1961)
61-9	Takuji YANABU Sukeaki YAMASHITA Teruo NAKAMURA Kunio TAKAMATSU Akira MASAIKE Shigeru KAKIGI Dai-Ca NGUYEN Kiyohiko TAKIMOTO	$O^{16}(d, \alpha)N^{14}$ Reaction with Deuterons near 15 MeV.	J. Phys. Soc. Japan **16** 2594 (1961)
61-10	Kiichi KIMURA Yoshiaki UEMURA Masateru SONODA Takuji YANABU Ryutaro ISHIWARI Jun KOKAME Isao KUMABE Sukeaki YAMASHITA Hidekuni TAKEKOSHI Kozo MIYAKE Hidetsugu IKEGAMI Hirokazu FUJITA	A 105 cm Fixed Frequency Cyclotron of Kyoto University.	Bull. Inst. Chem. Res., Kyoto Univ., **39** 368 (1961)
62-1	Kiichi KIMURA Yoshiaki UEMURA Ryutaro ISHIWARI Jun KOKAME Kiyoji FUKUNAGA Akira KATASE Jiro MUTO Isao KUMABE Hiroshi OGATA Taro OHAMA Yasuya OHMORI	Elastic Scattering of Protons from B^{11}, Al, P, Co, and Cu from 6 to 7.4 MeV.	J. Phys. Soc. Japan **17** 9 (19632)

Table 6-1. (Continued).

Ref. No.	Author	Title	Journal
62-2	Azuma OKUDA Yasuyuki YAMADA	Foliar Absorption of Nutrients III. Comparison of Folier Absorption with Root Absorption in Potassium Phosphate Double-labeled with ^{42}K and ^{32}P.	Soil Science and Plant Nutrition **8** 14 (1962)
62-3	Teruo NAKAMURA Kunio TAKAMATSU Akira MASAIKE Shigeru KAKIGI Dai-Ca NGUYEN Sukeaki YAMASHITA Takuji YANABU	Angular Distributions of the Alpha Particles from the (p, α) Reactions on Na^{23} and K^{39} at 6.9~7.3 MeV.	J. Phys. Soc. Japan **17** 19 (1962)
62-4	Takuji YANABU Sukeaki YAMASHITA Teruo NAKAMURA Kunio TAKAMATSU Akira MASAIKE Shigeru KAKIGI Dai-Ca NGUYEN Kiyohiko TAKIMOTO	C^{12} and O^{16} (d, α) Reactions by 15~20 MeV Deuterons. (in Japanese)	Genshikaku Kenkyu (circular in Japanese) **7** 275 (1962)
62-5	Kunio TAKAMATSU	(d, α) Reactions on F^{19}, Ne^{20}, P^{31} and S^{32} at 14.7 MeV.	J. Phys. Soc. Japan **17** 896 (1961)
62-6	Takuji YANABU Sukeaki YAMASHITA Teruo NAKAMURA Kunio TAKAMATSU Akira MASAIKE Shigeru KAKIGI Dai-Ca NGUYEN Kiyohiko TAKIMOTO	Al^{27} (d, α) Mg^{25} Reaction at 14.7 MeV.	J. Phys. Soc. Japan **17** 914 (1962)
62-7	Isao KUMABE Takeshi KOMATSUZAKI Shigeharu TOMITA Tetsuji YAMAKI Yasumasa YAMADA	Protons from Several Elements Bomberded with 30-MeV Alpha Particles.	J. Phys. Soc. Japan **17** 1526 (1962)
63-1	Kozo MIYAKE	A Survey of Recent Development of the Radiation Detector. (in Japanese)	Genshikaku Kenkyu (circular in Japanese) **8** 33 (1963)
63-2	Junji SHIMIZU Kyoichi MIYASHITA Mamoru TAKADA Yoshiyuki SUGAWA	P-N Junction Semiconductor Radiation Detector.	Mitsubishi Denki LABORATORY REPORTS **4** 495 (1963)
63-3	Takuji YANABU Sukeaki YAMASHITA Teruo NAKAMURA Kunio TAKAMATSU Akira MASAIKE Shigeru KAKIGI Dai-Ca NGUYEMN Kiyohiko TAKIMOTO	(d, α) Reactions on C^{12} and O^{16} with Deuterons in the Energy Range from 15 MeV to 20 MeV.	J. Phys. Soc. Japan **18** 742 (1963)
63-4	Sukeaki YAMASHITA	The (p, p′ α) Reaction. (in Japanese)	Genshikaku Kenkyu (circular in Japanese) **8** 233 (1963)
63-5	Jun KOKAME Ryutaro ISHIWARI Kozo MIYAKE Jiro MUTO Hidehiko ITOH Taro OHAMA Kazuhiro UEDA Sadamu TAHIRA Kota BABA	Scattering of Protons from Be^9, B^{11}, Al^{27} and P^{31} in the Energy Range of 8~14 MeV. (in Japanese)	Genshikaku Kenkyu (circular in Japanese) **8** 339 (1963)

Table 6-1. (Continued).

Ref. No.	Author	Title	Journal
64-1	Jun KOKAME	Direct- and Compound Nucleus-Process in the Inelastic Scattering of Protons from Light Odd Nuclei.	Genshikaku Kenkyu (circular in Japanese) **8** 604 (1964)
64-2	Yoshiaki UEMURA Hirokazu FUJITA Shuzo KAKUI Masakatsu SAKISAKA Funio FUKUZAWA Mitio TOMITA Koji YOSHIDA Shoji OKUMURA Shinji IMANISHI Kazuo KOBAYASI Takayuki TAKEUCHI Taiji NAKATA	Fundamental Studies on Heavy Ion Reactions. I (in Japanese)	Genshikaku Kenkyu (circular in Japanese) **8** 617 (1964)
64-3	Isao KUMABE Hiroshi OGATA Makoto INOUE Yasuhiko OKUMA Jiro MUTO	Elastic and Inelastic Scattering of 28.5 MeV Alpha Particles by Medium-Weight Nuclei.	J. Phys. Soc. Japan **19** 147 (1964)
64-4	Jun KOKAME Kiyoji FUKUNAGA Nobuyuki INOUE Hitoshi NAKAMURA	Excitation of Unnatural-Parity States in (α, α') Scatterings on O^{16}, Ne^{20}, Mg^{24} and Si^{28}.	Physics Letters **8** 342 (1964)
64-5	Masao HANAOKA	Injuries by Radiation, especially by Neutrons on Blood and Hematopoietic Organs. (in Japanese)	Hdb. Hematology, ed. by Jap. Hematol. Soc. **3** 541 (1964)
64-6	Kiyohiko TAKIMOTO	Quasi-Free Alpha-Alpha Collisions in Nuclei with 28 MeV Alpha Particles. (in Japanese)	Genshikaku Kenkyu (circular in Japanese) **9** 297 (1964)
64-7	Yoshiaki UEMURA Hirokazu FUJITA Shuzo KAKUI Masakatsu SAKISAKA Fumio FUKUZAWA Mitio TOMITA Koji YOSHIDA Shoji OKUMURA Shinji IMANISHI Kazuo KOBAYASHI Takayuki TAKEUCHI Taiji NAKATA	Fundamental Studies on Heavy Ion Reactions. II (in Japanese)	Genshikaku Kenkyu (circular in Japanese) **9** 363 (1964)
64-8	Takuji YANABU Sukeaki YAMASHITA Shigeru KAKIGI Dai-Ca NGUYEN Kiyohiko TAKIMOTO Yasumasa YAMADA Kouya OGINO	Alpha Emitting Reactions on Be^9, B^{10} and B^{11} Induced by Protons, Deuterons and Alpha-Particles.	J. Phys. Soc. Japan **19** 1818 (1964)
64-9	Takuji YANABU Sukeaki YAMASHITA Teruo NAKAMURA Hiroshi OGATA Shigeru KAKIGI Dai-Ca NGUYEN Kiyohiko TAKIMOTO Kouya OGINO Makoto INOUE Yasuhiko OKUMA	Al and Ni $(p, p' \alpha)$ Reactions Induced by 55 MeV Protons. (in Japanese)	Genshikaku Kenkyu (circular in Japanese) **9** 421 (1964)
65-1	Kiyoji FUKUNAGA	Elastic and Inelastic Scatterings of Polarized Protons from Be^9 and Al^{27}.	J. Phys. Soc. Japan. **20** 1 (1965)

Table 6-1. (Continued).

Ref. No.	Author	Title	Journal
65-2	Jun KOKAME Kiyoji FUKUNAGA Hitoshi NAKAMURA	The Excited Core Model of Light Nuclei in (α, α') Scattering.	Physics Letters **14** 234 (1965)
65-3	Jun KOKAME Kiyoji FUKUNAGA	Differential Cross Sections of (p, p) and (p, p′) Scattering from Several Odd-A Nuclei in the Energy Range of 6 to 7.5 MeV.	Bull. Inst. Chem. Res., Kyoto Univ., Supplement. P. 1 Feb. 1965
65-4	Jun KOKAME Kiyoji FUKUNAGA Hitoshi NAKAMURA Nobuyuki INOUE	Differential Cross Sections of (α, α) and (α, α) Scattering from B^{11}, C^{12}, C^{13}, O^{16}, Ne^{20}, Mg^{24}, Si^{28} and P^{31}.	Bull. Inst Chem. Res, Kyoto Univ., Supplement. p. 26 Feb. 1965
65-5	Takuji YANABU Sukeaki YAMASHITA Teruo NAKAMURA Kunio TAKAMATSU Akira MASAIKE Shigeru KAKIGI Dai-Ca NGUYEN Kiyohiko TAKIMOTO	Differential and Integral Cross Sections of the (p, α') and (d, α) Reactions on Some Light Nuclei.	Bull. Inst. Chem. Res., Kyoto Univ., Supplement. p. 41 Feb. 1965
65-6	Takuji YANABU Sukeaki YAMASHITA Teruo NAKAMURA Kunio TAKAMATSU Akira MASAIKE Shigeru KAKIGI Dai-Ca NGUYEN Kiyohiko TAKIMOTO	Differential and Integral Cross Sections of the Reaction $C^{12}(d, \alpha)B^{10}$ and $O^{16}(d, \alpha)N^{14}$ in the Deuteron Energy Range from 15 MeV to 20 MeV.	Bull. Inst. Chem. Res., Kyoto Univ., Supplement, p. 68 Feb. 1965
65-7	Jun KOKAME Kiyoji FUKUNAGA Hitoshi NAKAMURA Nobuyuki INOUE	Elastic and Inelastic Scattering of 28.4 MeV Alpha-Particles from O^{16}, Ne^{20}, Mg^{24} and Si^{28}.	J. Phys. Soc. Japan **20** 475 (1965)
65-8	Jun KOKAME Kiyoji FUKUNAGA	Estimation of Direct- and Compound-Nuclear Reaction Cross Sections in $Al^{27}(p, p')Al^{27*}$ in the Energy Range of 6.5 to 14 MeV.	J. Phys. Soc. Japan **20** 649 (1965)
65-9	Ryutaro ISHIWARI	Ionization Yield of the $N^{14}(n, p)C^{14}$ Reaction in Air.	J. Phys. Soc. Japan **20** 658 (1965)
65-10	Takuji YANABU Sukeaki YAMASHITA Kiyohiko TAKIMOTO Kouya OGINO	Quasi-Free Alpha-Alpha Collisions in Be^9 and C^{12} at 28 MeV.	J. Phys. Soc. Japan **20** 1303 (1965)
65-11	Yoshiaki UEMURA Hirokazu FUJITA Tadahiro MARUYAMA Masakatsu SAKISAKA Fumio FUKUZAWA Mitio TOMITA Kouya OGINO Kohji YOSHIDA Shoji OKUMURA Nobutsugu IMANISHI Taiji NAKATA	Fundamental Studies on Heavy Ion Reaction III. Charge Changing Collisions of Carbon Ions. (in Japanese)	Genshikaku Kenkyu (circular in Japanese) **10** 303 (1965)
65-12	Isao KUMABE	DWBA Analysis of Alpha Scattering. (in Japanese)	Genshikaku Kenkyu (circular in Japanese) **10** 369 (1965)
65-13	Jun KOKAME	The Excitation of 3^+ State of Mg^{24} by (α, α') Scattering. Analysis by Dr. Taro Tamura. (in Japanese)	Genshikaku Kenkyu (circular in Japanese) **10** 425 (1965)

Table 6-1. (Continued).

Ref. No.	Author	Title	Journal
65-14	Shigeru KAKIGI	(α, d) and (α, t) Reactions on Be^9, F^{19} and Al^{27} at 28.6 MeV.	J. Phys. Soc. Japan **20** 1967 (1965)
65-15	Nobutsugu IMANISHI Masakatsu SAKISAKA Fumio FUKUZAWA Yoshiaki UEMURA	Medium Dependence of Charge Changing Collisions for 9.7 MeV Carbon Ions.	J. Phys. Soc. Japan **20** 2100 (1965)
65-16	Kazuhiko HOSONO Ryutaro ISHIWARI Yoshiaki UEMURA	Energy Loss of Alpha Particles through Matter at 28 MeV.	Bull. Inst. Chem. Res. **43** 323 (1965)
65-17	Seishi MATSUKI Sukeaki YAMASHITA Kozo MIYAKE	Time Resolution of a Transitorized Time-of-Flight System.	Bull. Inst Chem. Res. **43** 330 (1965)
65-18	Tetsumi TANABE Jun KOKAME Ryutaro ISHIWARI	Construction of a Thin Magnetic Lens Type Beta-Ray Spectrometer.	Bull. Inst. Chem. Res. **43** 315 (1965)
65-19	Kiyoteru OTOZAI Sanshiro KUME Mutsuo KOYAMA Toshikazu MITSUJI Tomota NISHI Ichiro FUJIWARA	Excitation Functions for the Reactions Induced by Deuterons on Ce^{142} up to 14.2 MeV.	Submitted to Nuclear Physics.
65-20	Isao KUMABE Hiroshi OGATA Shigeharu TOMITA Makoto INOUE Yasuhiko OHKUMA	Elastic and Inelastic Scattering of 28.4 MeV Alpha Particles by Sn, Cd, Ag, Cu and Ti.	Submitted to J. Phys. Soc. Japan.

As a matter of course, published works are not the whole of research activities. Rather, unpublished daily works are the basis of research. Among these unpublished works, some concerning the laboratory techniques and instrumentations will be compiled and published in near future, but others will remain in the ground of this laboratory forever.

ACKNOWLEDGEMENTS

Ending this report, many recollections and reflections recur to the author's mind. Innumerable persons helped to start the laboratory, to construct the cyclotron, to complete the equipments and to accomplish the work. Among those persons, the author would like to thank especially the past Presidents of Kyoto University, Professor Dr. Risaburo TORIGAI and Professor Dr. Shunjiro HATTORI for their assistance in the early stage of the construction of this laboratory. Thanks are also due to the past and present Directors of the Institute for Chemical Research, the late Professor Dr. Senji UCHINO, Professor Dr. Masao HORIO, Professor Dr. Sankichi TAKEI, the late Professor Dr. Risaburo NAKAI, Professor Dr. Rempei GOTOH and Professor Dr. Sango KUNICHIKA. The generosities and patient coopperations in various ways given by the staff of the Institute for Chemical Research are appreciated. The authorities of the Ministry of Education and those of Kyoto University are also sincerely acknowledged for their courtesy and financial support. The goodwill given by the authorities of Kyoto City Hall and by the executives of Kansai Electric Power Co., Inc. is finally appreciated.